PROCEEDINGS

OF THE

NATIONAL ACADEMY OF SCIENCES

INDIA

1961

Vol. XXX SECTION - A Part I

NATIONAL ACADEMY OF SCIENCES, INDIA
ALLAHABAD

The *Proceedings of the National Academy of Sciences, India*, is published in two sections: Section A (Physical Sciences) and Section B (Biological Sciences). Four parts of each section are published annually (since 1960).

The Editorial Board in its work of examining papers received for publication is assisted, in an honorary capacity, by a large number of distinguished scientists. Papers are accepted from members of the Academy *in good standing*. In case of a joint paper, one of the authors must be a member of the Academy. The Academy assumes no responsibility for the statements and opinions advanced by the authors. The papers must conform strictly to the rules for publication of papers in the *Proceedings*. A total of 50 reprints are supplied free of cost to the author or authors. The authors may have any reasonable number of additional reprints at cost price, provided they give prior intimation while returning the proof.

Communications regarding contributions for publication in the *Proceedings*, books for review, subscriptions etc., should be sent to the General Secretary, National Academy of Sciences, India, Lajpatrai Road, Allahabad-2 (India).

Annual Subscription for both Sections: Rs. 65; for each Section: Rs. 35 (including Annual Number); Single Copy: Rs. 7.50; Annual Number Rs. 5

PROCEEDINGS

OF THE

NATIONAL ACADEMY OF SCIENCES

INDIA

1961

VOL. XXX SECTION - A PART I

THE MASS—FREQUENCY FUNCTION IN GALACTIC CLUSTERS

By

O. P. GUPTA *and* R. S. KUSHWAHA

Department of Astronomy and Astrophysics, University of Delhi, Delhi-6

[Received on 14th November, 1960]

ABSTRACT

An important question in present-day astronomy is the distribution of stars in different masses, called the mass-frequency function. For a system like neighbourhood of Sun or stars in a large volume of galaxy, the whole stellar-population may not have been born at the same time and, therefore, the present mass-frequency function may be a combination of different mass-frequency functions of stars at the time of their birth. In the present work an attempt has been made to study the observed mass-frequency function of a group of stars which is believed to be born at the same time. Most probably galactic clusters represent such system. It is assumed that the birth of all the stars comes about as a single event. Theory of random-fragmentations can be applied to these systems. The theoretical mass-frequency function has been compared with the observed one in case of several galactic clusters. The two are found in reasonable agreement.

These galactic clusters being very young, it is found that evolution does not have any appreciable effect on these distributions. The linear representation of mass-frequency function in logarithmic variables, as assumed by previous workers, appears to differ from the observed mass-frequency function towards the low mass end. There is definitely a curvature in the observed curve. A parabola, therefore, is fitted with the help of least square solution. It is found that it represents the observed curve fairly well in the whole range. From the comparison of the observed curve with the theoretical curve for random-fragmentation, the original masses of the various clusters are estimated. They are found to be of the right order.

INTRODUCTION

According to the present belief, the stars are born from condensations in large intersteller clouds. These condensations may start at various points within a very large cloud. The stars in various regions of the galaxy are also born in the same way at different times. At a particular moment, a group of stars are born. They may follow a particular pattern in their mass distribution. If the birth of stars is a continuous process or if present population of the stars is a combination of several such births then the present-day mass-frequency function

should be a combination of such mass-distributions. Therefore, to have any idea of mass-distribution in the case of an instantaneous single-event like birth of the stars, one has to observe a group of stars which should have a simultaneous birth. Probably, the most plausible groups of such stars are the galactic clusters.

The study of the mass-frequency function and its probable analytical form was made by Ferrarid' Occhieppo (1952), Saltpeter (1955) and G. Jaschek and M. Jaschek (1957). They tried to represent the function by a power law of the form

$$\frac{dN}{dm} = C\, m^{-\alpha} \tag{1}$$

where N represents the number of stars having masses lying between m and $(m+dm)$ and C is some constant.

The former two confined to the study of stars in solar neighbourhood whereas the last one studied the case of three galactic clusters, using the observations of Johnson and Knuckles (1955), Johnson (1952) and Mawridis (1956). Since then a number of other galactic clusters have been observed in details by Mitchell and Johnson (1958), Walker (1956, 57, 58, 59), Johnson and Sandage (1956), Sandage (1958), Burbidge and Sandage (1958) and Arp & Sandage (1959). Also the ideas about the evolution of the main sequence stars have been clearified in details by Schwarzschild (1958), Kushwaha (1957) and Heyney (1959). Consequently the present study is of some interest.

OBSERVATIONAL MATERIAL

For the present study we have chosen the following clusters :—

TABLE I

Cluster	Age in years	Number of stars	Distance Modulus	Sources For		
				Age	Number	Distance
M 67	4×10^9	500	9·6	Van den Bergh (1957)		Johnson (1957)
NGC7789	$(0{\cdot}5-4)\times10^9$	586	11·36	Burbidge & Sandage (1958)		
NGC6940	$(0{\cdot}5-4)\times10^9$	110	10·0	Walker (1958)		
Praesepe	5×10^8	193	6·0	Heyney (1959)	Johnson (1952)	Johnson (1957)
Hyades	5×10^8	189	3·03	Heyney (1959)	Johnson & Knuckles (1955)	
M 11	$(0{\cdot}6-5)\times10^8$	599	1·21	Johnson, Sandage & Wahlquist, (1956)		Johnson (1957)
Pleiades	6×10^7	289	5·5	Heyney (1959)	Mitchell & Johnson (1958)	Johnson (1957)
NGC129	8×10^6	103	11·0	Arp & Sandage (1959)		
NGC2264	3×10^6	210	9·7	Walker (1955-56)		Johnson (1957)

M 67 :— This cluster was first studied in detail by Johnson and Sandage (1955). The photographic photometry for about 450 stars and photoelectric photometry for 59 stars was done by making use of combinations of plates and filters described there. The errors in U, B, V magnitudes were found to be large and so they did not give the magnitudes and colours of the individual members. But the magnitudes were found to be on the Johnson's U, B, V system. As this is perhaps the oldest galactic cluster, uncertainty due to evolutionary effect and the lack of reliable magnitudes of individual stars, is large.

NGC 7789 :—The cluster is rich in membership and is also old but the definiteness of the membership of each star is not yet established. The study does not show any differential reddening. The magnitudes given are on the U, B, V system.

NGC 6940 :—A three colour photoelectric photometry has been done only for those stars whose membership is established. The membership of the rest is determined statistically from the counts of the stars in different parts of cluster area. Reddening is found to be non-uniform over the area of the cluster. It is in the vicinity of a rich field and hence there is an uncertainty in the membership of the stars.

Praesepe :— Measurements of colour and magnitude for 133 physical members and 17 non-members were made photoelectrically and that for 60 other stars was done by Haffner and Heckmann (1937, 1940). There may be enough number of double stars but the reddening is found to be negligible.

Hyades :— The magnitudes are given on the U, B, V system. The three colour photoelectric observations were made on most of the known cluster members. The membership of all the stars is not very definite on the basis of proper motion and radial velocity measurements.

M 11 :— The three colour photometric observations on 400 stars was made by the interpolation between photoelectric standards. Reddening is found to be large. Out of these the membership of many stars is not deter mined with definiteness.

Pleiades :— The two or three colour photometry is available for all members except six of them. The photoelectric observations are good but photographic ones are not accurate. In our calculation only members and probable members have been used. The magnitudes are on U, B, V system.

NGC 129 :— The photometric data for 192 stars is available but the most probable members being only 103. Measurements on 26 stars were taken to be as standard ones and the magnitudes for the rest of the stars were interpolated. The magnitudes are on U, B, V system. A differential reddening is found here.

NGC 2264 :—This cluster has a dark background and hence the field stars don't create any uncertainty in determining the membership. The reddening is found to be uniform and small. The magnitudes of 149 non-variable stars photoelectrically and that of 61 stars photographically have been obtained. The data of some of the stars is not reliable due to the fact that there is an irregular brightness of the emission nebulosity.

COMPUTATION OF MASSES OF INDIVIDUAL STARS

The procedure adopted for the computation of mass of each of the cluster members was as follows. The apparent visual magnitudes m_v obtained observationally were stransferred to absolute visual magnitude M_v by making use of the distance modulus. The bolometric correction and effective temperature T_e for colour index (B – V) for the corresponding individual stars was taken from Schwarzschild (1958). Applying bolometric corrections to absolute visual magnitudes M_v, absolute bolometric magnitudes M_b were determined. The actual mass computations were carried out with the help of following equation given by R. M. Petrie (1950)

$$\log m = +0{\cdot}548 - 0{\cdot}144\, M_c + 0{\cdot}002\, M_c^2 \qquad (2)$$

where M_c is given by

$$M_c = M_b + 2 \log (T_e/5200) \qquad (3)$$

To calculate the corrected magnitude M_c from the absolute bolometric magnitude M_b, the effective temperature T_e was required. This was obtained as mentioned above.

OBSERVED MASS-FREQUENCY CURVE

From the above calculated masses, counts were made for total number of stars with masses greater than a certain value of m. This number was represented by N_m. The following Table 2 gives this distribution for the various clusters where the mass is represented in terms of the solar units.

TABLE 2

Mass-frequency distribution for various clusters

Log N_m

log m \ Clusters	NGC 7789	NGC 6940	Praesepe	Hyades	M11	Pleiades	NGC 129	NGC 2264
−0·6			2·286	2·277		2·461		
−0·5			2·286	2·277		2·449		
−0·4			2·279	2·274		2·401		2·322
−0·3			2·248	2·250		2·324		2·316
−0·2	2·768		2·152	2·137		2·212		2·299
−0·1	2·768		2·004	1·991	2·601	2·076	2·013	2·260
0	2·664	2·041	1·857	1·826	2·589	1·940	1·969	2·173
+0·1	2·505	2·037	1·644	1·672	2·443	1·820	1·833	2·097
+0·2	2·286	1·919	1·505	1·301	2·297	1·663	1·602	2·021
+0·3	2·090	1·568	1·255	1·041	2·143	1·462	1·398	1·929
+0·4	2·029	1·362	1·079	0·602	1·919	1·230	1·146	1·792
+0·5	1·748	1·000	0·477	0·477	1·644	1·041	0·903	1·663
+0·6	1·519	0·699			1·505	0·845	0·699	1·477
+0·7	1·255	0·602			1·342	0·699	0·602	1·322
+0·8	1·041	0·301			0·954	0·602		1·041
+0·9	0·845				0·301			0·845
+1·0	0·477							0·477
+1·1								0·301

(For cluster M67 the distribution could not be found in above mentioned intervals as the magnitudes of the individual members were not available.)

The observational curve for the mass-frequency function was plotted with $\log N_m$ as abscissa and $\log m$ as ordinate.

MASS-FREQUENCY DISTRIBUTION FOR RANDOM FRAGMENTATION

The following theoretical expression giving the distribution of elements of various sizes for the case of random fragmentation is given by Auluck and Kothari (1954).

$$N(V) \sim (2\pi/\sqrt{3})\, N_0\, (V/V_0)^{1/3} \exp\left[-3\,(V/V_0)^{1/3} \right] \qquad (4)$$

where N (V) represents the number of elements with volume $\geqslant$ V. N_0 – the total number of fragments.

V_0 – average volume of fragments.

If we can assume that the original cloud had uniform density throughout then this volume distribution of various elements will also represent the mass distribution of various condensations *i.e.*, stars. Therefore, to compare the theoretical and the observed distribution, a theoretical curve is plotted with $\log (V/V_0)$ as ordinate and $[\log N(V) - \log (2\pi/\sqrt{3}\, N_0)]$ as abscissa. Figures 1 (*a*), and 1 (*b*) give the comparison of the observed curve and this theoretical curve.

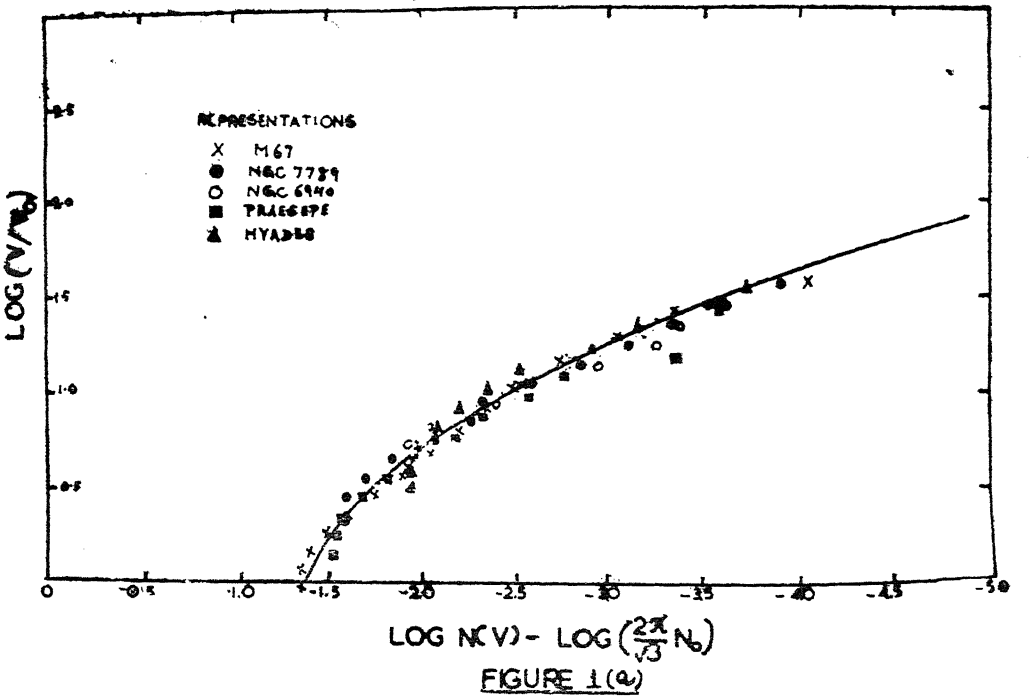

FIGURE 1(a)

It can be seen from this curve that in general the theoretical distribution fits reasonably well with the observed distribution, which confirms the present belief that almost all the stars in the galactic clusters were born simultaneously.

The previous workers have represented this mass-frequency function as a power law of the form given by expression (1). To convert this into our representation we integrate from m to ∞ and get

$$\log N_m = \log C_1 - (\alpha - 1) \log m \qquad (5)$$

where N_m is the total number of stars with masses greater than a certain value of mass m and C_1 is another constant.

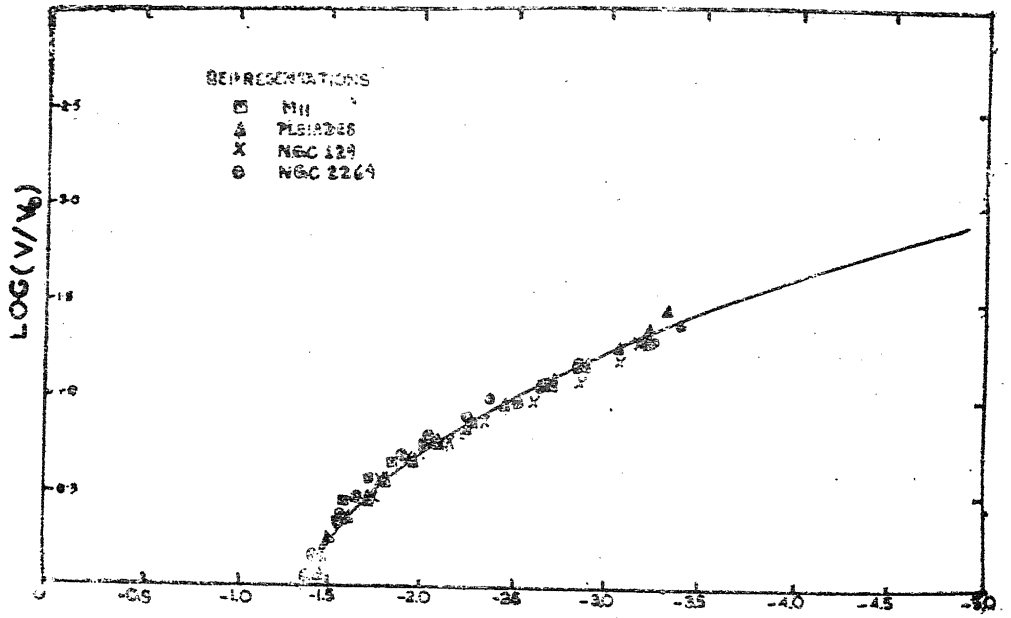

FIGURE 1(b)

From the observational material this graph was plotted with $\log N_m$ against $\log m$. The best possible straight line was fitted through the above observed points for various clusters and from there the value of α was derived. These are given in Table 3.

TABLE 3

Cluster	Value of α	Age in years
M 67	2·3	4×10^9
NGC 6940	3·4	$(0{\cdot}5-4) \times 10^9$
NGC 7789	2·9	$(0{\cdot}5-4) \times 10^9$
Hyades	2·7	5×10^8
Praesepe	2·5	5×10^8
M11	3·1	$(0{\cdot}6-5) \times 10^8$
Pleiades	2·5	6×10^7
NGC 129	3·0	8×10^6
NGC 2264	2·3	3×10^6

It can be concluded from the table that α has a tendency to increase with the age. Clusters M67, M11 and NGC 129 show discordance. The magnitudes for individual members of M67 was not available. For the cluster M11, the study of luminosity function show that it contains many yellow giants similar to M67 and the distance modulus also is uncertain and hence the age of the cluster may be more than the given one. The cluster NGC 129 is young and observational magnitudes and membership is not very definite. Therefore, the values of α for these may not be very reliable.

QUADRATIC MASS-FREQUENCY FUNCTION

From figures 1(*a*) and 1(*b*), it is obvious that there exists a definite curvature, specially towards the low mass end. Therefore, a parabola instead of a straight line was fitted. The various parabolae fitting the cases of various clusters were obtained with the help of least square solution. These can be represented as follow :—

M67	$\log N_m = 1{\cdot}271 - 1{\cdot}937 \log m - 0{\cdot}598 (\log m)^2$
NGC 7789	$\log N_m = 2{\cdot}608 - 1{\cdot}286 \log m - 0{\cdot}826 (\log m)^2$
NGC 6940	$\log N_m = 2{\cdot}166 - 1{\cdot}805 \log m - 0{\cdot}719 (\log m)^2$
Praesepe	$\log N_m = 1{\cdot}837 - 1{\cdot}641 \log m - 1{\cdot}343 (\log m)^2$
Hyades	$\log N_m = 1{\cdot}813 - 1{\cdot}933 \log m - 1{\cdot}909 (\log m)^2$
M 11	$\log N_m = 2{\cdot}543 - 0{\cdot}752 \log m - 1{\cdot}723 (\log m)^2$
Pleiades	$\log N_m = 1{\cdot}929 - 1{\cdot}345 \log m - 0{\cdot}573 (\log m)^2$
NGC 129	$\log N_m = 1{\cdot}932 - 1{\cdot}736 \log m - 0{\cdot}381 (\log m)^2$
NGC 2264	$\log N_m = 2{\cdot}205 - 0{\cdot}649 \log m - 0{\cdot}997 (\log m)^2$

EFFECT OF EVOLUTION

Out of all these clusters, Hyades was chosen to see the effect of evolution on the mass-frequency function. In the course of evolution the stars of main-sequence move in Hertzsprung-Russell diagram towards the giant region, thereby increase the luminosity and decrease the effective temperature. The present observed magnitudes actually correspond to the evolved positions in H-R diagram rather than original main sequence positions. The equation used for computation of mass is to be applied for the main sequence. Hence one has to reduce the observed magnitude to the corresponding main sequence magnitude. For this purpose the theoretically computed evolutionary tracks available [Kushwaha (57), Heyney (1959)] were used. With the help of these, the necessary tracks for individual stars were interpolated.

With the help of these interpolated tracks the magnitudes of the individual stars were obtained for their positions on the main sequence. From these magnitudes the masses of the individual stars were recalculated. It was found as expected that for most of the stars the effect was neglegible due to their masses being small. It was only in the case of few stars having larger masses that the effect was of any significance. On the whole the effect of this on the mass-frequency curve was not very appreciable. It only increased the scatter a little towards the large mass end.

Observed mass-frequency curves were superimposed on the theoretical curve given by the equation (4). The best fits were obtained as far as possible. The shifts in the ordinate and the abscissa gave the average mass m_0 (defined as the total mass of the original cloud divided by the number of fragmentations) and N_0 – the total number of fragmentations. From this one can have a rough estimate of the original mass of the cloud. This sort of fitting was done for the case of every cluster. The best fit to some extent was a matter of personal judgment. The values thus obtained for masses of clusters are given in Table 4.

TABLE 4

Masses of Clusters

Cluster	MASS	
	Calculated	From other sources
M 67	250 $M_\odot$	500 $M_\odot$
NGC 7789	1700 $M_\odot$	.....
NGC 6940	600 $M_\odot$	.....
Praesepe	400 $M_\odot$	700 $M_\odot$
Hyades	450 $M_\odot$	500 $M_\odot$
M11	1400 $M_\odot$	.....
Pleiades	500 $M_\odot$	500 $M_\odot$
NGC 129	450 $M_\odot$	.....
NGC 2264	700 $M_\odot$	450 $M_\odot$

The masses available from other sources, calculated from dynamical considerations are also given in third column of Table (4). In view of the approximate nature of the work one can conclude from the comparison of these masses that the above calculated masses are of the right order of magnitude.

CONCLUSIONS

From the above study it can be said that the mass-frequency function for the galactic clusters of stars is in general agreement with the theoretical distribution represented by equation (4). It means probably that these stars of the clusters were born more or less simultaneously.

From these clusters the analytical expression of mass frequency function given by equation (1) does not differ much from that for the solar neighbourhood. The curvature suggests that a parabola is better suited for the representation than the linear relation (5). The study of power law given by (1) and its variation with ages of clusters suggests that the power has got a general tendency to increase as the age of the cluster increases.

REFERENCES

1. Arp, H., and Sandage, A. 1959, *Ap. J.*, 130, 80.
2. Auluck, F. C., and Kothari, D. S. 1954, *Nature*, Vol. 174, 565.
3. Burbidge, E. M., and Sadage, A. 1958, *Ap. J.*, 128, 174.
4. Ferrari d' occieppo, K. 1952, *Mitt. Vienna obs.*, 6, 59.
5. Haffner and Heckmann 1937, Göttingen Veröff, No. 55.
6. Haffner and Heckmann 1940, Göttingen Veröff, No. 66, 67.
7. Heyney, L. G. 1959, *Ap. J.*, 129, 1.
8. Johnson, H. L. and Sandage, A 1955, *Ap. J.*, 121, 616.
9. Johnson, H. L. 1957, *Ap. J.*, 126, 121.
10. Johson, H. L., Wahlquist and Sandage, A. 1956, *Ap. J.*, 124, 81.
11. Johnson, H. L. 1952, *Ap. J.*, 116, 640.
12. Johnson, H. L., and Knuckles, C. F., 1955, *Ap. J.*, 122, 209.
13. Jaschek, C., and Jaschek, M. 1957, *P. A. S. P.*, 69, 33.
14. Kushwaha, R. S. 1957, *Ap. J.*, 125, 242.
15. Mawridis, L. 1956, *Zs. f. Ap.*, 41, 35.
16. Mitchell., R. I., and Johnson, H. L 1958, *Ap. J.*, 128, 31.
17. Petrie, R. M. 1950, *Pub. Dom. Ap. obs.*, Vol. VIII, No. 11.
18. Saltpeter, E. E. 1955, *Ap. J.*, 121, 161.
19. Sandage, A. 1958, *Ap. J.*, 128, 150.
20. Schwarzschild, M. 1958, Structure and Evolution of Stars.
21. Van den Bergh, Sidney 1957, *A. J.*, 62, 100.
22. Walker, M. F. (1955-56), *Ap. J. Suppl.* 2, 365, (No. 23).
23. Walker, M. F. 1957, *Ap. J.*, 125, 636.
24. Walker, M. F. 1958, *Ap. J.*, 128, 562.
25. Walker, M. F. 1959, *Ap. J.*, 130, 57.

PHYSICO-CHEMICAL STUDIES ON THE COMPOSITIONS OF COMPLEX ARSENITE, THIOSULPHATE AND ARSENATE OF METALS

Part 1. Systems $CuSO_4 - NaAsO_2$; (*ii*) $Bi(NO_3)_3 - Na_2S_2O_3$ and (*iii*) $CuSO_4 - Na_3AsO_4$

By

M. S. BHADRAVER *and* J. N. GAUR

Departments of Chemistry, Lohia College, Churu; and University of Rajasthan, Jaipur

[Received on 30th August, 1960]

ABSTRACT

The formation of grassy green coloured compound between $CuSO_4$ and sodium arsenite (pH 9·3) has been reported. The composition of copper arsenite arrived at by conductometric method is $Cu(AsO_2)_2$. It is interesting to note that no complex formation takes place by the interaction of $CuSO_4$ and $NaAsO_2$. The formation of the complex, $Na_3Bi(S_2O_3)_3$ in the molecular ratio of 1:3 ($Bi(NO_3)_3$: $Na_2S_2O_3$ has been confirmed by electrometric titrations between bismuth nitrate and sodium thiosulphate at different concentrations of the reactants both by direct and reverse methods. The composition of the product obtained by the interaction of $CuSO_4$ and Na_3AsO_4, has been investigated by the potentiometric titrations between the reactants. The complex formed can be expressed by the formula $CuKAsO_4$.

A survey of literature shows that great deal of analytical work has been done on the composition of copper arsenite by Stevenhagen, Sharples, Reichard, Simon and C. A. Krauss[1]. In recent years the formation of copper arsenite in aqueous medium was studied by Luchinski and Churlikina[2]. On mixing sodium arsenite and copper sulphate solution, copper arsenite was formed, the composition of which depend on the condition of precipitation. Thus $2CuO, As_2O_3, 2H_2O$ was formed by precipitating from cold solutions, while $CuO, As_2O_3, 2CuO, As_2O_3$ or $3CuO, As_2O_3, 3H_2O$ (depending upon the concentration of $NaAsO_2$) was formed by precipitating from hot solutions. The reaction between CuO and As_2O_3 in aqueous solution proceeds very slowly yielding CuO, As_2O_3 greenish blue powder. L. Malaprade[3] has reported the formation of bismuth thiosulphate and gave the formula of the complex as $Na_3Bi(S_2O_3)_2$, but no systematic physico-chemical methods have been applied for the study of the complex. Analytical study have only been done on the composition of copper arsenate complex. The results of these workers are undecisive and there is no coordination between the various views given so far. Keeping in view the difficulties associated with analytical work *i.e.*, change of composition of the compound during precipitation, laborious technique, uncontrollable factors etc., and to throw more light on the composition of bismuth thiosulphate, copper arsenite and copper arsenate, physico-chemical studies have been adhered to and the results are incorporated in this paper.

EXPERIMENTAL

A. R., B. D. H. samples of $CuSO_4$, $NaAsO_2$, Na_3AsO_4 and $Bi(NO_3)_3$ were used. Solutions were estimated according to standard methods. Sodium arsenate solution was standardised by the method of Williamson[4]. Sodium arsenite solution was estimated as described by Vogel[5].

(*a*) *Conductometric measurements* :

Air free conductivity water was used for the preparation and further dilution of all solutions. The conductance was measured on Kohlrausch Universal Bridge (W. G. Pye Ltd.). The titration cell was immersed in an electrically maintained thermostat. The conductance obtained after each addition was corrected for the dilution effect by multiplying the observed conductance by V/X, where V refers to the total volume of the solution and X ml. is the volume of the reactant already taken in the cell. Titrations were also carried out in varying %age of alcohol upto 30%.

(*b*) *Potentiometric measurements* :

Potentiometric titrations were carried out by using the electrode system:—

Pt | $CuSO_4$ or other solution | KCl | Calomel

E. M. F. of the solutions was measured on Cambridge pH meter. Using different concentrations of the two salts in solution direct and reverse titrations were followed. Curves were plotted between the volume of the titrant and E (obsd.).

(*c*) *Job's method of Continuous Variation* :

Complex forming sytem : Several sets of mixtures containing copper sulphate and sodium arsenite in the ratio of 1:1, 1:2 and 1:3 etc. were prepared. The total volume of the mixtures were kept constant (50 ml.). The difference in conductivities was calculated and the divergencies from the additive values were then plotted as a function of the mixture.. The maxima in the curve show the ratio of the reactants for the formation of the compound in question.

DISCUSSION

The formation of metallic arsenites depends upon the H^+ ion concentration of the medium and is therefore a function of pH.

It is observed that when $CuSO_4$ (pH 5·1) solution is added to sodium meta arsenite solution (pH 9·3) in cold at room temperature, a grassy green precipitate of copper arsenite is formed. It is further observed from conductometric titrations that a sharp break occurs in the molecular ratio of 1:2 of the reactants ($CuSO_4$:$NaAsO_2$). Therefore it can be concluded that the reaction between copper sulphate and meta sodium arsenite occurs in that ratio. It is interesting to note that a maxima is observed in the curves plotted between difference in conductivities and the volume of $CuSO_4$ solution added in c. c.

The electrometric titration curves indicate the formation of the complex, $Na_2Bi(S_2O_3)_3$, the product obtained by the interaction of $Bi(NO_3)_3$ and sodium thiosulphate solution, where the molecular ratio of the reactants is 1 : 3 ($Bi(NO_3)_3$: $Na_2S_2O_3$). Our results are in confirmity of the observations of Malaprade (*loc.cit.*)

The results of potentiometric titrations between copper sulphate and Na_3AsO_4

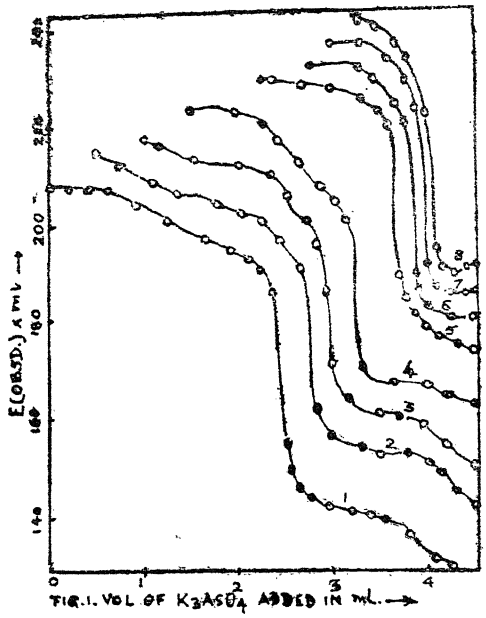

has been represented in (Fig. 1), it is obvious to note from the Fig. 1 that a sharp fall in potential is obtained at the ratio of reactants $CuSO_4$: Na_3AsO_4 as 1:1.

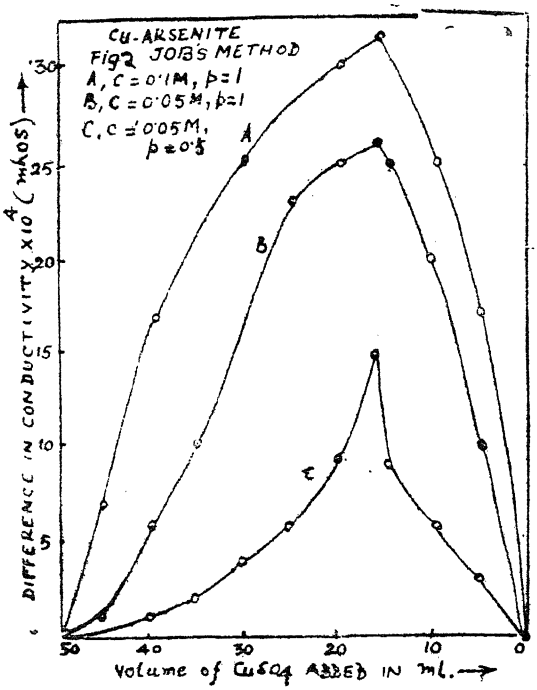

The composition of the complex formed can be best represented by the formula $CuKAsO_4$.

The details will be published elsewhere.

REFERENCES

1. C. A. Krauss, *Vide* Mellor J. W., A Comprehensive Treatise of Inorganic and Theoretical Chemistry, Vol. IX, p. 121 (1952).
2. G. P. Luchinski and V. F. Churilkina, *J. Gen. Chem., U. S. S. R.*, 10, 1425, 31 (1940).
3. L. Malaprade, *Ann. Chim. anal. chim. Appl.*, 22, 5 (1940).
4. Williamson, *J. Soc. Dyers. Col.*, **12**, 86 (1896).
5. Vogel A. I., Quantitative Inorganic Analysis, 2nd Edn. Longmans, p. 342 (1952).

TABLE 2

Nitrification in presence of 5 mg. P

Treatment	pH		Mineral N in mg.				Total N (Mineral + Organic) in mg.
	Initial	Final	NH_3-N	NO_2-N	NO_3-N	Total	
10 mg. N	7·85	7·70	0·812	0·054	1·846	2·712	9·87
20 „ N	7·80	7·60	0 938	0·089	3·541	4·568	19·81
30 „ N	7·85	7·50	1·148	0·092	5·500	6·740	29·82
40 „ N	7·90	7·60	1·666	0·085	3·038	4·789	39·90

A study of the data in Table 2 brings out clearly that an addition of phosphorus resulted in a marked enhancement of nitrification, giving higher amounts of nitrate and other forms of mineral nitrogen than those obtained without P (Table 1). The maximum amount of nitrate nitrogen formed was 5·5 mg. as against only 2·215 mg. in the absence of P at the same level of N. This indicates that phosphorus exerts a beneficial influence on N-availability. In this case also, the level of 30 mg. N per flask produced the highest amount of NO_2-N, NO_3-N and total mineral nitrogen. The low return in mineral nitrogen after 30 mg. N suggests that beyond this level there was an increase in the conversion of mineral nitrogen into microbial tissue. The initial and final pH did not show much difference.

TABLE 3

Nitrification in presence of 10 mg. P

Treatment	pH		Mineral N in mg.				Total N (Mineral + Organic) in mg.
	Initial	Final	NH_3-N	NO_2-N	NO_3-N	Total	
10 mg. N	8·00	7·50	0·910	0·060	3·094	4·064	9·87
20 „ N	7·90	7·55	1·134	0·084	6·358	7·576	20·02
30 „ N	7·85	7·50	1·484	0·110	10 000	11·594	29·99
40 „ N	7·90	7·55	2·296	0·088	4·643	7·027	39·90

The data in Table 3 further demonstrate that the presence of phosphorus has a definite stimulating effect on the process of nitrification. Moreover, there was a corresponding rise in nitrification as the level of P was increased from 5 mg. to 10 mg. per flask. The amount of NO_3-N produced with 30 mg. N in the presence of 5 mg. P per flask was 5·5 mg., whereas it reached a value of 10 mg. in the presence of 10 mg. P. The data also indicate that as compared to the highest amount of NO_3-N the maximum quantities of NH_3-N and NO_2-N were appreciably much less, being only 2·296 mg. and 0·11 mg. respectively. It may be inferred that under favourable conditions the nitrifying organisms convert these forms to NO_3-N at

a rapid rate, allowing little for accumulation. In this series again, the greatest nitrification was noticed at 30 mg. level of N and there was no substantial difference between the initial and final reaction.

TABLE 4

Nitrification in presence of 15 mg. P

Treatment	pH		Mineral N in mg.				Total N (Mineral + Organic) in mg.
	Initial	Final	NH_3-N	NO_2-N	NO_3-N	Total	
10 mg. N	8·10	7·95	0·882	0·052	2·000	2·934	9·84
20 „ N	8·10	7·90	0·986	0·070	4·140	5·196	19·81
30 „ N	8·05	7·75	1·106	0·095	5·857	7·058	29·75
40 „ N	8·15	7·80	2·184	0·083	3·875	6·142	39·90

From a critical scrutiny of the figures given in Table 4 it will be seen that although the presence of phosphorus had promoted nitrification, an increase in its amount from 10 to 15 mg. per flask brought about a significant depression in the formation of NO_3-N. As shown in Table 3, the maximum quantity of NO_3-N formed in the presence of 10 mg. P was as high as 10·0 mg. per flask, but this value fell down to 5·857 mg. when the level of P was increased to 15 mg. Other forms of N also recorded a depression generally. This may be due to toxicity of this higher level of P. Like the previous experiments, best nitrification was recorded at the level of 30 mg. N per flask.

TABLE 5

Nitrification in presence of 20 mg. P

Treatment	pH		Mineral N in mg.				Total N (Mineral + Organic) in mg.
	Initial	Final	NH_3-N	NO_2-N	NO_3-N	Total	
10 mg. N	8·10	7·90	0·868	0·043	1·519	2·430	9·87
20 „ N	8·05	7·90	0·994	0·062	3·375	4·431	19·95
30 „ N	8·10	7·80	1·078	0·078	3·880	5·036	29·99
40 „ N	8·10	7·85	1·834	0·078	2·678	4·590	40·01

A careful perusal of the figures in Table 5 illustrates that an increase in the level of phosphorus from 15 to 20 mg. per flask caused a further reduction in the process of nitrification. The amount of NO_3-N in the presence of 15 mg. P was 5·857 mg. (cf. Table 4), and only 3·88 mg., practically as low as in the absence of P, when the level of phosphorus was raised to 20 mg. per flask. This observation further confirms the toxic effect of higher levels of P on nitrification. The maximum NO_3-N production was noted at 30 mg. level of N in this case as well.

The effect of varying levels of P on nitrification has been represented graphically in figure I, which reveals that the amount of NO_3-N increased with an increase in the level of P from 5 to 10 mg. per flask. An increase beyond this level resulted in pronounced retardation of nitrification, showing 10 mg. P as the optimum level for an efficient nitrification. It also shows that 30 mg. N is the optimum level of N for the same purpose.

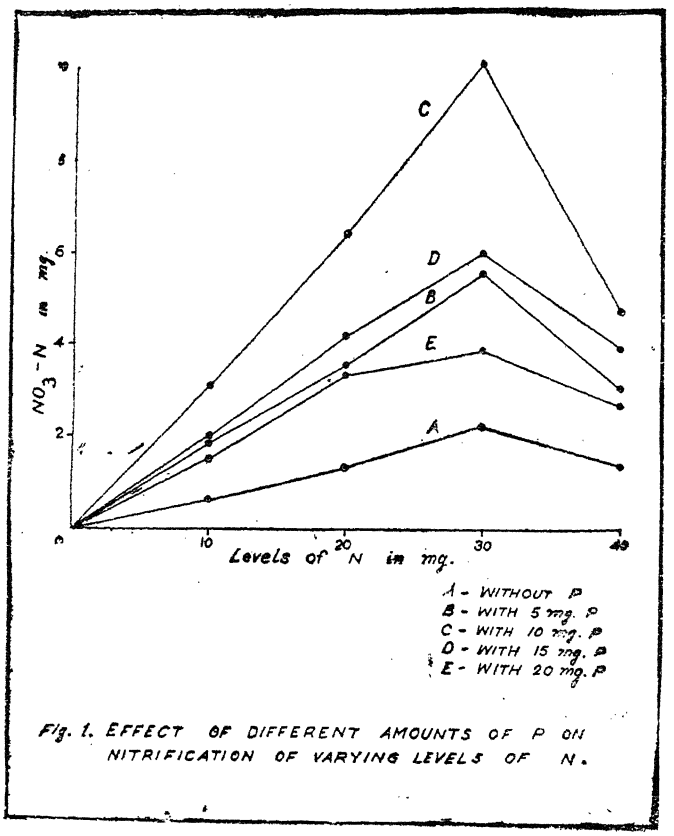

Fig. 1. EFFECT OF DIFFERENT AMOUNTS OF P ON NITRIFICATION OF VARYING LEVELS OF N.

CONCLUSIONS

The results reported in this paper reveal that the addition of phosphorus along with nitrogen enhances the availability of the latter. This may be attributed to the fact that phosphorus is equally essential as nitrogen for the building up of protoplasm and as such, the presence of phosphorus in the medium is conducive to microbial development and activity. On the contrary, a deficiency or complete lack of phosphorus leads to a decrease in the number and activity of these organisms, thereby resulting in poor nitrification. This is in agreement with the observations of Waksman (1927) and Shrikhande (1948). The increase in nitrification was, however, noticed only up to the level of 10 mg. P per flask, and then there was a gradual decrease in the formation of NO_3-N as the level of P was increased to 15 and 20 mg. This shows that the beneficial influence of phosphorus on nitrification is limited to a certain level; the higher levels reflected a toxic effect.

As regards nitrification at the individual levels of nitrogen, a corresponding rise was obtained as the amount of nitrogen added to each flask was increased successively from 10 to 30 mg. But when the amount was increased to 40 mg., a significant diminution in this process was observed. On the other hand, there was a continuous rise in the release of NH_3-N with an increase in the quantity of nitrogen supplied to the medium. Nevertheless, since the amount of NH_3-N was, in general, relatively much smaller, it may be reasonable to conclude that the best nitrification occurred at the level of 30 mg. N. This indicates that both the presence of N and P and their balance are equally important for their mutual absorption. The need of recognizing this fact when applying these fertilizers to the soil particularly in the form of mixtures is, therefore, emphasized. There was no marked difference in the initial and final pH values of the medium, presumably due to the neutralization of the various acids produced during microbial activity by calcium carbonate added in the culture solution.

ACKNOWLEDGEMENT

The author wishes to express his thanks to Dr. J. G. Shrikhande, M.Sc., Ph.D. (Lond), A. R. I. C. for his keen interest during the progress of the investigation.

REFERENCES

1. Breazeale, J. F. (1928). *Tech. Bull. Ariz. agric Exp. Sta.*, **19**, 465.
2. Fred, E. B., and Hart, E. B. (1915). *Univ. Wis. agric. Exp. Sta. Res. Bull.*, 35.
3. Shrikhande, J. G., (1948). *Curr. Sci.*, **17**, 364.
4. Shrikhande, J. G., and Yadav, J. S. P. (1954). *J. Indian Soc. Soil Sci.*, **2**. 115-120.
5. Sircar, S. M. and Sen, N. K. (1941). *Indian J. agric. Sci.*, **II**, 193-204.
6. Waksman, S. A. (1927). Principles of Soil Microbiology. Williams & Wilkins, Baltimore Md. U. S. A.
7. White-Stevens, R. H., and Wessels, P. H. (1944). *J. Amer. Soc. Agron.* **36**.
8. Winogradksy, S. (1904). Lafar's "Handb. techn. mykol". **3**, 132-181 (also Fred, E. B. and Waksman, S. A. 1928, Laboratory Manual of General Microbiology. McGraw-Hill Book Company, Inc. New York, page 22).
9. Yadav, J. S. P., and Shrikhande, J. G. (1955). *Proc. Nat. Acad. Sci.*, (India) 24A, 557.

CHEMISTRY OF VANADIUM : PART VII

VISCOMETRIC STUDIES ON THE FORMATION OF COMPOUNDS OF VCl_3 WITH SOME TRANSITION METAL CHLORIDES IN ABSOLUTE ALCOHOL

By

SARJU PRASAD *and* KAILASH NATH UPADHYAYA

Chemical Laboratories, Banaras Hindu University, Varanasi

[Received on 30th December, 1960]

ABSTRACT

The formation of double compounds of VCl_3 with the chlorides of Fe (ic), Co, Ni, Cu (ic), Zn, Cd and Hg (ic) has been studied viscometrically. These compounds have also been isolated in all the cases except in the case of ferric chloride, their properties studied and structures discussed.

Peterson[1] and Piccini and Giorgis[2] studied the formation of double fluorides of vanadium in trivalent state with monovalent and divalent cations. With alkali metals the compounds of the type $M_3[VF_6]$ anhydrous or $M_2[VF_5H_2O]$ or $M[VF_4.2H_2O]$ and with divalent metals (Co, Ni, Zn or Cd) of the type $M''[VF_5.H_2O].6H_2O$ or formed. Stahler[3] prepared complex chlorides of vanadium by concentrating VCl_3 and alkali metal chlorides saturated with HCl which are all of the type $VCl_3.2MCl,H_2O$ (M = alkali metal). Lock and Edward[4] obtained $KVCl_4$ from a mixture of VCl_3 and KCl dissolved in HCl.

A careful review of the literature shows that the formation of double chlorides of VCl_3 with any transition metal chlorides has not been studied. The present work was therefore, undertaken with a view to studying the formation of these compounds viscometrically and also by isolating them wherever possible.

ANALYTICAL

Vanadium was estimated in dil. H_2SO_4 solution by reduction with SO_2, removal of SO_2 by CO_2 and titrating against standard $KMnO_4$ at 70°C, Fe as Fe_2O_3, Co as pyridine complex, Ni as dimethylglyoxime complex, Zn as ZnO, Cd as $CdSO_4$, Hg as HgS and Cu iodometrically.

EXPERIMENTAL

All the chemicals used were of Merck's or B. D. H. extra pure quality and the alcohol was distilled twice over quick lime and finally over anhydrous copper sulphate. VCl_3 was prepared by the method of Weinland and Feige[5], anhydrous zinc and iron chlorides by passing chlorine over heated metal, and anhydrous chlo-

rides of Cu (ic), Cd, Co and Ni by heating the hydrated chlorides either as such or in a current of HCl. These were dissolved in absolute alcohol and the metal and chlorine estimated in a known volume of the solution. The solution then diluted to give 0·1M solution in each case.

The monomeric system was followed in determining the viscosity of the mi ed solutions. Two sets of experiments were carried out. In one quantity of the VCl_3 soln was fixed and that of the other chloride varied and in the second the quantity of the other chloride was fixed and that of VCl_3 varied. The total volume was made upto 50 c.c. with alcohol in each case. Viscosities of different compositions were plotted against the volume of the chloride solutions whose volume was varied as shown in figs. 1 and 2.

FIG 1

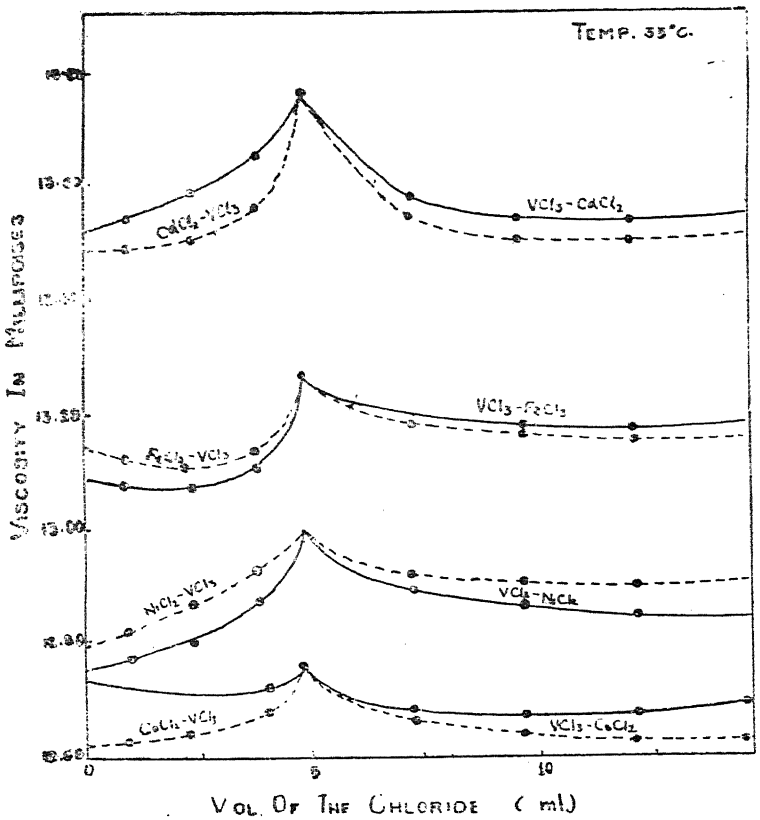

The mixture of solutions corresponding to the peak observed in the graphs was concentrated and the compound crystallised in vacuum. It was dried over freshly fused $CaCl_2$ in a vacuum desiccator and analysed. The results are given in the Table.

TABLE

Formation of compounds of VCl_3 with some transition metal chlorides in abs. alcohol

S No.	Chlorides	Colour of the compounds	Vanadium %		Other Metal %		Chlorine %		Org. matter %		Probable formulae
			obs.	calc.	obs.	calc.	obs.	calc.	obs.	calc.	
1.	$CoCl_2$	bluish green	15·02	15·26	17·80	17·65	53·00	53·16	14·18	13·78	CO $[VCl_5C_2H_5OH]$
2.	$NiCl_2$	dark green	15·01	15·30	17·72	17·62	52·92	53·28	14·35	13·81	Ni $[VCl_5C_2H_5OH]$
3.	$CuCl_2$	greyish blue	15·38	15·08	18·50	18·80	52·85	52·52	13·27	13·61	Cu $[VCl_5C_2H_5OH]$
4.	$ZnCl_2$	greyish white	15·19	14·99	19·12	19·24	52·70	52·24	12·99	13·53	Zn $[VCl_5C_2H_5OH]$
5.	$CdCl_2$	greyish green	13·28	13·17	28·89	29·06	45·36	45·88	12·47	11·90	Cd $[VCl_5C_2H_5OH]$
6.	$HgCl_2$	greyish black	10·24	10·73	42·38	42·23	37·60	37·37	9·78	9·68	Hg $[VCl_5C_2H_5OH]$

Fig. 2

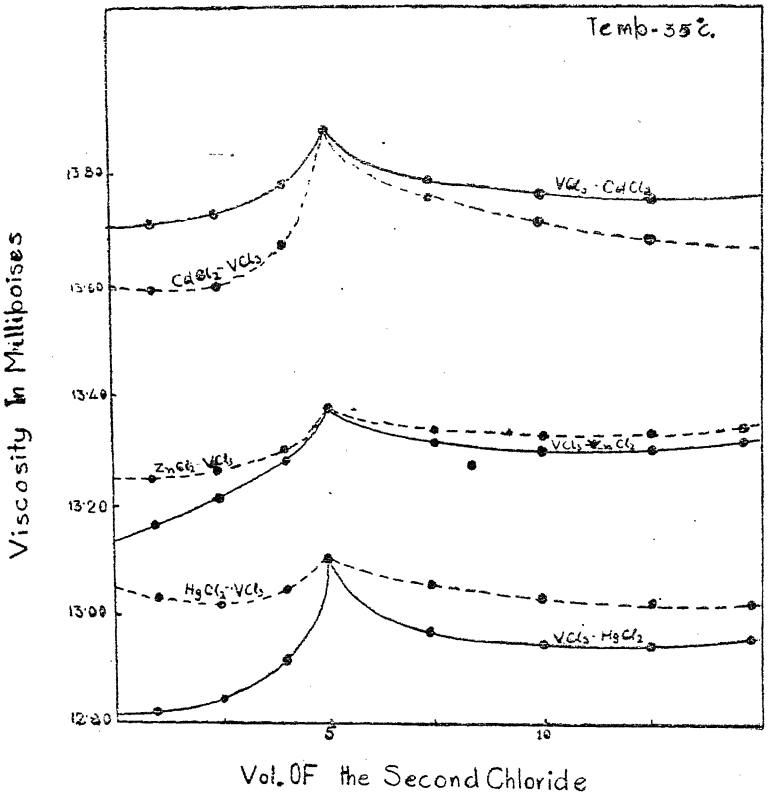

DISCUSSION

The analysis of the compounds shows that one molecule of alcohol is always present in all the compounds isolated and any attempt to expel this resulted in the decomposition of the compound. All the compounds are coloured, crystalline and hygroscopic and are easily hydrolysed by water, dilute acid and alkali solutions. They are soluble in alcohol, ethyl-acetate or acetone but insoluble in benzene, toluene, carbon tetrachloride or ether. When heated they decompose below 200°C.

An examination of the viscosity-concentration curves in both the set of experiments shows that the maxima are obtained at 1 : 1 proportion of VCl_3 to the metal chloride in each case, which indicates the formation of complex compounds at this composition. It is further confirmed by the isolation of these compounds in all the cases except ferric chloride, with which a pure compound was not obtained. On the basis of the results of the viscosity measurements and the analysis these compounds may be represented as M'' $[VCl_5C_2H_5OH]$.

ACKNOWLEDGEMENT

The authors' sincere thanks are due to the authorities of the Banaras Hindu Uuiversity for providing facilities.

REFERENCES

1. E. Peterson : *Ber.*, **21**, 3257 (1888); *J. prakt. Chem.*, **2**, 40, 44, 194, 271 (1889).
2. A. Piccini and G. Giorgis : *Gazz.*, **1**, 55 (1892).
3. A Stahler : *Ber.*, **37**, 4405 (1904).
4. J. Lock and G. H. Edward : *Am. Chem. Journ.*, **20**, 594 (1898).
5. R. F. Weinland and C. Feige : *Ber.*, **36**, 352 (1903).

POTENTIOMETRIC STUDIES ON THE OXALATO-COMPLEXES OF TITANIUM (IV)

By

SARJU PRASAD *and* JAIBENI PRASAD TRIPATHI

Chemical Laboratories, Banaras Hindu University, Varanasi

[Received on 30th December, 1960]

ABSTRACT

A systematic study on the formation of complex-compounds when a solution of titanium tetrachloride in HCl is treated with an aqueous solution of oxalic acid, sodium, potassium or ammonium oxalate has been carried out potentiometrically and results show the existence of several complex compounds in each system.

A series of complex titanyloxalates such as $K_2[O{=}Ti\ Ox_2].2H_2O$ have been reported by Pechard[1] Spence, Wrigley and Spence and Sons[2] prepared titanium oxalate by heating a mixture of titanium sulphate and alkali oxalate or titanium alkali sulphate with oxalic acid. Peter Spence & Sons Ltd.[3] obtained a precipitate of basic titanium oxalate by mixing Ti(IV) in mineral acids and solutions of oxalic acid, alkali or alkaline earth oxalates under suitable conditions, the presence of chloride ions gives a purer pruduct. Besides, Raman spectra and polarographic study also indicate the existence of the oxalato-complexes of titanium. Gupta[4] has studied the mode of vibration of the $C_2O_4^{--}$ions and obtained certain Raman shifts for potassium titanium oxalate. Pecsok[5] has investigated polarographic waves of Ti (IV) in $H_2C_2O_4$ solution at pH less than 3 and established the existence of oxalato-Ti (IV) ion.

The present work constitutes a study of the complex compounds formed between titanium tetrachloride with oxalic acid, sodium, potassium or ammonium oxalate.

EXPERIMENTAL

The chemicals used were of Merck's or B. D. H. Extra Pure quality and titanium tetrachloride was prepared by the method of Biltz, Sapper, and Wunneberg[6], and extracted with 2N HCl. The aqueous solutions of oxalic acid, and sodium, potassium or ammonium oxalate of 0·20M and 0·25M and titanic chloride in 0·5N HCl of 0·1M were prepared. The following cell is formed using saturated calomel as reference electrode and the metallic titanium or bright platinum wire as indicator electrode.

Ti or Pt	$TiCl_4$ 0·5N HCl	KCl (Sat.)	Hg_2Cl_2,KCl (Sat.)	Hg.

The potentials were measured by Pye model potentiometer and a sensitive mirror galvanometer was used to determine the null point.

10 c.c. of titanic chloride solution were taken in the titrating vessel, stirred well for about 10 – 15 mins. and the relative voltage (E) of the above cell was

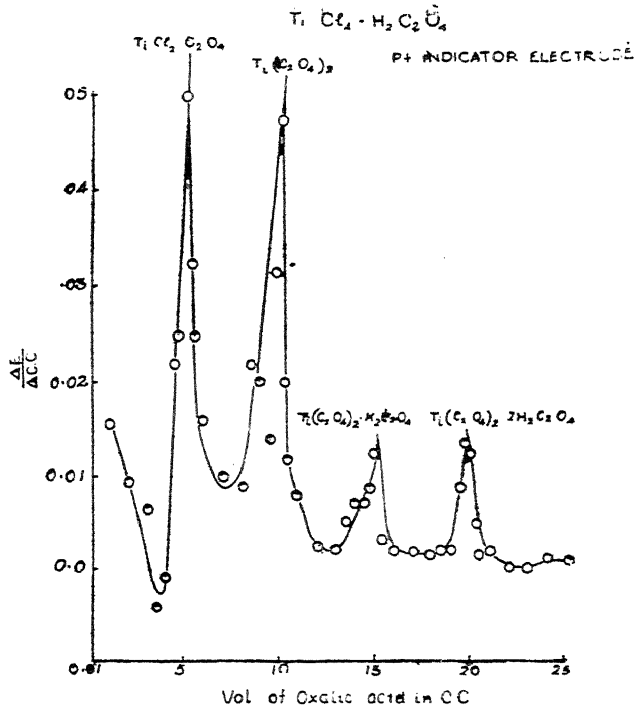
Ti Cl4 - H2 C2 O4
Pt INDICATOR ELECTRODE
Ti Cl2 C2 O4
Ti (C2 O4)2
Ti(C2 O4)2 H2 C2 O4
Ti(C2 O4)2 2H2 C2 O4
ΔE/ΔCC
0.5
0.4
0.3
0.2
0.1
0.0
0.01
5
10
15
20
25
Vol of Oxalic acid in CC

FIG. 1

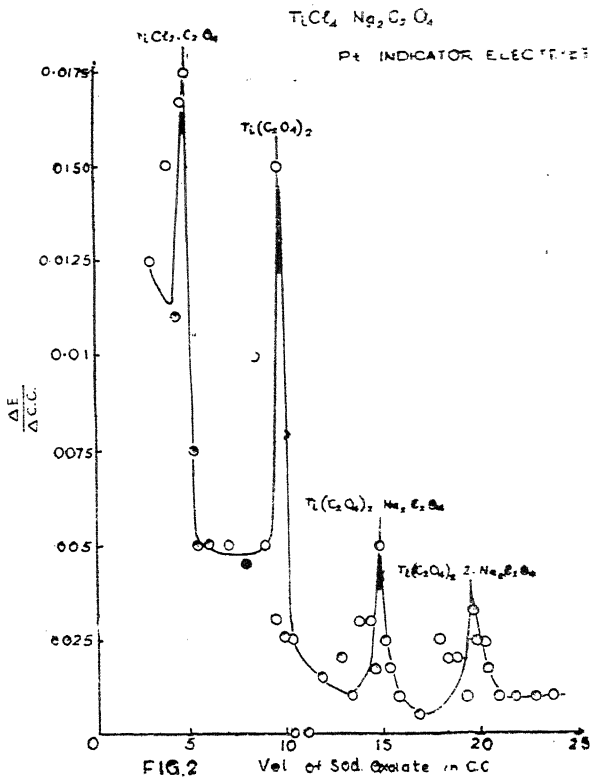
Ti Cl4 Na2 C2 O4
Pt INDICATOR ELECTRODE
Ti Cl2 . C2 O4
Ti(C2O4)2
Ti(C2O4)2 Na2 C2 O4
Ti(C2O4)2 2 Na2 C2 O4
ΔE/ΔCC
0.0175
0.015
0.0125
0.01
0.0075
0.005
0.0025
0
5
10
15
20
25
Vol of Sod. Oxalate in CC

FIG. 2

$Ti\,Cl_4$ $K_2C_2O_4$

Pt INDICATOR ELECTRODE

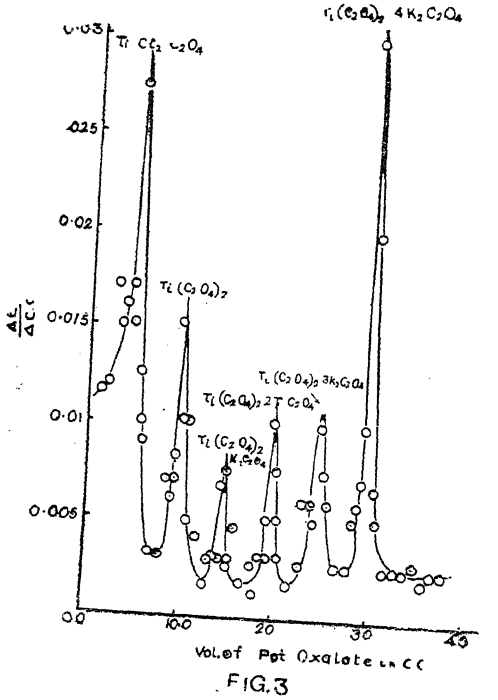

FIG. 3

$Ti\,Cl_4$-$(NH_4)_2C_2O_4$

Pt INDICATOR ELECTRODE

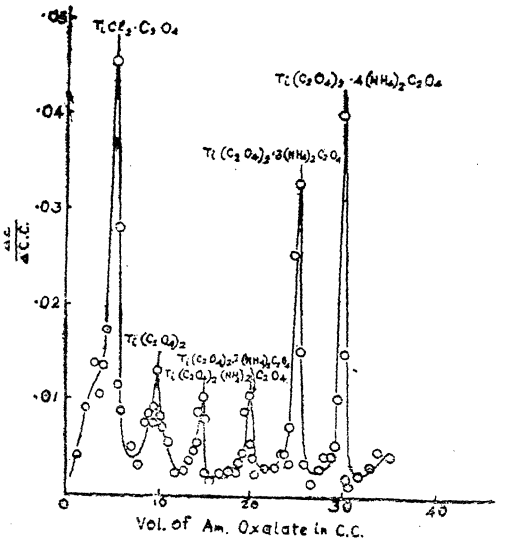

Fig. 4

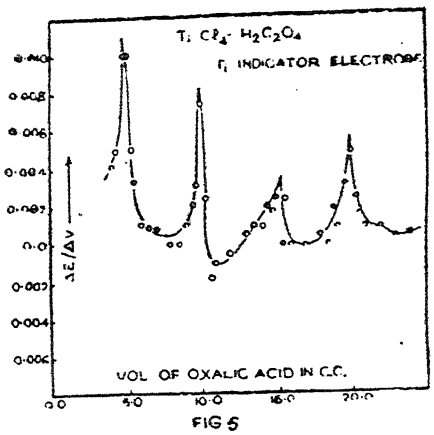

FIG 5

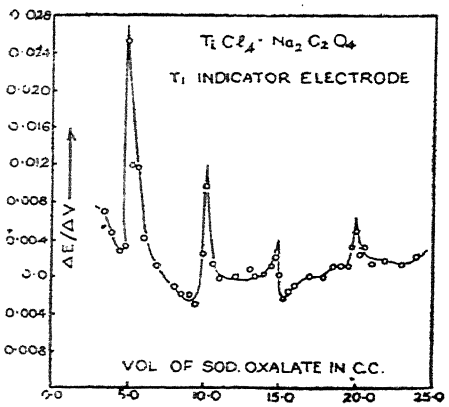

FIG.6

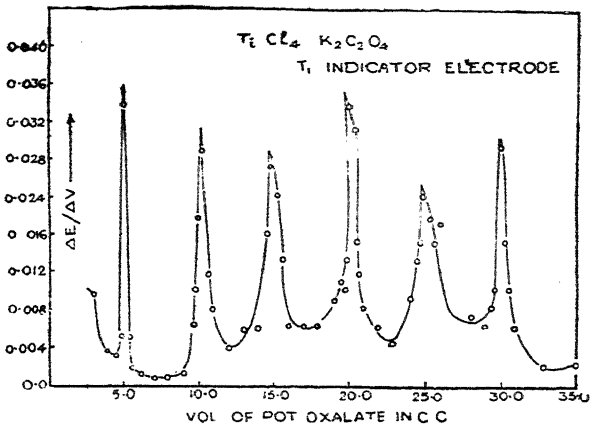

FIG.7

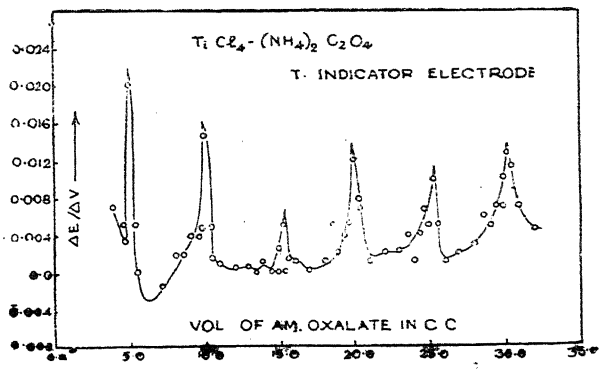

FIG.8

determined at the room temperature by balancing it against an accumulator cell. The oxalate solution was then added from the burette, stirred well for a few mins. and the voltage was determined. The $\triangle E/\triangle$ c.c. values were calculated at each volume and the graph $\triangle E/\triangle$ c.c. against the volume of oxalate solution in c.c. was drawn. The breaks in the curves correspond to complex compounds of compositions indicated by the volume of the oxalate solution added.

DISCUSSION

Figs. 1-4 and 5-8 in which the indicator electrodes were Pt and Ti metal respectively indicate the existence of four well-marked maxima corresponding to the molar proportions of titanium tetrachloride and the oxalates 1:1, 1:2; 1:3 and 1:4. Though the breaks occur at the same point in both the cases yet the peaks obtained with bright Pt are higher than those with Ti., the first two (1:1 and 1:2) may be explained by the assumption of two stage ionization of the former :

$$TiCl_4 \rightleftharpoons TiCl_2^{++} + 2Cl^-$$

$$TiCl_2^{++} \rightleftharpoons Ti^{++++} + 2Cl^-.$$

On further addition of the oxalate solutions, $[Ti.\ 3C_2O_4]^{--}$ and $[Ti.\ 4C_2O_4]^{----}$ radicals are formed, which are defined by the third and fourth breaks in the curves. The overall results correspond to the formation of the following four compounds in all the cases :

$TiCl_2.\ C_2O_4$; $Ti\ (C_2O_4)_2$;

$Ti\ (C_2O_4)_2.M_2\ C_2O_4$ or $M_2\ \frac{1}{4}[Ti\ (C_2O_4)_3]$

$Ti\ (C_2O_4)_2.2M_2\ C_2O_4$ or $M_4\ [Ti\ (C_2O_4)_4]$

where M denotes hydrogen, sodium, potassium or ammonium ion, but with potassium and ammonium oxalates two more maxima corresponding to the molar proportion of titanic chloride and potassium or ammonium oxalate 1:5 and 1:6 are obtained (vide figs. 3 and 4, 7 and 8). Those compounds may be represented as:

$$Ti\ (C_2O_4)_2.\ 3M_2C_2O_4$$

$$Ti\ (C_2O_4)_2.\ 4M_2C_2O_4.$$

ACKNOWLEDGEMENT

The authors' sincere thanks are due to the authorities of the Banaras Hindu University for providing facilities.

REFERENCES

1. Pechard, E., *C. R.* **116**, 1513 (1893).
2. Spence, H., Wrigley, H. and Spence and Sons, Brit., Nov. 26, 1914, 23089.
3. Peter Spence & Sons Ltd., Fr April 14, 1932.
4. Gupta. J., *Indian J. Phys.*, **10**, 465 (1936).
5. Peesok, Robert, L., *J. Am. Chem. Soc.*, **73** 1304 (1951).
6. Biltz, W., Sapper, A and Wunneberg, E., *Z. anorg. Chem.*, **203**, 277 (1932).

CHEMISTRY OF VANADIUM PART–VIII

VISCOMETRIC STUDIES ON THE FORMATION OF COMPOUNDS OF VCl_3 WITH PHENOLS IN ABSOLUTE ALCOHOL

By

SARJU PRASAD *and* KAILASH NATH UPADHYAYA

Chemical Laboratories, Banaras Hindu University, Varanasi

[Received on 30th December, 1950]

ABSTRACT

Viscometric measurements of the systems VCl_3-Phenols in abs. alcohol have been carried out. The results indicated by the viscosity- composition curves have been interpreted for the formation of compounds.

Vanadium trichloride is known to form 'ato' type complexes with phenols Sidgwick[1] has reported that grassgreen crystals of the composition $(NH_4)_3[V(C_6H_4O_2)_3].2H_2O$ are separated when a concentrated solution of VCl_3 is treated with catechol and ammonia is added. Many other phenolic compounds of vanadium in higher valency states are known which are all oxycompounds and mainly of the chelate type.

A review of the literature shows that the action of vanadium trichloride on pure phenols in organic solvents has not been studied either by analytical or by physicochemical methods. The present work was, therefore, undertaken with a view to studying the formation of compounds of VCl_3 and phenols in absolute alcohol by viscometric method.

EXPERIMENTAL

All the chemicals used were of Merck's or B. D. H. extra pure quality and the alcohol was distilled twice over quick lime and finally over anhydrous copper sulphate. VCl_3 was prepared by the method of Weinland and Feige[2], and dissolved in absolute alcohol and vanadium and chlorine estimated in a known volume of the solution. It was then diluted to give 0·1M solution. The phenol solutions of the same strength were also prepared in absolute alcohol in each case.

The monomeric system was followed in determining the viscosity of the mixed solutions. The quantity of the VCl_3 solution was fixed and that of phenol varied and the total volume was made upto 50 c. c. with alcohol in each case.

Viscosities of different compositions were plotted against the volume of the phenol solution (*cf.* Fig. 1 & II).

FIG. 1

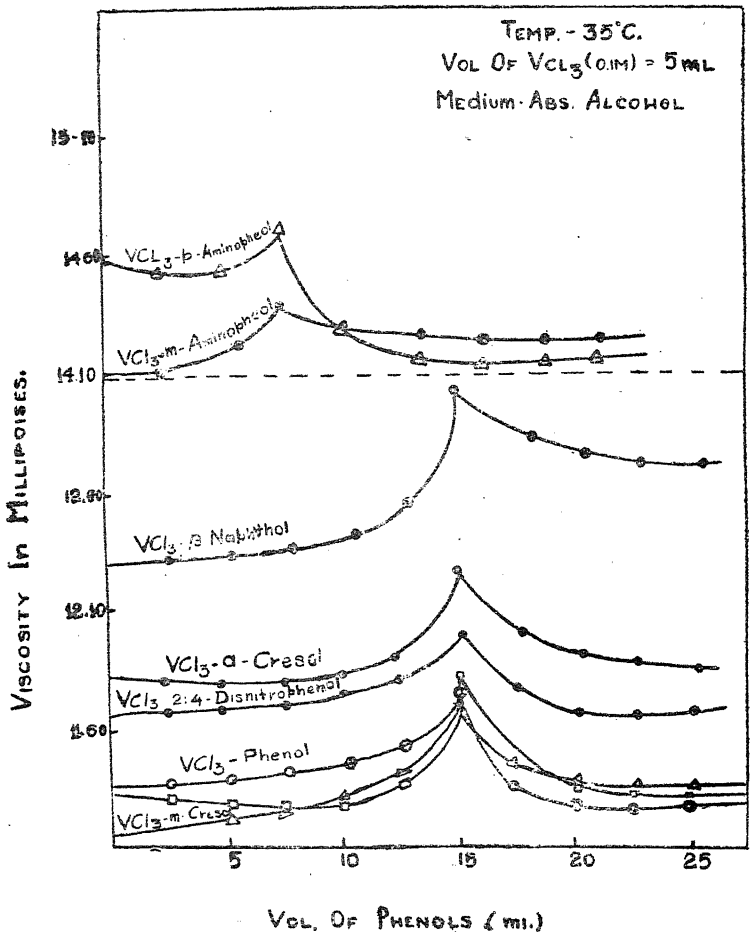

DISCUSSION

From the viscosity-composition curves it is evident that a distinct peak is obtained in each case, which indicates the formation of complex compounds. With nitrophenols and monohydroxy phenols it is obtained at 1 : 3 ratio of VCl_3 to phenol and with amino and polyhydroxy phenols except catechol at 2:3. In the case of catechol it is obtained at 1:1. It appears that the union of VCl_3 and phenol is

taking place in solution by coordination, the oxygen of phenolic OH group and N of NH_2 group serving as donor and vanadium as acceptor. The nitro group,

FIG. 2

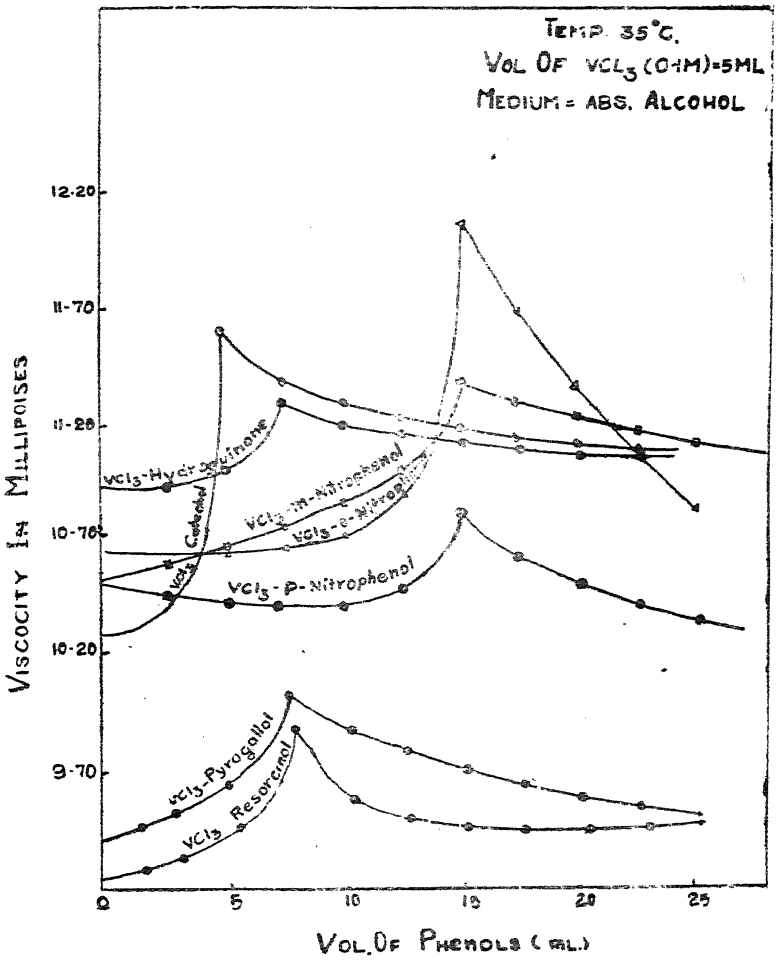

however, shows no tendency for coordination. On the basis of the above observations, these compounds may be assigned the following structures :

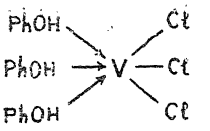

in the case of monohydroxy or nitrophenols,

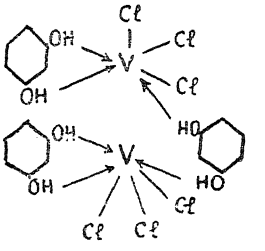

in the case of resorcinol

and

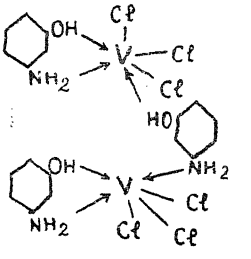

in the case of m-aminophenol

Attempts were made to confirm these results by isolating the compounds but it was not successful.

The authors' sincere thanks are due to the authorities of the Banaras Hindu University for providing facilities.

REFERENCES

1. N. V. Sidgwick : Chemical Elements and Their Compounds, London, Vol. I, 831 (1950).
2. R. F. Weinland and C. Feige : *Ber*, **36**, 352 (1903).

STUDY OF THE V^{IV} PRECIPITATES BY PHYSICO-CHEMICAL METHODS

PART I: ELECTROMETRIC STUDY OF VANADYL FERROCYANIDE

By

P. K. BHATTACHARYA *and* S. N. BANERJI

University of Saugor, Saugor (M. P.)

[Received on 8th Januar., 1961]

ABSTRACT

The reaction between vanadyl sulphate and potassium ferrocyanide has been studied by the application of monovariation methods in two ways. In the first case the volume of vanadyl sulphate was kept constant and that of equimolar potassium ferrocyanide varied. In the latter case the volume of potassium ferrocyanide was kept constart varying that of equimolar vanadyl sulphate.

Electrometric measurements were carried on using M/40 and M/60 solutions each of vanadyl sulphat and potassium ferrocyanide. The experimental curves in both the cases indicated a break nearly corresponding to the formation of vanadyl ferrocyanide $(VO)_2$ [Fe (CN,]. It was, however, seen that the equivalence point does not exactly correspond with the theoretical values of the solutions required. In the first case the volume of the solution required is slightly less and in the second case slightly more than the theoretical values.

The experiments, when repeated in presence of 10% and 20% alcohol, show that the volumes of solutions required gradually approch the theoretical values. It is clear, therefore, that the discrepancy between the observed and theoritical values is due to (*i*) the greater adsorption of VO^{++} ions by vanadyl ferrocyanide and (*ii*) its hydrolysis.

Attempts to study the applicability of potassium ferrocy anide as a gravimetric reagent have led to the investigation of its reactions with several common metal salts by analytical and physico-chemical methods. Bhattacharya and co-workers[1-5] have studied a number of common metal ferrocyanides. However, except with thallium[6], uranium[7] and thorium[8] not much work has been done towords the study of the ferrocyanides of rarer elements. There is no account in literature about the nature of vanadium ferrocyanide. It was, therefore, thought worthwhile to take up the conductometric and pH study of the reaction between vanadyl sulphate and potassium ferrocyanide.

EXPERIMENTAL

Solutions of vanadyl sulphate (B.D.H.) and B. D. H. Analar sample of potassium ferrocyanide respectively in conductivity water were used for the experiments. The conductance measurements were done with a Doran Conductivity Bridge, while a Beckman glass-electrode pH-meter, model H/2 was used for pH measurements.

Vanadyl sulphate and potassium ferrocyanide when mixed up in solution yield a yellowish precipitate. Monovariation method[9] was taken recourse to in order to determine the composition of the vanadyl ferrocyanide formed. The method was applied in two ways. In the first case, the volume of vanadyl sulphate (M/40) was kept constant (8 ml.) and the volume of potassium ferrocyanide (M/40) was varied still maintaining the total volume constant (20 ml.) by the addition of conductivity water. In the second case, the process was reversed by keeping the volume of $K_4Fe(CN)_6$ (M/40) constant (2 ml.) varying that of vanadyl sulphate of the same strength. Similar sets were prepared taking M/80 solutions. The conductance and pH measurements were carried out as usual. The experiments were repeated with 10% and 20% alcoholic solutions in the case of M/40 vanadyl sulphate and potassium ferrocyanide. A break is seen in the curves obtained by conductivity (fig. 1, 3, 5 and 7 curves A and B) and pH measurement (figs. 2, 4, 6, and 8 curves A and B) showing the formation of vanadyl ferrocyanide at that point.

DISCUSSION

It is seen that in the first case when the volume of vanadyl sulphate is kept constant (8 ml.) the curves exhibit a break corresponding to nearly 4 ml. of potassium ferrocyanide solution. In the second case also the break is obtained at about 4 ml. of vanadyl sulphate solution for a constant volume (2 ml.) of potassium ferrocyanide solution. These values nearly correspond to the theoretical amounts of $K_4Fe(CN)_6$ and $VOSO_4$ required for the formation of the compound $(VO)_2[Fe(CN)]_6$ according to the following equation:

$$2VOSO_4 + K_4Fe(CN)_6 = (VO)_2[Fe(CN)_6] + 2K_2SO_4$$

The possibility of the formation of $K_2VO[Fe(CN)_6]$ is thus ruled out. The slight increase in the conductance (fig. 1) in the beginning on the addition of potassium ferrocyanide to a constant volume of vanadyl sulphate is due to the replacement of VO^{++} ions by the relatively fast moving K^+ ions, till the attainment of the equivalence point. After this no more of vanadyl sulphate is left for being precipitated with potassium ferrocyanide and the whole of the potassium ferrocyanide added contributes to the conductance of the system resulting in a sharp rise.

The second case can be explained similarly. The conductance (fig. 3) increases till the equivalence point due to the replacement of $Fe(CN)_6^{4-}$ ions by the less mobile SO_4^{--} ions. A sharp increase in the conductivity, observed later, results from the addition of excess of vanadyl sulphate.

The pH of the system in the first case (fig. 2) undergoes a slight increase in the initial stages due to the neutralization of the free acid from the vanadyl sulphate by the alkali obtained from potassium ferrocyanide. The equivalence point where the whole of vanadyl sulphate is used up is indicated by the inflexion in the curve.

Addition of excess of potassium ferrocyanide causes a smooth increase in the pH of the system due to the basic nature of the added substance.

The pH of the mixture in the second case (fig. 4) first shows a slight decrease till the equivalence point due to the neutralization of the alkali from potassium ferrocyanide by the acid from vanadyl sulphate. Further decrease in pH after the equivalence point is attributed to addition of excess of acid salt vanadyl sulphate.

The amounts of solutions required however, do not exactly correspond with the theoretical values. It will be evident from the curves (fig. 1 and 2, curves A

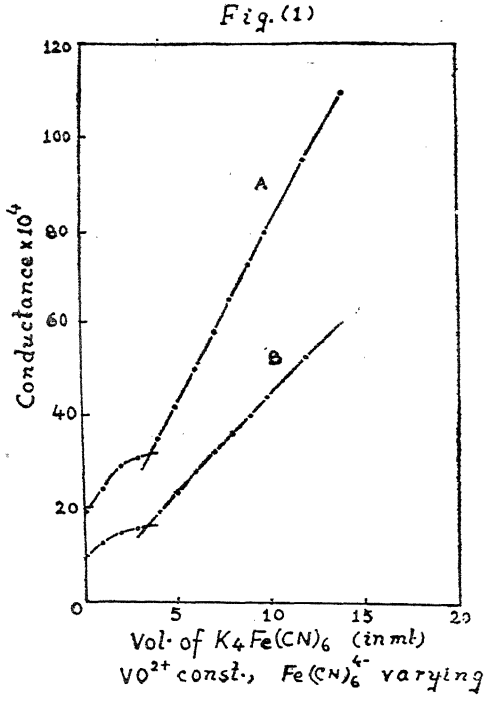

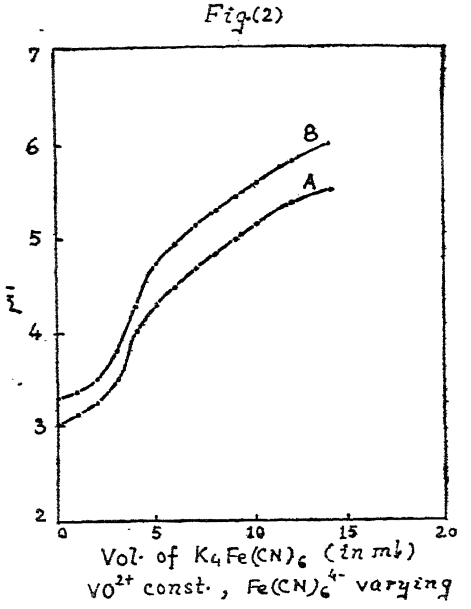

and B) that the volume of $K_4Fe(CN)_6$ required is slightly lower than the theoretical value. The curves (fig. 3 & 4, curves A and B), on the other hand, reveal that the volume of $VOSO_4$ sufficient for the formation of vanadyl ferrocyanide is a little more than the theoretical value. To explain this shift from the theoretical values, experiments with alcoholic solutions were carried out. A study of the curves with 10% (figs 5, 6, 7, & 8 curves A) and 20% alcoholic solutions (fig. 5, 6, 7, 8 curves B) respectively shows that the volumes of solutions required, gradually approach the theoritical value.

Fig.(3)

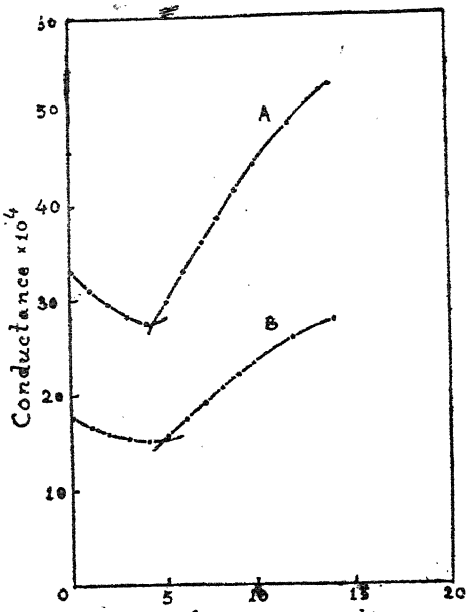

Fig.(4)

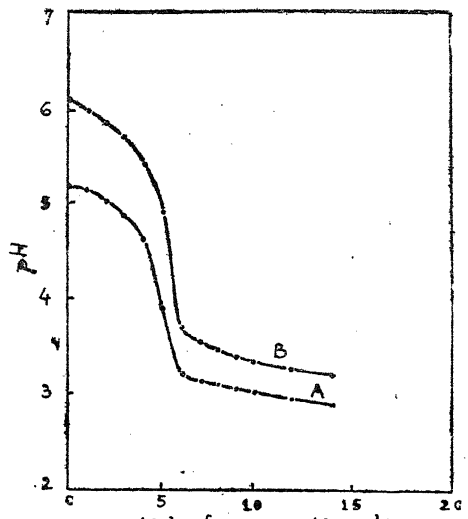

Fig.(5)

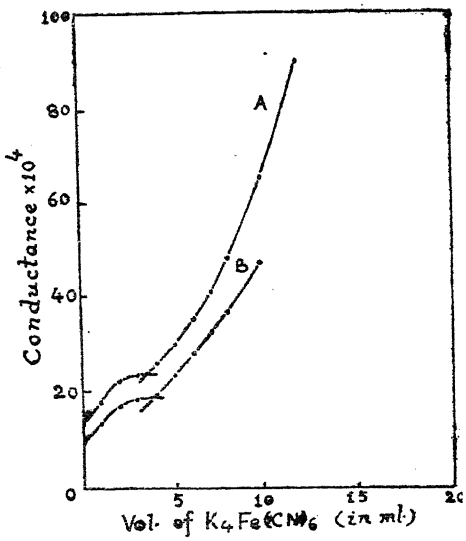

curve A: 10% alcohol
curve B: 20% alcohol

Fig.(6)

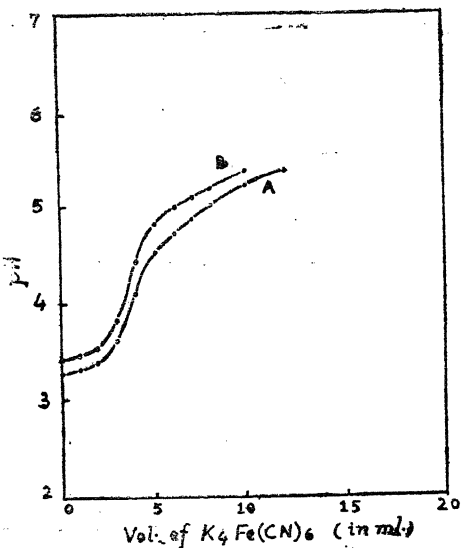

curve A: 10% alcohol
curve B: 20% alcohol

The discrepancy between the observed and theoretical values in aqueous medium and the subsequent agreement between the two values in partially alcoholic solutions, are in conformity with the results obtained by earlier workers (*loc. cit.*) on metallic ferrocyanides.

Fig. (7)

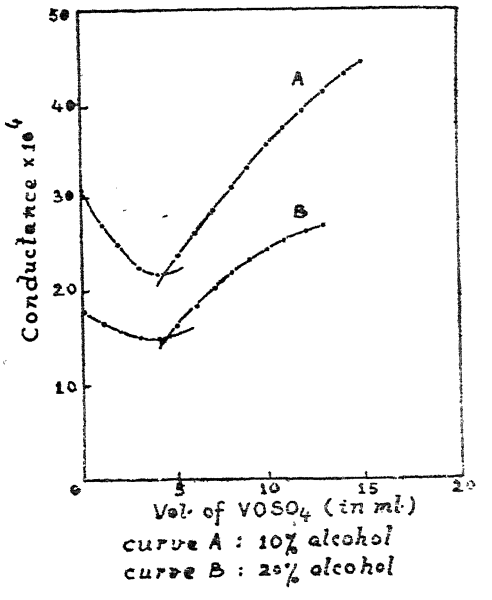

Fig. (8)

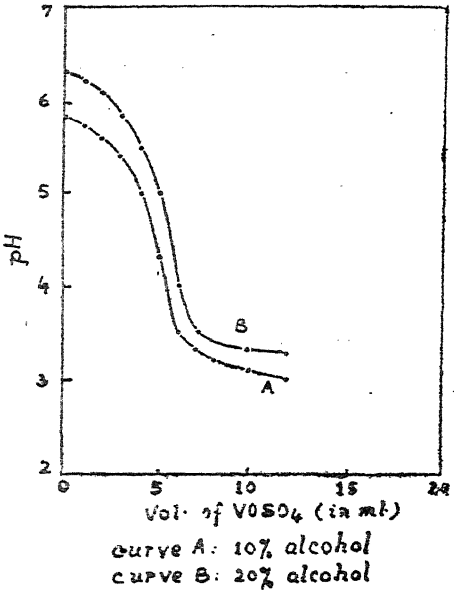

The reason for the discrepancy can be sought in the greater adsorption of the cation VO^{++} than that of $[Fe(CN)_6]^{4-}$ by vanadyl ferrocyanide and its probable hydrolysis in aqueous solution. The settling down of the vanadyl ferrocianide in solutions with excess of vanadyl ion indicates that there is relatively more adsorption of VO^{++} ions when $K_4Fe(CN)_6$ is added to vanadyl sulphate solution. There is, therefore, a decrease in the number of VO^{++} ions available for reaction with $K_4Fe(CN)_6$ and consequently the volume of $K_4Fe(CN)_6$ required for precipitation is less than the theoretical value. Due to the same reason the amount of vanadyl sulphate required is more when it is added to $K_4Fe(CN)_6$ solution. An extra amount of vanadyl sulphate is utilized for providing the adsorbed VO^{++} ions.

The results with alcoholic solutions indicate the possibility of hydrolysis of vanadyl ferrocyanide in aqueous medium to yield $[Fe(CN)_6]^{4-}$ resulting in the requirement of less $K_4Fe(CN)_6$ in the first case and more vanadyl sulphate in the second. In alcoholic solutions the hydrolysis and adsorption are suppressed, as a result of which the volumes of solutions required approach the theoretical values.

Studies on the adsorption and the quantitative nature of vanadyl ferrocyanide are in progress.

The authors express their thanks to Prof. A. K. Bhattacharya, Head of the Chemistry Department, University of Saugar, for his keen interest in the work.

REFERENCES

1. Bhattacharya and Saxena, *J. Ind. Chem. Soc.* **28**, 141 (1951)
2. Saxena, *J. Ind. Chem. Soc.*, **34**, 471 (1957)
3. Bhattacharya, and Gaur, *J. Ind. Chem. Soc.*, **28**, 473 (1951)
4. Bhattacharya and Saxena, *J. Ind. Chem. Soc.*, **29**, 284 (1952)
5. Bhattacharya and Gaur, *J. Ind. Chem. Soc.*, **24**, 487 (1947)
6. Fischer and Benzian, *Chem. Z.*, **26**, 49 (1902)
7. Andanasium, *Bul. Soc. romana, stiinte*, **30**, 69 (1928)
8. Bhattacharya and Gaur, *J. Ind. Chem. Soc.*, **31**, 467 (1954)
9. Nayar and Pandey, *Proc. Ind. Acad. Sci.* **27A**, 284 (1948)

A STUDY OF THE V^{IV} PRECIPITATES BY PHYSICO-CHEMICAL METHODS

PART II : ELECTROMETRIC STUDY OF VANADYL FERRICYANIDE

By

P. K. BHATTACHARYA *and* S. N. BANERJI

Department of Chemistry, University of Saugar, Saugor, M. P.

[Received on 8th January, 1961]

ABSTRACT

The precipitation of vanadyl ferricyanide has been studied electrometrically by means of Monovariation method in two ways (*i*) taking constant volume of vanadyl sulphate and varying that of equimolar potassium ferricyanide and (*ii*) vice versa.

The electrometric measurement data in case of M/40 and M/60 solutions, when plotted indicated the formation of vanadyl ferricyanide $(VO)K[Fe(CN)_6]$. It was however, seen that in the first case the volume of $K_3Fe(CN)_6$ required is less than the equimolar vanadyl sulphate, whereas in the second case the volume of vanadyl sulphate required is more.

The above experiments, when performed in presence of 10% and 20% alcohol bring a better agreement between the theoretical and observed values, showing thereby that the discrepancy may be due to the greater adsorption of VO^{**} ions by vanadyl ferricyanide and its hydrolysis to liberate $[Fe(CN)_6]^{3-}$ ions.

In part I of this series, we have studied the precipitation of vanadyl ferrocyanide electrometrically. We are reporting, here, the results of our observations with the system $VOSO_4$—$K_3Fe(CN)_6$ by conductometric and pH methods. Bhattacharya and co-workers have applied physico-chemical methods to investigate the ferricyanides of Ferrous[1], Ferric[2], Mercury[3], Cobalt[4], Zinc[5] Copper[6] and Cadmium[7]. Uranyl[8] salts have been shown to yield insoluble ferricyanide with $K_3Fe(CN)_6$. It seems no work has so far been done with vanadium salts and potassium ferricyanide.

EXPERIMENTAL

A gelatinous yellowish green precipitate is seen to be formed when a solution of potassium ferricyanide is added to vanadyl sulphate solution. Analysed samples of vanadyl sulphate and potassium ferricyanide were taken and conductometric and pH measurements were carried on with their solutions in conductivity water. Instead of using the method of direct titration, Monovariation method[9] has been utilized, by first keeping the volume of vanadyl sulphate constant (6 ml.) and varying that of equimolar potassium ferricyanide solution and next keeping the volume of $K_3Fe(CN)_6$ constant (5 ml.) altering that of equimolar vanadyl sulphate. The total volume was kept constant (20 ml.) in both the cases.

The results of the conductivity and pH measurements with M/40 and M/60 solutions have been plotted in figs. 1, 2, 3, 4, curves A and B. The results with

Fig. (1)

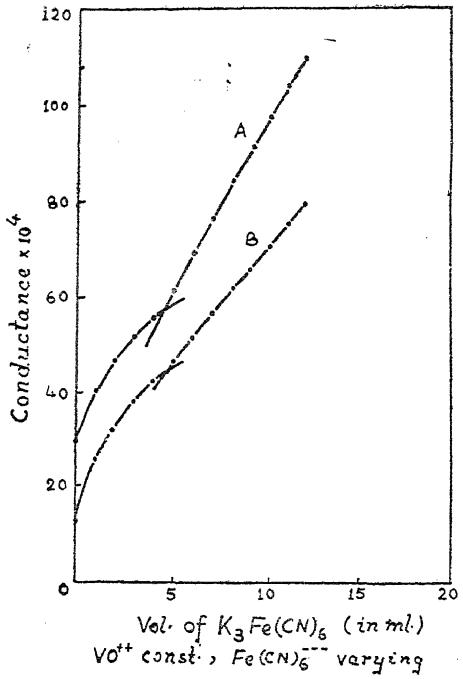

Fig. (2)

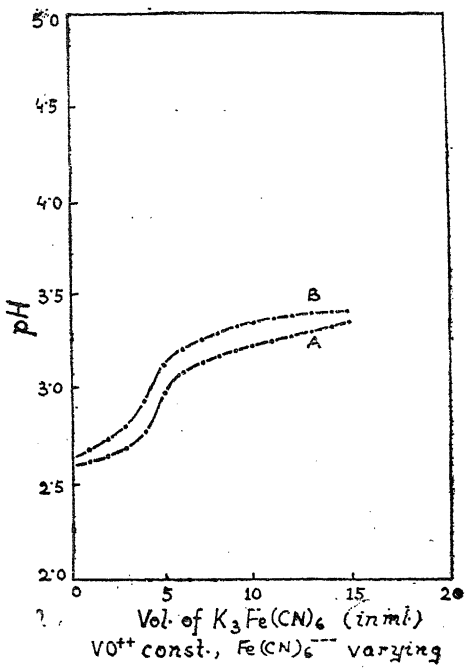

Fig. (3)

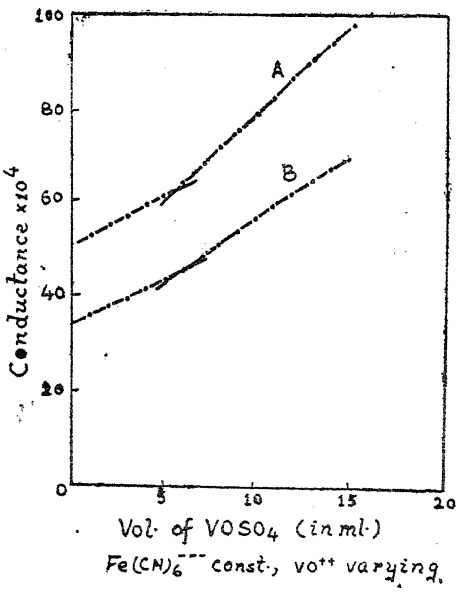

Fig. (4)

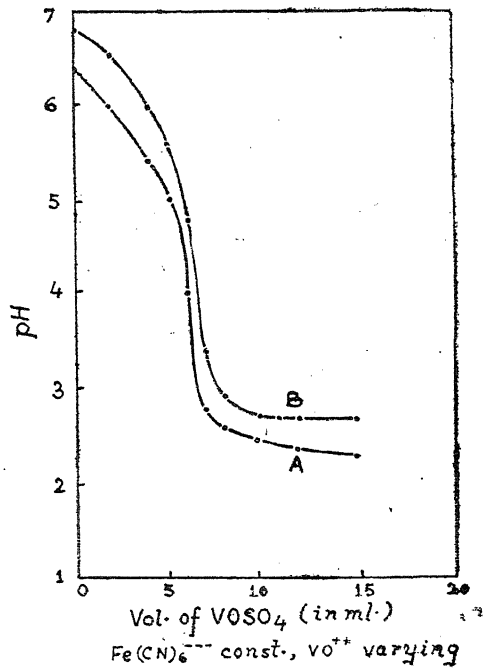

10% and 20% alcoholic solutions in the case of M/40 vanadyl sulphate and potassium ferricyanide solutions have been shown in figs. 5, 6, 7 and 8, curves A and B.

Fig. (5)

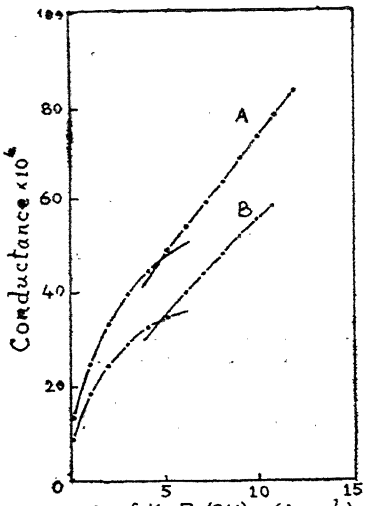

curve A: 10% alcohol
curve B: 20% alcohol

Fig. (6)

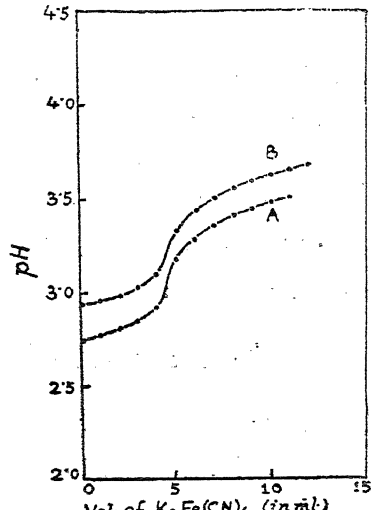

curve A: 10% alcohol
curve B: 20% alcohol

Fig. (7)

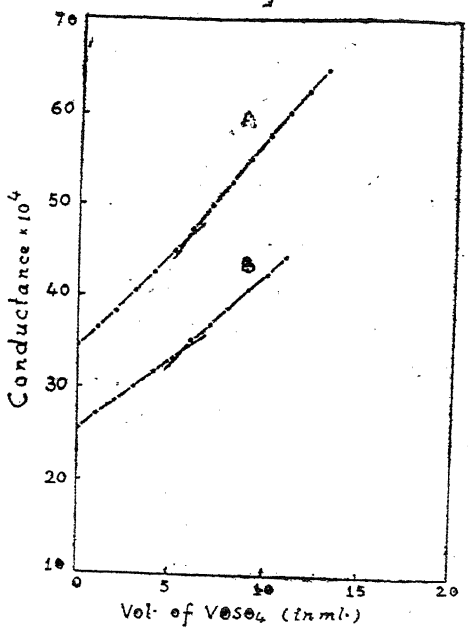

curve A: 10% alcohol
curve B: 20% alcohol

Fig. (8)

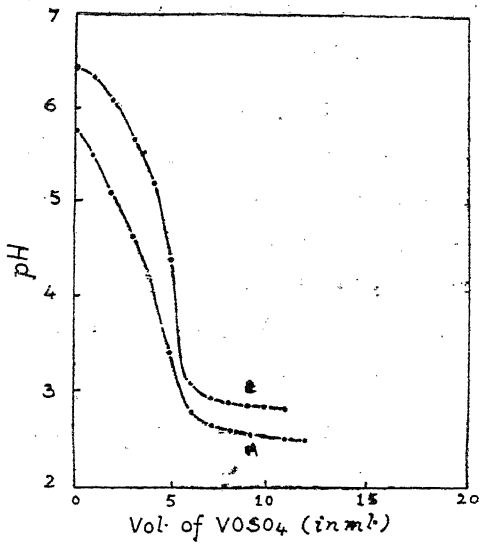

curve A: 10% alcohol
curve B: 20% alcohol

The breaks in the curves indicate the point where the vanadyl ferricyanide is formed.

DISCUSSION

A study of the nature of the curves reveals that either of the constituents remaining constant, the break corresponds to nearly equal volume of the variable equimolar component. It is clear, therefore, that equal volumes of equimolar vanadyl sulphate and potassium ferricyanide react to form vanadyl ferricyanide. The composition of the compound should, therefore, be VO K $[Fe(CN)_6]$ as seen in the following equation :

$$VOSO_4 + K_3[Fe(CN)_6] = VO\,K\,[Fe(CN)_6] + K_2SO_4$$

The nature of the conductivity and pH curves can be explained in the same way as has been done in part I of this communication.[10]

The volumes of solutions required are, however, not exactly equal, that of $K_3Fe(CN)_6$ being slightly less than the volume of equimolar vanadyl sulphate (figs 1 and 2, curves A and B). The curves in Figs. 3 and 4, on the other hand, show that the volume of vanadyl sulphate required is more than that of euimolar potassium ferricyanide. However, the curves with 10% and 20% alcoholic solutions (figs. 5, 6, 7, 8, curves A and B) show more and more agreement with theoretical values.

The discrepancy between the observed and the theoretical values in aqueous medium as against the aqueous-alcoholic can be explained in the same manner as in Part I from a consideration of relatively more adsorption of VO^{++} ions by vanadyl ferricyanide solution and the hydrolysis of vanadyl ferricyanide to liberate $[Fe(CN)_6]^{3-}$. The adsorption and hydrolysis of vanadyl ferricyanide are suppressed in alcoholic solutions, thus bringing a better agreement between the theoretical and observed values.

The authors express their thanks to Prof. A. K. Bhattacharya, Head of the Department of Chemistry, University of Saugar for his keen interest in the progress of work.

REFERENCES

1. Bhattacharya and Saxena, *J. Ind. Chem. Soc.*, **29**, 529 (1952).
2. Bhattacharya and Saxena, *J. Ind. Chem. Soc.* **29**, 263 (1952).
3. Saxena, *J. Ind. Chem. Soc.*, **34**, 415 (1957).
4. Khosla and Gaur, *J. Ind. Chem. Soc.*, **30**, 622 (1953).
5. Bhattacharya and Gaur, *J. Ind. Chem. Soc.*, **29**, 29 (1952).
6. Bhattacharya and Gaur, *J. Ind. Chem. Soc.*, **27**, 131, (1950).
7. Bhattacharya and Gaur, *J. Ind. Chem. Soc.*, **26**, 43 (1949).
8. Bhattacharya and Gaur, *J. Ind. Chem. Soc.*, **30**, 859 (1953).
9. Nayar and Pandey, *Proc. Ind. Acad. Sci.*, **27A**, 284 (1948).
10. Bhattacharya and Banerji, *Proc. Nat. Acad. Sci., India*, **30A**, 33 (1951).

PHYSICO CHEMICAL STUDY OF THE INSOLUBLE COMPOUNDS OF TRIVALENT CERIUM

PART I : ELECTROMETRIC STUDY OF CEROUS MOLYBDATE

By

M. C. SAXENA *and* A. K. BHATTACHARYA

Department of Chemistry, University of Saugar, Saugor, M. P.

[Received on 8th January, 1961]

ABSTRACT

The precipitation of cerous molybdate from cerous chloride and sodium molybdate has been studied electrometrically using the Monovariation method in two ways, (i) keeping the concentration of Ce^{+++} ions constant and varying that of MoO_4^{--} ions, and (ii) vice-versa.

The conductometric study in both the ways was carried out using equimolecular solutions of the reactants at three different dilutions, viz., M/30, M/40 and M/60. The experimental curves exhibit only one break nearly corresponding to the formation of normal cerous molybdate, $Ce_2(MoO_4)_3$.

It was observed in each case that the point of equivalence did not occur at the theoretical value. Thus the precipitation of cerous molybdate required a lesser amount of cerous chloride in the first case and greater of sodium molybdate in the second case, as compared to the calculated equivalent amounts. To find out whether this discrepancy was due to the hydrolysis of the precipitated cerous molybdate or due to unequal adsorption of cerous and molybdate ions by the precipitate, the above experiments were repeated in the presence of two different concentrations of alcohol, namely, 10% and 20%. The presence of alcohol did not bring about a closer approximation between the calculated and observed values, and hence it was assumed that the difference in the two values was due to a greater adsorption of Ce^{+++} ions than of MoO_4^{--} ions by the precipitated cerous molybdate.

In the case of pH study the experiments were performed in the same way as described above. The results of the pH measurements were found to be in complete accord with those of conductance measurements.

The composition of the precipitate was also confirmed by estimating analytically the cerium and molybdate contents in it.

The importance of the study of the composition of insoluble substances by Physico-chemical methods has been realized by a number of workers. The physico-chemical investigation of the composition of metallic molybdates has an interesting feature that the molybdate ion, according to Jander and co-workers[1], exists in the following states of aggregation depending on the pH of the solution, the various ions being pH reversible and supposed to exist in equilibrium

$$MoO_4^{2-} \rightleftharpoons Mo_3O_{11}^{4-} \rightleftharpoons Mo_6O_{21}^{6-}$$

pH 14 to 6·5 6·5 to 4·5 4·5 to 1·5

Gupta and Saxena[2,3] have carried out a potentionmetric study on mercury molybdate and concluded that normal mercury molybdate, HgO. MoO_3 is formed

at pH 2. The normal silver molybdate, Ag_2MoO_4 has been worked out physico-chemically by Saxena and Gupta[4,5]. They[6] have also reported from conductance measurements in aqueous and alcoholic-aqueous media, the formation of di- and tri- silver molybdates, the compositions of which are pH-dependent. Ramana Rao[7] has shown that for the precipitation of Ca, Sr, Ba and Cd molybdates a minimum pH of 4·18 is necesary.

P. Didier[8] prepared cerous molybdate by fusing a mixture of anhydrous cerous chloride and sodium molybdate and A. Cossa[9] observed that a solution of cerous salt gives a gelatinous white precipitate when treated with sodium molybdate; the precipitate becomes yellow and crystalline. No attempt has, however, been made to study this reaction physicochemically.

The authors here report the results of the electrometric studies on the reaction between cerous chloride and sodium molybdate. It has been observed that irrespective of the dilutions used, when either of the two reactants is added to a constant volume of the other, only normal cerous molybdate, $Ce_2(MoO_4)_3$ is formed. Freshly precipitated cerous molybdate is white and gelatinous in nature, but with lapse of time it becomes yellow and crystalline, an observation similar to that of Cossa (*loc. cit.*)

EXPERIMENTAL

Cerous chloride (B. D. H.) solution was prepared in conductivity water. The cerium content of the solution was extimated by precipitating cerium as cerous oxalate, subsequent ignition to ceric oxide and weighing as CeO_2. A recrystallized sample of sodium molybdate (E. Merck) was used, its solution being prepared in conductivity water. The conductance measurements were carried out at a temperature of 25° C, using a Doron Conductivity Bridge, and a glass electrode Beckman pH-meter was used for pH measurements.

In studying the system $CeCl_3 - Na_2MoO_4$-H_2O recourse was taken to the monovariation method[10], rather than the simple titration, because of the error involved in the titration due to volume changes during the operation, despite the volume correction being taken into consideration. The precipitation was studied in two ways, (i) keeping the concentration of Ce^{+++} constant and varying that of MoO_4^{--}, and (ii) vice-versa.

Conductometric Study :—

(*i*) Various samples were prepared by taking a constant volume (4ml.) of cerous chloride solution and increasing amounts (1 ml. to 16 ml.) of equimolar solution of sodium molybdate, the total volume being always kept constant (20 ml.) by the addition of conductivity water. Thus, three sets of solutions were prepared using M/30, M/40 and M/60 solutions each of cerous chloride and sodium molybdate,

Conductance measurements were carried out after allowing the solutions to stand for some time for the attainment of equilibrium.

Curves A, B and C in Fig. (1) represent the change in conductance with increasing volume (in ml.) of sodium molybdate solution. The conductance first decreases slightly as the fast-moving Ce^{+++} ions are being replaced by relatively slow-moving Na^{+} ions; the curves then exhibit a break indicating the complete precipitation of cerium as cerous molobdate. Further addition of sodium molybdate causes a rapid increase in conductance due to the excess of MoO_4^{--}-ions.

The precipitation reaction may be represented by the following equation, according to which cerous chloride and sodium molybdate combine in the ratio 2:3 to form cerous molybdate :

$$2\ CeCl_3 + 3Na_2MoO_4 \rightarrow Ce_2(MoO_4)_3 + 6\ NaCl.$$

(ii) In this case, to a constant volume (6 ml.) of sodium molybdate solution were added increasing amounts of equimolar cerous chloride solution (from 0 ml. to 14 ml.), keeping the total volume 20 ml. in each sample by the addition of conductivity water. Three sets of solutions were prepared as before taking M/30, M/40 and M/60 solutions, each of sodium molybdate and cerous chloride.

The conductometric study yields three curves, A, B and C as shown in Fig. (2). The conductance at first increases slightly due to the replacement of comparatively less mobile MoO_4^{--} ions by Cl^{-} ions, the rate of increase being still more after the equivalence point because of the addition of excess of Ce^{+++} ions.

In both the cases, (Fig. 1 and Fig. 2), it is seen that the break in the curves

Fig. (1)

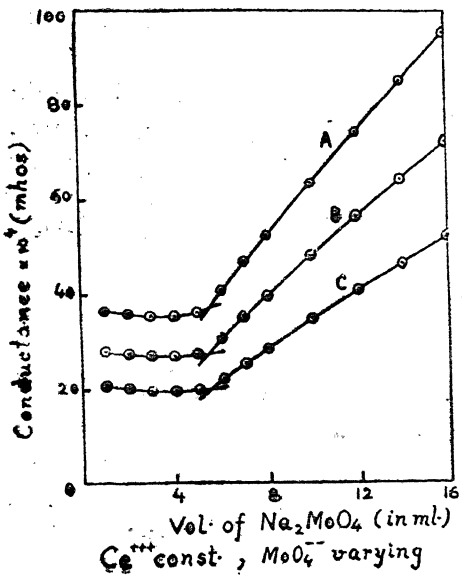

Fig. (2)

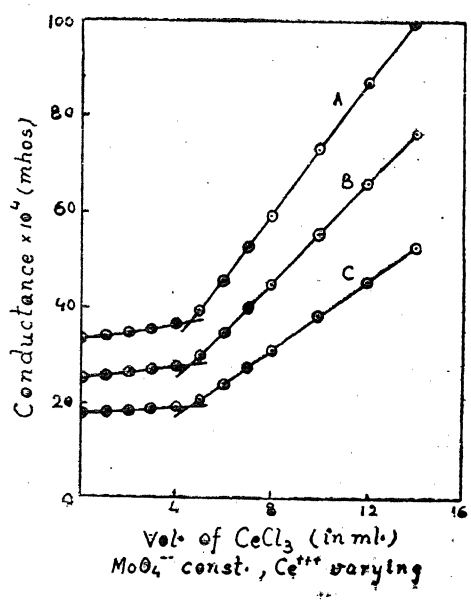

does not occur at the theoretical value. Thus Fig. 1 shows a lower experimental value and Fig. 2 a higher value than the theoretical ones. There can be two possible reasons for the departure of the experimental values from the theoretical values: (i) the hydrolysis of the precipitated cerous molybdate and (ii) the unequal adsorption of Ce^{+++} and MoO_4^{--} ions by cerous molybdate.

The effect of alcohol on the precipitation of cerous molybdate was studied by repeating the above experiments in the presence of different amounts of alcohol. Curves A and B in Figs. 3 and 4 show the results of conductometric study of the

Fig.(3)

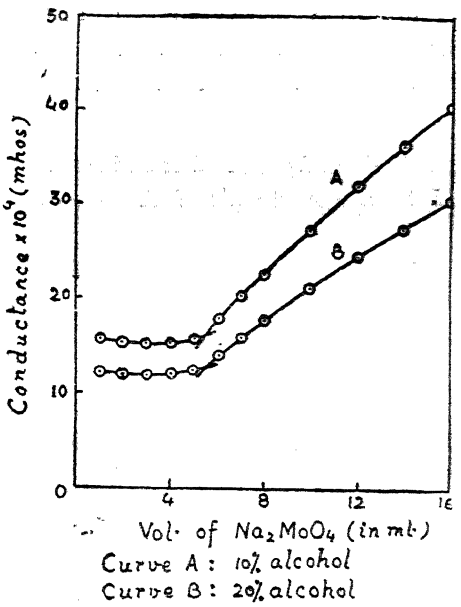

Fig.(4)

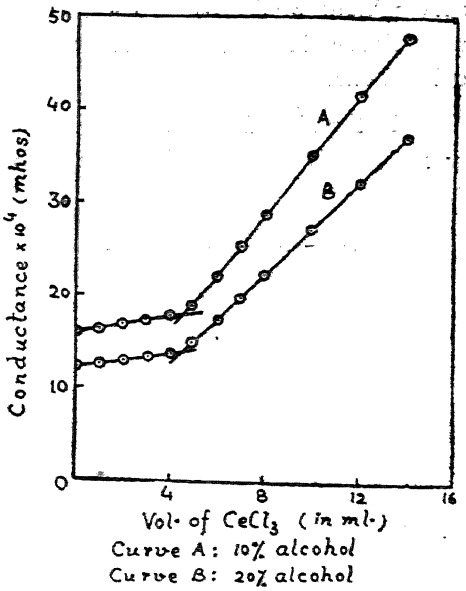

system using M/40 solutions of both the reactants in presence of 10% and 20% alcohol, respectively. The presence of alcohol does not seem to alter the experimental value, showing that hydrolysis should not be responsible for the difference in the experimental and theoretical values.

The difference in the calculated and experimental values may be explained on the assumption that cerous molybdate adsorbs more Ce^{+++} ions than MoO_4^{--} ions and hence in the first case a lower value, whereas in the second case a higher value is obtained.

pH Study :—

The experiments were preformed in the same way as in the case of conductometric measurements.

In the first case, *i. e.*, when the amount of cerous chloride was kept constant, and that of sodium molybdate varied, two sets of solutions were prepared using M/60 solutions of both the reactants in the first set and M/80 in the second set. A plot of the observed pH values against the volume (in ml.) of sodium molybdate solution yields two curves A and B as shown in Fig 6 which exhibit a point of inflexion at a lower value than the theoretical one, thus supporting the results of conductance measurements.

In the second case, cerous chloride was the variable component and sodium molybdate constant, the strength of the two reacting solutions in the two sets being the same as in the first case, *i. e.*, M/60 and M/80, respectively. The observed pH values when plotted against the volume (in ml.) of cerous chloride yield two curves A and B (Fig. 6). As seen in the case of conductometric study, the point of equivalence in both the curves is obtained at a higher value than the calculated one.

In Figs. 5 and 6 the two curves A and B were obtained from the first and second sets, respectively. A study of the curves in Fig. 5 shows that the pH of the system

(*Fig 5*)

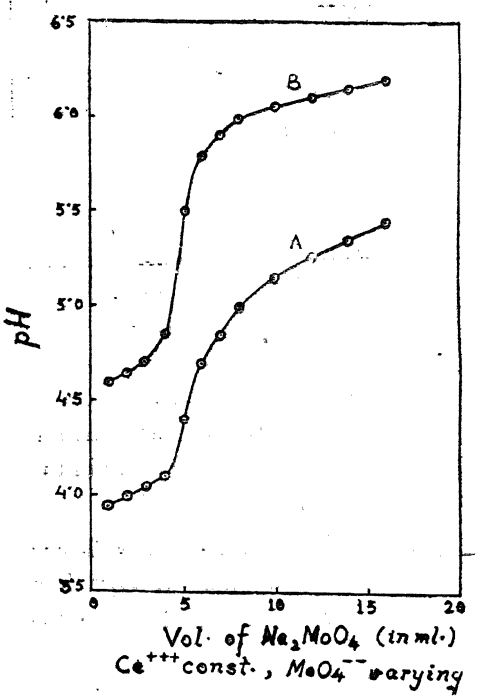

Fig.(6)

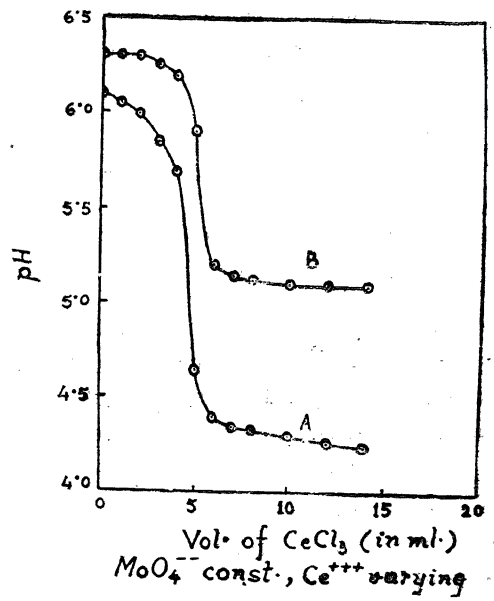

increases slowly in the initial stage with the gradual increase in the amount of sodium molybdate, which may be due to the neutralization of the free acid from

$CeCl_3$. Complete precipitation of cerous molybdate is indicated by a point of inflexion in the curve, after which the pH of the system rises steadily due to the excess of sodium molybdate which is an alkaline salt.

In the second case (Fig. 6) the pH of the system first decreases slightly, *i. e.*, there is an increase in the hydrogen-ion concentration of the system, which may be explained on the similar reasonings as done in the first case, that along with the precipitation of cerous molybdate, increasing volume of $CeCl_3$, by virtue of its acidic nature due to partial hydrolysis, neutralizes the alkali of the sodium molybdate. The point of inflection shows the completion of the precipitation and further addition of $CeCl_3$ results only in a slight decrease in the pH.

The above experiments were now repeated in the presence of alcohol. For cerous chloride as the constant component, the experimental curves are shown in Fig. 7; and when sodium molybate is kept constant the curves obtained are shown in Fig. 8. In both the figures, *i. e.*, in Figs. 7 and 8 Curve A refers to 10%

Fig. (7)

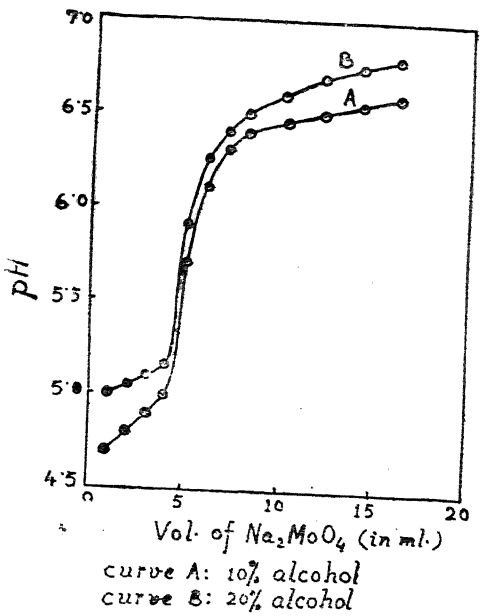

Fig. (8)

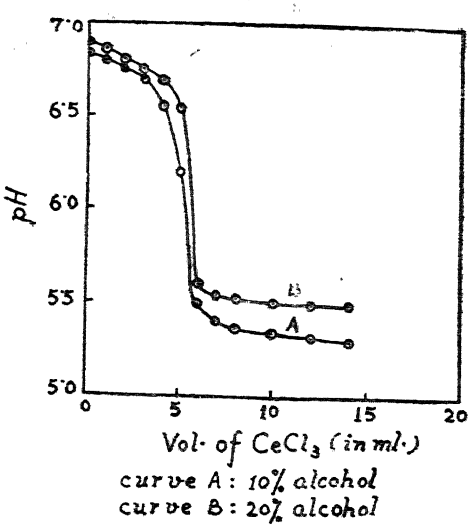

alcohol and curve B to 20% alcohol. No shift in the position of equivalence point seems to occur even in the presence of alcohol.

It is thus seen that the results of the pH measurements are in good accord with those of conductance.

The analytical data on the estimation of cerium and molybdate in the purified and dried sample of precipitate obtained by mixing the equivalent amounts of the solutions of cerous chloride and sodium molybdate, support the results obtained by conductivity and pH measurements, that is, only normal cerous molybdate $Ce_2(MoO_4)_3$ is formed on mixing the two reactants.

REFERENCES

1. G. Jander et al, *Ber.*, **194**, 383, (1930).
2. C. M. Gupta and R. S. Saxena, *J. Ind. Chem. Soc.*, **35**, 617-18 (1958).
3. C. M. Gupta and R. S. Saxena, *Z. Naturforsch.*, **13b**, 557-59 (1958).
4. C. M. Gupta and R. S. Saxena, *Rajasthan University Studies*, Physical Sciences, p. 91-95, (1958).
5. G. Charlot and D. Bezier, Quantitative Inorganic Analysis John Willey and Sons, London, p. 293 (1957).
6. C. M. Gupta and R. S. Saxena, *Current Science*, **28**, 280-81 (1959).
7. D. V. Ramana Rao, *J. Sci. Ind. Res.*, **13B**, 309 (1954).
8. P. Didier, *Compt. Rend.*, **102**, 823 (1886).
9. A. Cossa, *ibid*, **98**, 990 (1884); **102**, 1315 (1886).
10. M R. Nayar and C. S. Pandey, *Proc. Ind. Acad. Sci.*, **27A**, 284 (1948).

PHYSICO CHEMICAL STUDY OF THE INSOLUBLE COMPOUNDS OF TRIVALENT CERIUM

PART II: ELECTROMETRIC STUDY OF CEROUS TUNGSTATE

By

M. C. SAXENA *and* A. K. BHATTACHARYA

Department of Chemistry, University of Saugar, Saugor, M. P.

[Received on 8th January, 1961]

ABSTRACT

The precipitation of cerous tungstate has been studied electrometrically by means of the Monovariation method in two ways. In the first case cerous chloride was the constant component and sodium tungstate was the variable one, whereas in the second case the volume of sodium tungstate was kept constant varying that of cerous chloride.

Electrometric measurements of the system using M/40 and M/60 solutions, each of cerous chloride and sodium tungstate revealed that normal cerous tungstate, $Ce_2(WO_4)_3$ is formed on mixing the two reacting solutions. It was, however, seen that the point of equivalence did not occur at the calculated value. In the first case a lower experimental value, whereas in the second case a higher value was obtained.

The above experiments, when repeated in the presence of 10% and 20% alcohol, respectively, showed that the presence of alcohol does not affect the position of the equivalence point. This indicated that the difference in the experimental and theoretical values should not be due to the hydolysis of the precipitated cerous tungstate. The difference could, however, be explained on the assumption that cerous tungstate adsorbs more Ce^{+++} ions than WO_4^{--} ions.

The physico chemical methods have been found many a times to give better and conclusive results than the analytical procedures in determining the composition of metallic tungstates. The reason is, that the precipitation of a metallic tungstate is affected by factors like aggregation of tungstate ion, pH of the medium, etc. Various types of tungstate ions have been described, the formation of which depends upon the hydrogen ion concentration of the medium[1], the more important and well defined being the normal, para and meta tungstates. Thus the normal tungstates have been said to precipitate from alkaline solutions, the para-tungstates from weakly acid solutions and the meta-tungstates under specified conditions, from strongly acidified solutions of sodium tungstate.

The formation and precipitation of mercury tungstate have been studied from electrometric titrations by Saxena and Gupta[2]. They have shown the existence of

a normal mercury tungstate, $HgO.WO_3$ between pH 3 and 4. Saxena and Gupta[3] have found from the results of conductometric titrations between copper sulphate and sodium tungstate that a normal copper tungstate is formed at pH 6·0 – 6·5, whereas at lower pH values (4·8 to 5·2) the precipitate obtained is that of copper meta-tungstate. Some other examples[4] of the physico chemical studies of metallic tungstates are also available in the literature.

Tammann[5,6] observed evidence of the formation of cerous tungstate, $Ce_2(WO_4)_3$, when ceric oxide is heated with tungsten trioxide. According to Cossa and Zecchini[7,8], an amorphous pale yellow precipitate of cerous tungstate is formed on adding a solution of cerous sulphate to that of sodium tungstate; the precipitate becomes crystalline after heating to redness. Hitchcock[9] has shown that a solution of sodium tungstate gives a precipitate with solutions of cerium salts. According to him the precipitation is not complete and the addition of alcohol causes the precipitation of other cerium salts along with the cerium tungstate in solution. Didier[10] and Traube[11] have separately obtained cerous tungstate following two different analytical procedures. Different types of analytical methods have been adopted by some workers in preparing various tungstates of cerium. Thus, Rogers and Smith[12] have prepared ammonium cerous tungstate, Högbom[13] has obtained sodium cerous tungstate, Didier[14] has prepared a complex tungstate, $Na_2Ce_2(WO_4)_4$, and Carobbi and Tancredi[14] have suggested the existence of three crystalline compounds in the system $Ce_2(WO_4)_3 - Na_2WO_4 - H_2O$ at 25°C. A yellow cerous metatungstate has been prepared by Scheibler[15]. The compounds cerium potassium tungstate and cerium sodium tungstate have been obtained by Sillen and Sundvall[16].

The preceding lines, which record in brief the available literature on the various tungstates of cerium, show that, though considerable amount of work has been done on the cerium tungstates by a variety of analytical procedures, no attempt whatsoever has been made to investigate by physico-chemical methods, the nature of the reaction between cerous salts and sodium tungstate in solution. We, therefore, thought it worthwhile to undertake a systematic electrometric study of the system $CeCl_3 - Na_2WO_4 - H_2O$ and to see the effect of alcohol, if any, on the precipitation of the tungstate of Ce (III).

EXPERIMENTAL

Standard cerous chloride solution was prepared in the same way as described in Part – I of this paper (this journal, page). Sodium tungstate of analar quality was used, and its solution was prepared in conductivity water. A Doron Conductivity bridge and a Beckman glass-electrode pH Meter were used for measuring conductance and pH, respectively.

The interaction between cerous chloride and sodium tungstate was studied by means of the Monovariation method[19] in two ways.

In the first case the volume of cerous chloride solution was kept constant (4 ml.) varying that of sodium tungstate solution (from 0 ml. to 16 ml.), the total volume being always made upto 20 ml. by the addition of conductivity water. Two sets of solutions were prepared using equimolar solutions of cerous chloride and sodium tungstate, the strength of the two solutions being M/40 in the first set and M/60 in the second set. The experimental conductometric data when plotted against the volume (in ml.) of sodium tungstate yielded two curves A and B as shown in Fig. 1. A similar plot of pH data is represented by the curves A and B in Fig. 2. It is seen from the curves A and B. (Fig. 1.) that the gradual increase of

Fig.(1)

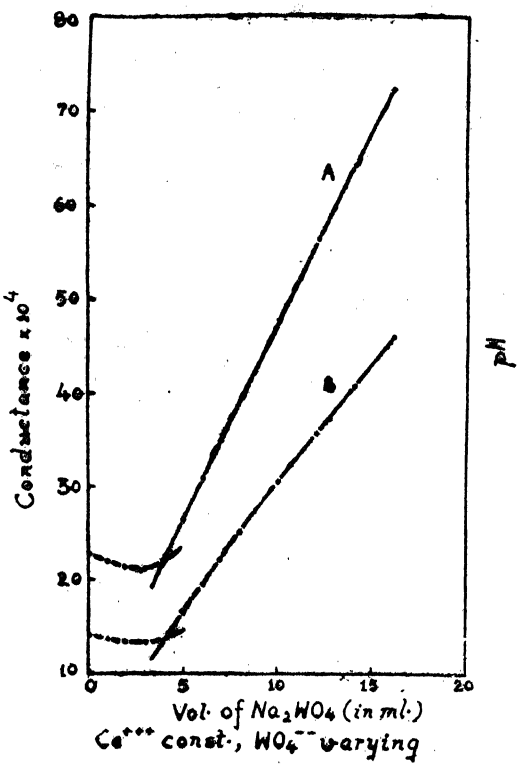

Fig.(2)

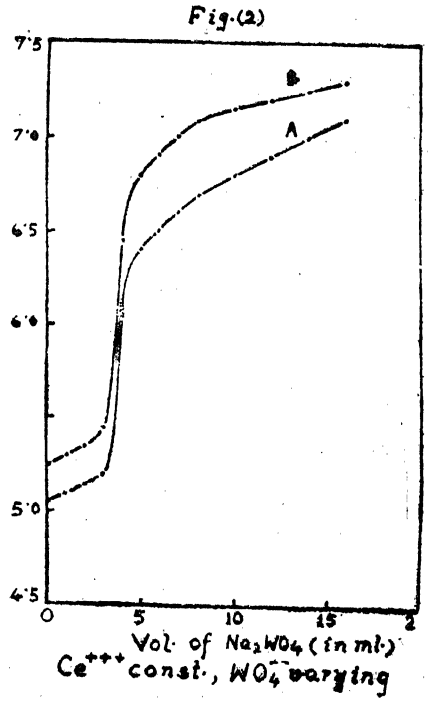

sodium tungstate first causes a slight decrease in the conductance. This is because of the removal of fast-moving Ce^{+++} ions by relatively slow-moving Na^{+} ions. A further increase in the amount of sodium tungstate causes a rapid increase in the conductance, the point of equivalence being shown by a break in both the curves. The conductance increases rapidly after the equivalence point due to the addition of excess of WO_4^{--} ions.

The curves, A and B, in Fig. 2 support the results obtained conductometrically, the point of equivalence in this case being represented by a point of inflexion in the two curves. With the gradual addition in the amount of sodium tungstate, the pH of the medium rises, because of the basic nature of sodium tungstate.

Secondly, the curves A and B in Figs. 3 and 4, which have been obtained

Fig. (3)

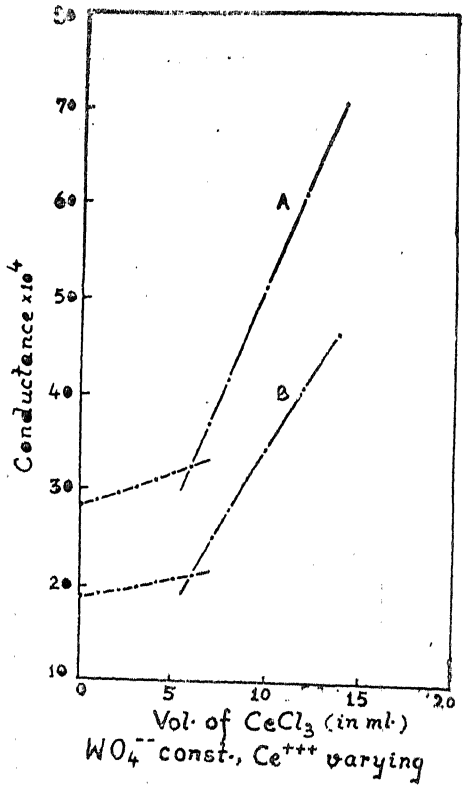

Fig. (4)

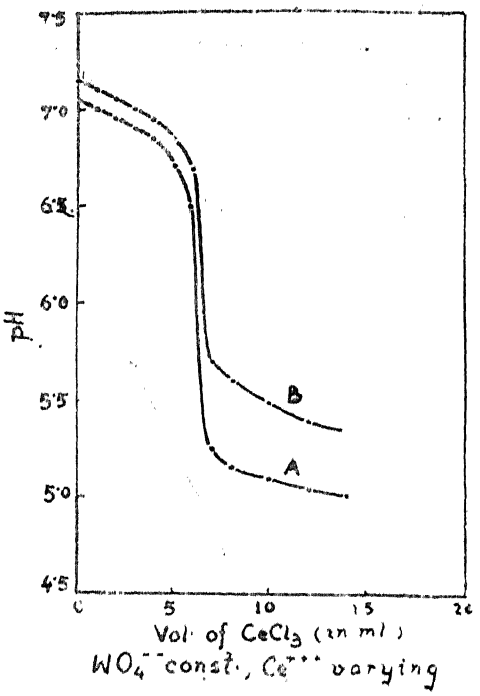

by keeping the amount of sodium tungstate constant and varying that of cerous chloride, confirmed the previous observations. As expected in this case, it is seen from Fig. 3 that the conductance first increases slightly due to the replacement of relatively less mobile WO_4^{--} ions by Cl^- ions, the rate of increase being still more after the equivalence point. The rapid increase in conductance is due to the addition of excess of Ce^{+++} ions. The results of the pH measurements (Fig. 4) are in agreement with those of conductance. This time the pH of the medium is lower throughout due to the removal of WO_4^{--} ions and addition of Cl^- ions. The nature of the curves may be discussed as has been done in part I of the series.

The electrometric observations as recorded in the Figs. 1, 2, 3 and 4 confirm the formation and precipitation of only one tungstate of cerium (III) on

mixing together the solutions of cerous chloride and sodium tungstate. As seen from the experimental curves, the $Ce^{+++}:WO_4^{--}$ ratio remains the same irrespective of the fact whether cerous chloride solution is added to the solution of sodium tungstate or, vice-versa. The position of the breaks in the various curves nearly corresponds to the formation of a normal cerous tungstate, $Ce_2(WO_4)_3$. However, it is worth noting that curves in Figs. 1 and 2 show a lower experimental value than the theoretical one. On the other hand a higher experimental value is exhibited by the curves in Figs. 3 and 4.

The above experiments were repeated in the presence of two different concentrations of alcohol, viz., 10% and 20%. Each of the two Figs. 5 and 6

Fig. (5)

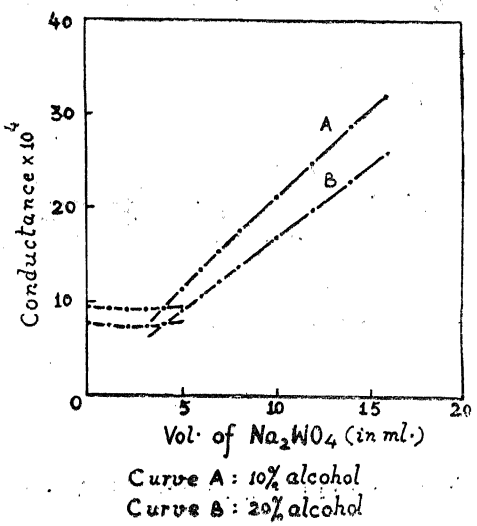

Fig. (6)

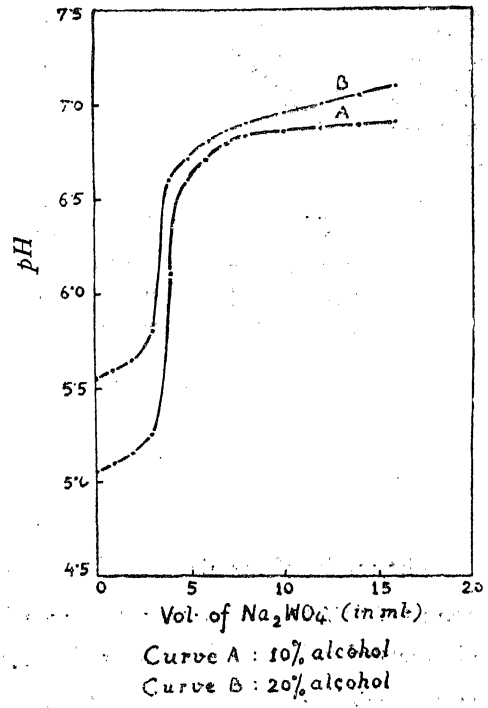

6 contains two curves A and B, the curve A representing the change of the measured property (conductance or pH) with respect to the increasing amount of sodium tungstate in the presence of 10% alcohol, and the curve B exhibiting the data obtained in the presence of 20% alcohol.

In Figs. 7 and 8 are shown the curves A and B obtained in the presence of 10% and 20% alcohol, respectively, the constant component in this case being sodium tungstate, cerous chloride being the variable one.

Fig. (7)

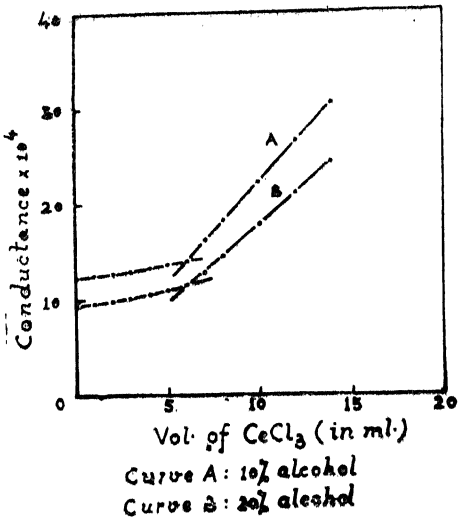

Fig. 8

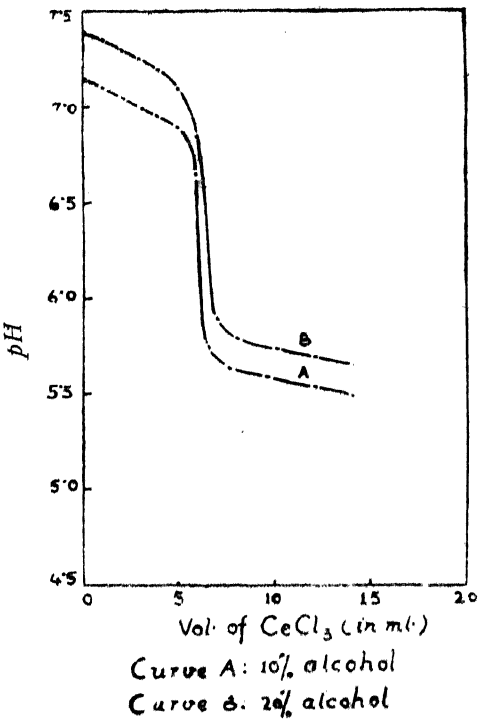

The results of the electrometric study of the system in the presence of different amounts of alcohol do not seem to give a better agreement between the calculated and observed values. This shows that the difference between the two values is not due to hydrolysis of the precipitate. The difference in the theoretical and experimental values, may, however, be explained on the assumption that the precipitated cerous tungstate adsorbs more Ce^{+++} ions than WO_4^{--} ions and hence in the first case a lower, whereas in the second case a higher value is obtained.

REFERENCES

1. H. J. Emeleus and J. S. Anderson, Modern Aspects of Inorganic Chemistry, Third Edition (Revised and Reset), 1960, p. 322.
2. R. S. Saxena and C. M. Gupta, *J. Ind. Chem. Soc.*, **36**, 845 (1959)
3. R. S. Saxena and C. M. Gupta, *Curr. Sci*, **27**, 437 (1958)
4. R. S. Saxena and C. M. Gupta, *J. Ind. Chem. Soc.*, **35**, 830 (1958); *J. Sci. Ind. Res.* **17B**, 136, 503 (1958), *Z. physikal Chem.*, **19**, 94 (1959)
5. G. Tammann, *Zeit. anorg. Chem.*, **149**, 21 (1925)
6. G. Tammann and W. Rosenthal, *ibid*, **156**, 20 (1926)
7. A. Cossa, *Gazz Chim. Ital.*, **9**, 118 (1879); **10**, 467 (1880); **16**, 284 (1886)
8. A. Cossa and M. Zecchini, *ibid*; **10**, 225 (1880)
9. F. R. M. Hitchcock, *J. Am. Chem. Soc.*, **17**, 483 (1895)
10. P. Didier, *Compt. Rend.*, **102**, 823 (1886)
11. H. Traube, *Centr. Min.*, 679 (1901)
12. A. Rogers and E. F. Smith, *J. Am. Chem. Soc.*, **26**, 1474 (1904)
13. A. J. Hogbom, *Bull. Soc. Chim.*, (2), **42**, 2 (1884); *Oefvers. Svenska* Akad. Forh. **40**, 5 (1884)
14. G. Carobbi and G. Tancredi, *Gazz. Chim. Ital.*, **58**, 45 (1928)
15. C. Scheibler, *Jour. prakt. Chem.* (1), **80**, 204 (1860)
16. Lars G. Sillen and Herman Sundvall, *Arkiv Kemi, Mineral, Geol.* **17A**, No. 10, 1-18 (1943); *Chem. Zentr.* **I**, 271 (1944)
17. M. R. Nayar and C. S. Pandey, *Proc. Acad. Sci.*, **27A**, 284 (1948)

STUDIES IN CHROMIUM ARSENITE SOL

PART II :—EFFECT OF TEMPERATURE AND DILUTION ON THE VISCOSITY AND CONDUCTIVITY OF THE SOL AT VARIOUS STAGES OF DIALYSIS

By

P. C. JAIN *and* S. N. BANERJI

Department of Chemistry, University of Saugar, Saugar

[Received on 13th January, 1961]

ABSTRACT

Observations show that in the case of impure sol the viscosity decreases with increase of temperature. However, in the purified sol the decrease is followed by an increase. Similar behaviours have been noted in the vlaues of ϕ. This may be due to the formation of loose aggregates at higher temperatures.

It is interesting to note that when the sols are diluted, the viscosity at all stages of purity decreases with the increase of temperature. Hence it may be assumed that the tendency of the particles to form loose aggregates is lost on dilution.

The specific conductivity of the sol decreases on dilution. The temperature of zero conductance lies between —20°C to —30°C; and the temperature coefficient of conductivity has value in between 1·5% and 2·5% per degree rise of temperature to the value at 30°C.

INTRODUCTION

In a previous communication[1], we have reported the observations in surface tension, viscosity, conductivity and stability of chromium arsenite sol at different stages of purity at 30°C.

We are reporting, here, the results of our studies on the effect of temperature and dilution on the viscosity and conductivity of the above sol at various stages of dialysis.

EXPERIMENTAL

The sol was prepared and its constituents were estimated in the same way as has been described in the preceding paper[1]. The percentage composition of the sol at various stages of purity is given in the fig. 1 and table 1.

The measurements of viscosity and conductivity of the original and diluted sols were made at different temperatures under identical conditions by keeping the

viscometer and the conductivity cell in an electrically heated thermostat maintained at the desired temperature.

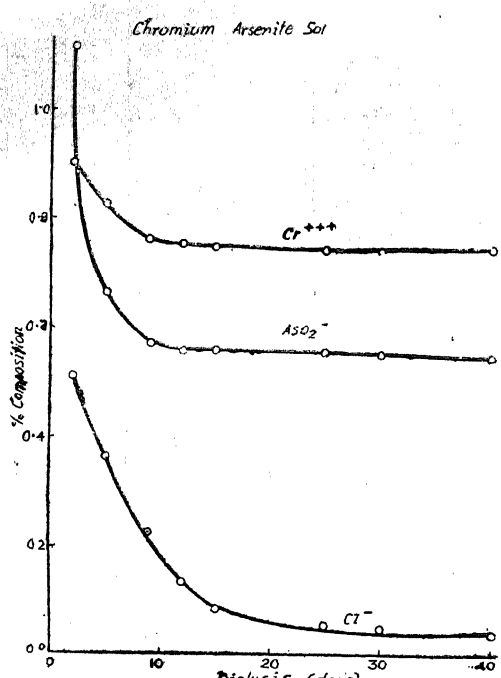

Fig. 1 - Percentage composition of the sol at different stages of dialysis.

The change in viscosity for every 10°C rise of temperature has been taken as the temperature coefficient of viscosity and the rise in specific conductivity per degree rise of temperature to the conductivity at 30°C as that of conductivity.

The experimental results are given in the following tables.

TABLE 1

Percentage composition of the sol at various stages of dialysis

Stages of dialysis	days of dialysis	Percentages of		
		Cr^{+++}	AsO_2^-	Cl^-
I	2	0·9004	1·1150	0·5107
II	5	0·8225	0·6638	0·3842
III	9	0·7572	0·5685	0·2248
IV	12	0·7749	0·5548	0·1344
V	15	0·7452	0·5540	0·0801
VI	25	0·7401	0·5535	0·0546
VII	30	0·7395	0·5535	0·0484
VIII	40	0·7395	0·5535	0·0403

TABLE 2

Effect of temperature on the viscosity of the sol at different stages of dialysis

temp.	sol I		sol II		sol III		sol IV		sol V		sol VI		sol VII		sol VIII	
	visc.	visc. coef.	visc.	v sc. coef.	visc.	visc. coef.	visc.	visc. coef.	visc.	visc. coef.	visc.	visc. coef.	visc.	visc. coef.	visc.	visc. coef.
30°C	0·8600		0·8433		0·8438		0·8470		0·8548		0·8834		0·9302		1·1130	
		—0·1558		—0·1542		—0·1542		—0·1493		—0·1560		—0·1609		—0·1722		—0·2370
40°C	0·7042		0·6891		0·6896		0·6977		0·6983		0·7225		0·7580		0·8760	
		—0·1176		—0·1141		—0·1110		—0·1190		—0·1191		—0·1235		—0·1298		—0·0725
50°C	0·5866		0·5750		0·5786		0·5787		0·5797		0·5590		0·6282		0·8035	
		—0·0884		—0·0857		—0·0888		—0·0862		—0·0851		—0·0871		—0·0908		+0·0234
60°C	0·4982		0·4893		0·4898		0·4925		0·4936		0·5119		0·5374		0·8269	

TABLE 3

Effect of temperature on the viscosity of sol 2 (diluted two times)

temp.	sol I/2		sol II/2		sol III/2		sol IV/2		sol V/2		sol VI/2		sol VII/2		sol VIII/2	
	visc.	visc. coef.	visc.	visc. coef.	visc.	visc. coef.	visc.	visc. coef.	visc.	visc. coef.	visc.	visc. coef.	visc.	visc. coef.	visc.	visc. coef.
30°C	0·8441		0·8280		0·8300		0·8301		0·8320		0·8405		0·8620		0·9624	
		—0·1546		—0·1453		—0·1460		—0·1453		—0·1460		—0·1425		—0·1537		—0·1836
40°C	0·6895		0·6822		0·6840		0·6848		0·6860		0·6980		0·7083		0·7788	
		—0·1091		—0·1116		—0·1120		—0·1120		—0·1128		—0·1228		—0·1319		—0·1399
50°C	0·5804		0·5706		0·5720		0·5728		0·5732		0·5752		0·5764		0·6389	
		—0·0919		—0·0884		—0·0889		—0·0890		—0·0892		—0·0904		—0·0821		—0·1072
60°C	0·4885		0·4822		0·4831		0·4838		0·4840		0·4848		0·4943		0·5317	

TABLE 4

Effect of temperature on the viscosity of the sol /4 (diluted four times)

temp.	sol 1/4		sol II/4		sol III/4		sol IV/4		sol V/4		sol VI/4		sol VII/4		sol VIII/4	
	visc.	visc. coef.	visc.	visc. coef.	visc.	visc. coef.	visc.	visc. coef.	visc.	visc. coef.	visc.	visc. coef.	visc.	visc. coef.	visc.	visc. coef.
30°C	0·8369		0·8255		0·8262		0·8265		0·8268		0·8283		0·8482		0·9168	
		—0·1568		—0·1518		—0·1520		—0·1522		—0·1516		—0·1400		—0·1598		—0·1761
40°C	0·6801		0·6737		0·6742		0·6743		06752		0·6883		0·6884		0·7407	
		—0·1097		—0·1057		—0·1057		—0·1056		—0·1059		—0·1162		—0·1123		—0·1320
50°C	0·5704		0·5680		0·5685		0·5687		0·5693		0·5721		0·5761		0·6087	
		—0·0880		—0·0950		—0·0953		—0·0949		—0·0953		—0·0901		—0·0875		—0·0936
60°C	0·4824		0·4730		0·4732		0·4738		0·4740		0·4820		0·4886		0·5151	

TABLE 5

Values of ϕ of the sol at different temperatures using Guth-Simha's equation

temp.	sol I	sol II	sol III	sol IV	sol V	sol VI	sol VII	sol VIII
30°C	0 02585	0·01933	0·01962	0·02027	0·02383	0·03454	0·05097	0·09984
40°C	0·02644	0·0183 0	0·01865	0·02041	0·02213	0·03401	0·04883	0·09007
50°C	0·02386	0·01702	0·01729	0·01923	0·01986	0·03050	0·04564	0·11310
60°C	0·02227	0·01603	0·01630	0·01833	0·01912	0·03132	0·04642	0·15600

TABLE 6

Effect of temperature on the specific conductivity $\times 10^3$ of the sol at different stages of dialysis

temp.	sol I		sol II		sol III		sol IV		sol V		sol VI		sol VII		sol VIII	
	sp. cond.	temp. coef.	sp. cond.	temp. coef.	sp. cond.	temp coef.	sp. cond.	temp. coef.	sp. cond.	temp. coef.	sp. cond.	temp. coef.	sp. cond.	temp. coef.	sp. cond.	tem. coef.
30°C	8·9050		4·2000		2·5920		2·1918		1·6801		1·0919		1·0060		0·7880	
		2·1%		2·0%		2·0%		1·8%		2·3%		1·9%		2·0%		2·1%
40°C	10·8200		5·0408		3·1210		2·5799		2·0412		1·2560		1·2060		0·9480	
		2·1%		2·0%		2·0%		1·6%		2·3%		2·0%		2·2%		1·7%
50°C	12·7701		5·8802		3·6208		2·9281		2·4479		1·5191		1·4400		1·0561	
		2·2%		2·1%		2·0%		1·9%		2·3%		2·0%		2·0%		1·6%
60°C	14·8004		6·8399		4·1189		3·4080		2·8600		1·7520		1·6320		1·1762	

TABLE 7

Effect of temperature on the specific conductivity $\times 10^3$ of sol/2

temp.	sol I/2	sol II/2	sol III/2	sol IV/2	sol V/2	sol VI/2	sol VII/2	sol VIII/2
30°C	4·5690	2·3240	1·4900	1·2001	0·9178	0 6139	0·5543	0·3993
40°C	5·9610	2·8001	1·7402	1·3829	1·2165	0·7426	0·6592	0·5066
50°C	6·6899	3·3019	2 0379	1·6449	1·4900	0·8750	0·7748	0·5841
60°C	7·7469	3·8742	2·4578	1·9432	1·6929	1·0250	0·9059	0 6437

TABLE 8

Effect of temperature on the specific conductivity $\times 10^3$ of sol/4

temp.	sol I/4	sol II/4	sol III/4	sol IV/4	sol V/4	sol VI/4	sol VII 4	sol VIII/4
30°C	2·5590	1·3660	0·8158	0·7247	0·4871	0·3496	0·3089	0·2178
40°C	3·1941	1·6462	1·0102	0·7999	0·6534	0·4158	0·3722	0·2911
50°C	3·630	1·9209	1·2079	0 9702	0·7920	0·5029	0·4475	0·3208
60°C	4·3509	2·2568	1·4650	1·1286	0·8950	0·5940	0·5340	0·3643

RESULTS

Table 2 shows that at all stages of dialysis the viscosity decreases with temperature till the sol attains high purity. In the latter case the viscosity initially decreases with temperature and then increases. At a still higher temperature it sets to a gel. There is a continuous decrease in the viscosity values with temperature in the case of diluted sols (tables 3 & 4).

Similarly, the values of ϕ decrease initially with dialysis and temperature, followed by a slow increase with dialysis and decrease with temperature and finally a rapid increase with both dialysis and temperature.

The conductivity of the original and the diluted sols increases with temperature (tables 6, 7 & 8).

Plots of Log η vs. reciprocal of absolute temperature (1/T) show that straight lines are obtained in all the cases except in sols VII and VIII, where the graphs are curvilinear and this is more pronounced in sol VIII than in sol VII (fig. 2).

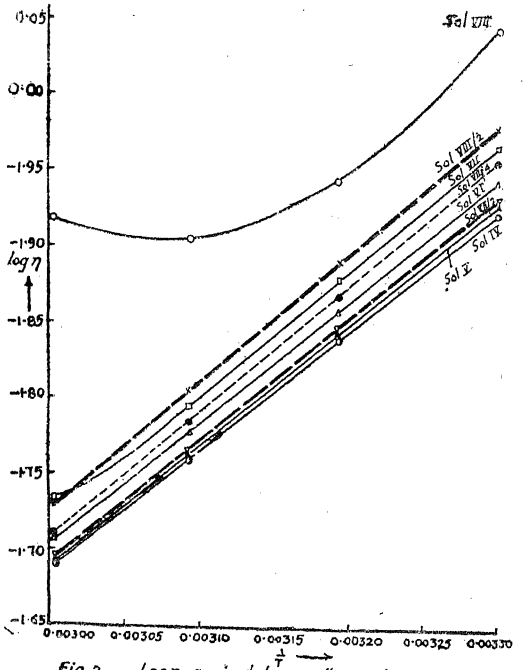

Fig. 2 – Log η against $\frac{1}{T}$ for the systems of chromium arsenite sol at various stages of dialysis.

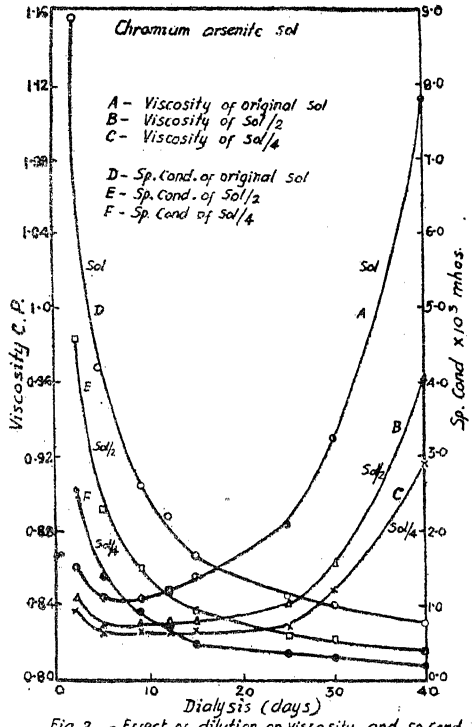

Fig. 3 – Effect of dilution on viscosity and Sp Cond. of the sol at different stages of dialysis

The general pattern of the viscosity (fig. 3 curves A, B, C) and the conductivity curves (fig. 3 curves D, E, F) of the original and diluted sols does not change.

Fig. 4 shows the graphs for specific conductivity against temperature. In all cases straight lines are obtained. Extrapolations to zero conductance give the temperature of zero conductance between – 20°C to – 30°C. The values of the temperature coefficient of conductivity lie in between 1·8% and 2·5% to the conductance at 30°C.

Viscosity—

Changes in the viscosity of very dilute suspension have been variously ascribed to the changes in solvation, particle or molecular weight, particle or molecular shape, solute-solute interaction and the degree of orientation of asymmetric

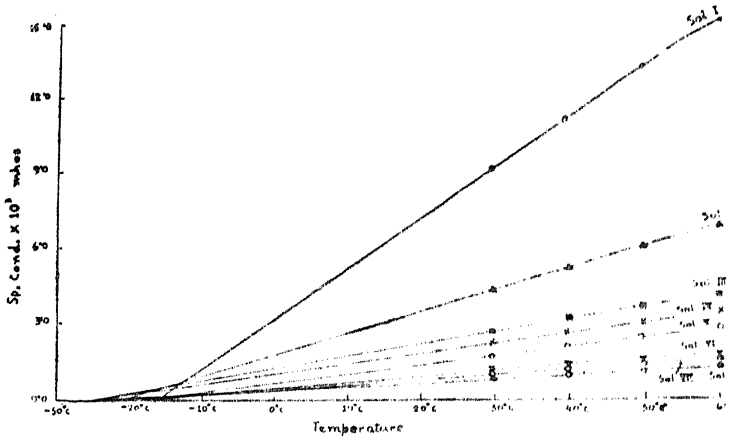

Fig. 4 — Sp. Cond. of chromium arsenite sol at different temperatures under various stages of dialysis

particles. The effect of temperature on the viscosity of a liquid has been represented by Grunberg and Nissan[2] by the following equation:—

$$\eta = K\ \phi_1\ (T, v)_{\bullet}\ \phi_2\ (T, v) \qquad (1)$$

where η is the coefficient of viscosity, K a constant characteristic of the liquid and ϕ_1 (T, v) and ϕ_2 (T, v) are the functions of temperature and volume. Experiments have shown that as long as the type of association remains the same, the viscosity-temperature function can be represented by the simplified equation *i.e.*,

$$\eta = A_{\cdot}e^{-\frac{E\ visc.}{R'T}} \qquad (2)$$

where A is a constant related to molecular weight and density, E is the activation energy of flow, that is, the energy necessary to destroy the mutual coherence between the molecules thus giving an information concerning the type of association between the particles.

Evisc. has been ascribed by Andrade[3] as due to the energy of interaction between a pair of molecules of liquid while Frenkel[4] considers it as the energy required to liberate a molecule from the sphere of coordination and to effect a jump into the new equilibrium position. Attempts have also been made to relate Evisc. to Van der Waals constant 'a'[5], to latent heat of vaporisation,[6] to internal pressure[7], and to latent heat of fusion[8]. It seems that according to these ideas Evisc. represents the energy required to break certain bonds between the molecules.

From equation (2) it is seen that the plots of log η against 1/T should give straight lines if the sol behaves normally. Fig. 2 shows that in all cases straight lines are obtained except when the sol attains high purity (sols VII & VIII) where the curves are curvilinear. At higher temperatures, the stabilising electrolyte of the sol particles is given out and the Brownian motion increases. Consequently

with the increase in the number of collisions among the particles and desorption of the stablising ions, there is formation of a large number of loose aggregates. The medium behaves abnormally and the curves are curvilinear. Transition from one straight part of the curve to another is probably due to the transition from one type of association to another, the latter imparting enhanced asymmetry to the aggregates. It is observed that the negativity of the viscosity coefficient decreases with increase in temperature (sols VI, VII & VIII). This further supports the idea of association of the particles at higher temperatures. Similar conclusions were arrived at in the studies of chromium tungstate[9] and chromium arsenate sols[10].

It is interesting to draw a comparasion between the curves for log η against 1/T (fig. 2) for the original sols VII and VIII and those for the diluted ones VIII/2, VIII/4 and VII/2. The former give curved lines while the latter straight ones. It may, therefore, be assumed that the tendency of the sol particles to form loose aggregates is lost on dilution.

Table 5 shows the values of ϕ at different stages of d ialysis and with temperature. The value first decreases, then increases gradually and finally rapidly. The initial decrease is due to the removal of adsorbed electrolytes from the surface of sol particles causing a decrease in the effective volume. The gradual increase is mainly due to the aggregation of the sol particles. Increase in temperature results in a decrease in hydration and therefore, the value of ϕ also decreases. But the increase of ϕ with increase of temperature in the later stages of dialysis (table 5, sols VII & VIII) is due to the formation of increased number of loose aggregates with weak crystallographic axes leading to greater approach to gel structure.

Conductivity :—

Every sol particle is regarded as charged particle surrounded by an electrical double layer of opposits charge. When the sol particle moves, the double layer retards its motion due to the effects of (1) time of relaxation and (2) assymmetry. The frictional resistance of the medium which is dependent upon the speed of the particle and its radius and upon the viscosity of the medium also retards the motion.

Decrease in the conductivity with dialysis in the initial stages is caused by the removal of stabilising electrolyte as well as other ions present as impurities. Small values of conductivity in the purer sols is due to the fact that the number of current carrying ions or the particles is small. The larger charge carried by the colloidal particles is not sufficient to compensate their smaller number. The temperature coefficient of conductivity lies in between 1·8% and 2·3% which is nearly equal to the value for an ordinary electrolyte. Hence the increase in conductivity with temperature seems to be due to the increase in the mobility of the current carrying ions. At higher temperatures when the adsorbed electrolyte which stabilises the sol, is given out gradually, the sol becomes less stable and more conducting with the consequence that the rate of formation of loose aggregates increases in the purified sols.

REFERENCES

1. Jain, P. C. and Banerji, S. N., 1961, *Proc. Nat. Acad. Sci.* (Forthcoming).
2. Grunberg, L. and Nissan, A. H., *Trans. Farad Soc.*, **45**, 29, (1949).
3. Andrade, E. N., *Phil. Mag.*, **17**, 497, (1934).
4. Frenkel Ya, *Z. Physik.*, **35**, 662 (1926); *Ibid.*, **33**, 58 (1937).
5. Andrade, E. N., *Phil. Mag.*, **17**, 698 (1934).
6. Andrade, E. N. and Friend, J. N., *Z. Physik.*, **31**, 542 (1935).
7. MacLeod, D. E., *Z. Physik.*, **19**, 61 (1923).
8. Ward, A. C., *Z. Physik*, **33**, 92 (1937).
9. Jain, P. C. and Banerji, S. N., *Jour Saug. Univ.*, **7**, 35 (1958).
10. Jain, P. C. and Banerji, S. N., *Jour. Saug. Univ.*, **8**, 42 (1960).

STUDIES IN CHROMIUM ARSENITE SOL

PART III:—CHANGES IN EXTINCTION, pH AND ELECTRICAL CONDUCTIVITY OF THE SOL DURING COAGULATION UNDER DIFFERENT STAGES OF DIALYSIS

By

P. C. JAIN *and* S. N. BANERJI

Department of Chemistry, University, of Saugar, Saugor

[Received on 13th January, 1961]

ABSTRACT

Extinction measurements show that coagulation of the sol is accelerated with the addition of increasing amounts of electrolyte and a constant maximum flocculation is reached. At higher concentrations, the extinction begins to decrease due to the formation of loose flocs that scatter lesser light than those formed at relatively lower concentrations.

With the addition of increasing amounts of K_2SO_4, the pH of the sol increases. This is due to the adsorption of H_3O^+ ions on the partly neutralised colloid surface and consequent increase of OH^- ions concentration in the medium.

There is a continuous decrease in the conductivity of the sol with the progressive addition of the electrolyte. This has been ascribed to the greater penetrating power of SO_4^{--} ions as also their power of neutralising the positive charges of the sol particles. With the result, that they can not contribute to the total conductivity of the mixture of sol plus electrolyte. Moreover, the increased radius of the micelles and the salt-effect also play their roles in decreasing the conductivity of the sol to some extent.

INTRODUCTION

In previous communications[1] we have dealt with the surface tension, viscosity, conductivity and stability of chromium arsenite sol under different stage of dialysis, temperature and dilution.

We have studied in this paper the changes in extinction, pH and electrical conductivity with the addition of an electrolyte, K_2SO_4, to the sol at different stages of dialysis with a view to investigate the mechanism of coagulation of the sol. The results are similar to those obtained with chromium tungstate,[2] and chromium arsenate sols.

EXPERIMENTAL

The sol was prepared by the usual method as described in part I of this series of studies. The composition of the sol at various stages of dialysis as determined has been shown in table 1.

The extinction measurements were made with a photoelectric colorimeter (Lichtelektrisches Kolorimeter Modell VI) using red filter and 10 ml. rectangular cuvette. A series of eleven electrolyte solutions, the concentrations of which were systematically varied keeping the total volume (20 ml.) constant in all cases, was

taken. Each one of these was added separately to 20 ml. of the sol in test tubes. Extinction measurements were made after thorough mixing. Fig. 1 represents the

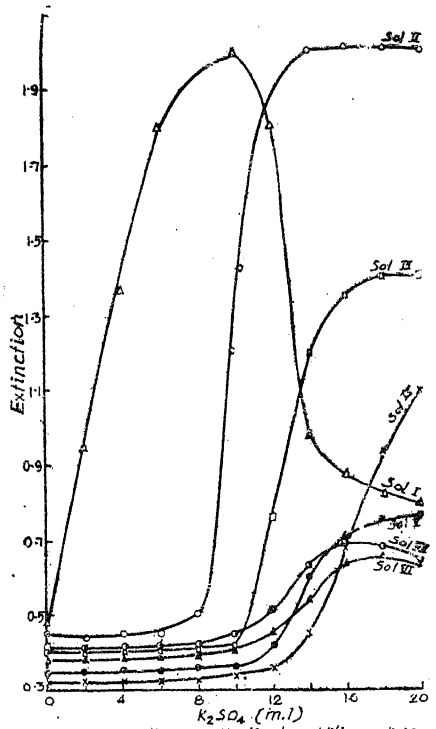

Fig. 1 - Variation of extinction by addition of K_2SO_4 to chromium arsenite sol at different stages of purity.

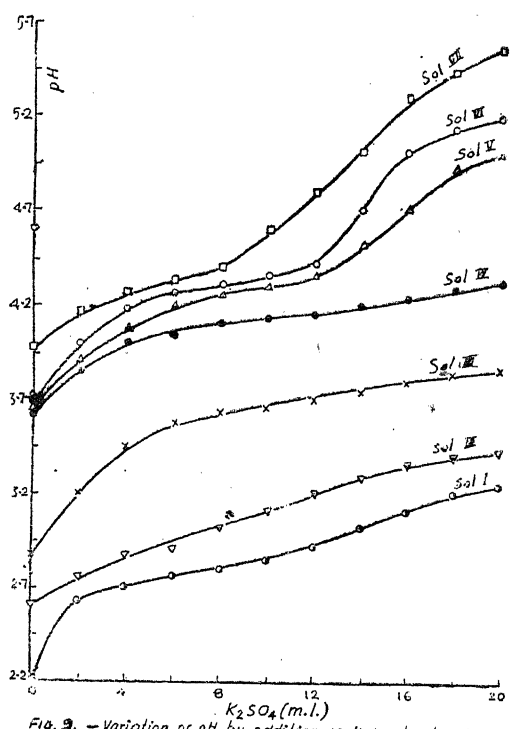

Fig. 2 - Variation of pH by addition of K_2SO_4 to chromium arsenite sol at different stages of purity

observations of extinction with varying amounts of electrolyte. The concentrations of electrolyte used at different stages of purity of the sol have been shown in table I.

Beckman (Model-M) pH-meter was used for determination of pH of the mixture of sol plus electrolyte. Fig. 2 indicates the changes of pH obtained on the addition of increasing amounts of electrolyte.

TABLE 1

Percentage composition of the sol and the concentrations of electrolyte used at different stages of dialysis

Stages of dialysis	Days of dialysis	Percentages of			Concentrations of electrolyte
		Cr^{+++}	AsO_2^-	Cl^-	
I	2	0·9004	1·1150	0·5707	2M/3
II	5	0·8225	0·6638	0·3842	M/20
III	9	0·7572	0·5655	0·2248	M/50
IV	12	0·7552	0·5590	0·0801	M/70
V	15	0·7401	0·5536	0·0546	M/80
VI	25	0·7400	0·5535	0·0500	M/100
VII	30	0·7395	0·5535	0·0484	M/100

TABLE 2

Values of the conductivity $\times 10^3$ (m hos) of the mixture of sol plus electrolyte (K_m) and of the electrolyte alone (K_e).

20 ml. sol + x ml. electrolyte + y ml. water = 40 ml.

Volume of electrolyte x ml.	Sol I		Sol II		Sol III		Sol IV		Sol V		Sol VI		Sol VII	
	K_m	K_e	K_m	K_e	K_m	K_e	K_m	K_e	K_m	K_e	K_m	K_e	K_m	K_e
0·0	5·040	...	2·184	...	1·301	...	1·029	...	0·840	...	0·607	...	0·535	...
2·0	10·56	7·110	2·474	1·054	1·392	0·252	1·116	0·213	0·919	0·199	0·696	0·154	0·601	0·154
4·0	17·52	14·58	2·688	1·464	1·512	0·557	1·200	0·420	0·959	0·300	0·768	0·336	0·644	0·336
6·0	24·13	21·42	2·976	2·008	1·608	0·755	1·349	0·658	0·992	0·390	0·804	0·436	0·694	0·436
8·0	30·16	27·60	3·394	2·613	1·740	1·104	1·416	0·864	1·044	0·505	0·866	0·580	0·749	0·580
10·0	34·80	32·31	3·844	3·182	1·848	1·247	1·512	0·912	1·138	0·655	0·924	0·690	0·820	0·690
12·0	40·80	38·40	4·319	3·768	1·980	1·505	1·632	1·126	1·212	0·777	0·984	0·774	0·888	0·774
14·0	46·80	44·77	4·821	4·341	2·124	1·720	1·753	1·442	1·296	0·975	1·080	0·876	0·984	0·876
16·0	50·40	48·72	5·315	4·841	2·393	2·028	1·860	1·584	1·356	1·076	1·224	0·978	1·082	0·973
18·0	56·40	54·50	5·832	5·323	2·520	2·160	1·946	1·686	1·644	1·383	1·344	1·220	1·323	1·220
20·0	62·40	60·03	6·360	5·350	2·750	2·406	2·040	1·784	1·812	1·580	1·536	1·420	1·516	1·420

The conductivities of the mixture of sol plus electrolyte (K_m) and those of the electrolyte alone (K_e) were determined and are given in table 2. The latter were subtracted from the former so as to give the values of the conductivities of the sol itself on the addition of increasing amounts of electrolyte. Fig. 3 therefore, shows the changes in the conductivity of the sol as a result of progressive addition of electrolyte.

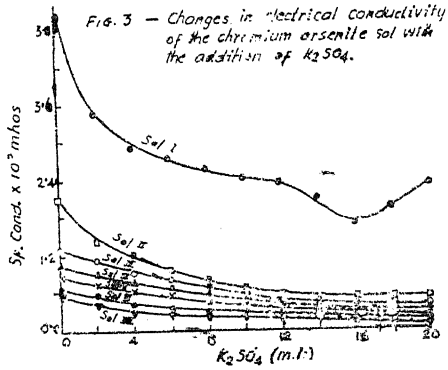

FIG. 3 — Changes in electrical conductivity of the chromium arsenite sol with the addition of K_2SO_4.

DISCUSSION

Extinction :—

When coagulation takes place, the extinction of light increases causing a decrease in the intensity of the light striking the photocell. This change of extinction is related to the type of aggregates formed and also to the rate of sedimentation following coagulation. It is seen from fig. 1 that initially the extinction-concentration curves are more or less horizontal. The coagulation is accelerated with increasing amounts of electrolyte until at a concentration it is maximum. Considering the repulsion between the particles arising from double layers and the London forces of attraction, Hamaker[4] obtained different types of resultant curves of potential energy. For the stability of a sol it is necessary that a maximum of sufficient height $>$ KT, where K is Boltzmann constant and T absolute temperature, should exist in the potential curves. On the addition of electrolyte, the double layer is compressed and the neutralisation of the charges takes place. In the absence of the energy barrier, the London van der Waals forces of attraction will prevail leading to rapid coagulation as observed by the sudden rise in the extinction curves. The repulsion between the double layers is not completely removed, therefore reorientation of the particles takes place giving rise to better contacts and denser structure. As a result of this the particles formed are highly scattering. At higher concentrations, however, the curves begin to fall. This is because in the absence of the repulsive action between the particles, the London attraction predominates with the consequence that the particles stick where they touch each other and form loose flocs. As they have irregular surface, the scattered radiations from such surface are interally reflected with the result that the amount of scattered light is less than that by a compact spherical surface.

A somewhat different behaviour is observed in the highly purified sols (sol VI & sol VII) where the addition of even a small amount of electrolyte (insufficient for normal coagulation) gives rise to lace-like structure. The partly discharged particles are attached to each other at very few spots and in the abstance of denser structure, the extinction values are low.

pH :—

Thomas and coworkers[5] noted an increase in pH of a sol of hydrous ferric oxide on the addition of an electrolyte. They have reported similar results with hydrous oxide sols of aluminium, thorium, beryllium and zirconium. Weiser[6] has also reported that the sol of hydrous chromium oxide acidified with HCl shows an increase in pH on the addition of K_2SO_4. It may be mentioned that workers other than Weiser have prefered to call these sols of hydrous oxide peptised by HCl as the sols of corresponding oxychlorides. They have further suggested that these hydrous oxide colloidal particles consisted of olated and oxolated hydroxy compounds of of Werner type and the increase in pH with the addition of a neutral electrolyte to these sols can be attributed to the replacement of OH^- and Cl^- ions in the diffused portion of the double layer and accounted for the change in pH as due to the displacement of pH^- group.

The above explanations do not appear to be probable from the X-ray studies of Böhm and coworkers[8], Fricke and Havestadt[9] and later on Weiser and Milligan[10]. Similar to these conclusions have been reached by Rai and Ghosh[11]. After a study of the coagulation of lyophobic sols by means of radioactive tracer atmos* Glazman, Strazhesko, Zhel'vis and Chervyatsova[12], hold that the coagulation process is connected not only with the surface of the sol particles but also with inner part of their electrical double layer. As is well known, the peptising ions always show a relation to the material of the particles, they fit into its crystal lattice, and it is just this fitting into lattic which makes these ions the potential determining ions. Taking in view these facts and also the fact that the concentration of Cr^{+++} ions is relatively large, the structure of the colloidal unit of chromium arsenite sol may be representated as :

$$\left[Cr(AsO_2)_3 . xH_2O \right]^{Cr^{+++}}_{H^+} \Big\} \; yCl^-$$

Thus implying that the positive charge and the stability are attributed to the chromium ions and H^+ which constitute the fixed part of the double layer while chloride ions form the diffused outer layer. On the addition of sulphate ions, the thickness of the double layer is decreased due to their high penetrating capacity. Hence, neutralisation of the charges on the surface of the sol particles takes place with the consequence that a partly neutralised surface is formed. It has the tendency to adsorb such ions as are capable of producing the same electric charge as that of the colloid unit[11]. Therefore, H_3O^+ ions from the medium are adsorbed on such surfaces increasing thereby the OH^- ion concentration in the system. Thus the pH of the sol goes on increasing with the progressive addition of the electrolyte.

Conductivity :

While studying the changes in conductivity during coagulation of hydrous oxide sol of Iron and other sols, Rai and Ghosh (*loc. cit.*) noted a decrease in conductivity on progressive addition of K_2SO_4. They explained it by saying that the Helmholtz double layer becomes fainter due to higher despersion of colloidal units and consequently contributing to lesser conductivity.

It is well known that in a sample binary electrolyte solution, the ionic conductivities of the counter ions and the by-ions as well as of the polyions are additive to give the observed conductivity of the solution. It is seen from fig. 3 that the conductivity of the sol itself decreases continuously as a result of the addition of

increasing amounts of electrolyte. The decrease is more remarkable for purer sols than for impure ones.

Two factors are expected to play important roles in the decrease of conductivity of a sol with the addition of electrolyte. One is the decrease in the thickness of the double layer while the other is the change in its charge density as a result of neutralisation with the coagulating ions. Due to the first factor the attraction between the two parts of double layer will increase. As a result, there will be more electrostatic attraction by the oppositely charged outer layer on the moving sol particle, thus decreasing its mobility. Low concentrations of the electrolyte mainly reduce the stability of the sols by the compression of the double layer, but further additions lead to a rapid fall in the stability due to the reduction of the surface potential at all concentrations of electrolyte.[13] Evidently, upto the point of addition of SO_4^{--} ions equivalent to rapid coagulation, nearly all of them penetrate into the complex double layer and hence no longer contribute to the conductivity of the mixture, although while substracting the conductivity of K_2SO_4 solutions (Ke) from the combined conductivity of the mixture of sol plus K_2SO_4 (Km), it was assumed that the conductivity of SO_4^{--} ions remains the same. Hence there will be greater fall in conductivity of the sol itself with the progressive addition of increasing amounts of electrolyte until the stage of rapid coagulation is reached. It has also been observed that there is a salt-effect[14] produced by the addition of K_2SO_4 on the conductivity of the polycharged colloid particles, but it is fairly small as compared to that produced by it in coagulating the sol.

The smaller decrease observed thereafter the rapid coagulation is of course due to the salt-effect as well as to the aggregation of the micelles when the resultant radius will increase and the mobility will decrease.

REFERENCES

1. Jain, P. C. and Banerji, S. N., *Proc. Nat. Acad. Sci. India*, (Forthcoming).
2. Jain, P. C. and Banerji, S. N., *J. Ind. Chem. Soc.*, **36**, 323 (1959).
3. Jain, P. C. and Banerji, S. N., *ibid*, (communicated).
4. Hamaker, H. C., *Rec. trav. Chim.*, **56**, 3 (1937).
5. Thomas, A. M. and Whitehead, T. H., *J. Phys. Chem*, **35**, 27 (1931).
6. Weiser, H. B., *J. Phys. Chem.*, **227**, 338 (1920).
7. Iyer, *Proc. Ind. Acad. Sci.*, **1**, 372 (1934).
8. Bohm, J., *Z. anorg. Chem*, **149**, 203 (1925).
   Bohm, J., and Niclassen, H., *Z. anorg. Chem.*, **132**, 7 (1923).
9. Fricke, H., and Havestadt, L., *Z. anorg. Chem.*, **188**, 357 (1930) *ibid.*, **196**, 120 (1931)
   Fricke, H., *Kolloid-Z.*, **56**, 166 (1931).
10. Weiser, H. B., and Milligan, W. O., *J. Phys. Chem.*, **40**, 40 (1936).
11. Rai, R. S. and Ghosh, S., *Proc. Nat. Acad. Sci. India*, **23**, 48, 142 (1954); *ibid.*, **25**, 190 (1956); *Kolloid-Z.*, **142**, 104 (1955).
12. Glazman, Y. M., Strazhesko, D. N., Zhel'vis, E. F. and Cherbyatsova, L. L., *Chem. Abstr.*, **54**, 45*b*, (1960).
13. Packter, A., *Kol'oid-Z.*, **150**, 60 (1957); **154**, 62 (1958), *ibid.*, **160**, 160; 1959, *ibid.*, **163**, 41; (1959), *Z. Physik. Chem.*, **211**, 40.
14. Onsager, L. and Fuoss, R. M., *J. Phys. Soc.*, **3**, 246 (1948).

CHEMISTRY OF VANADIUM. PART IX

FORMATION OF COMPOUNDS OF VCl_3 WITH ORGANIC SUBSTANCES

By

SARJU PRASAD *and* P. V. S. JAGANNADHA SARMA

Chemical Laboratories, Banaras Hindu University, Varanasi

[Received on 8th February, 1961]

ABSTRACT

Some compounds of VCl_3 with organic substances have been prepared, their properties studied and their structures discussed.

INTRODUCTION

In earlier communications[1] the action of vanadium-trichloride on some amines and heterocyclic bases was studied. The work has now been extended to study the action of vanadium-trichloride on some amines, nitranalines, aminobenzoic acids, and some other organic compounds in organic solvents.

EXPERIMENTAL

Vanadium-trichloride was prepared by the method described by Weinland and Feige[2] and was finally extracted with ether. The chemicals used were of B. D. H. or Merck's extra pure quality. Ether was distilled over metallic sodium.

In all the cases Ether was used as the solvent except in the case of *p*-Nitranaline, *p*-amino Benzoic acid and 8-hydroxy quinoline when the reaction was carried out in ethyl acetate medium.

In all the cases except Biuret and Michler's ketone a saturated solution of organic compound in ether was slowly added to the ethereal solution of vanadium-trichloride, with constant shaking till the precipitation was complete. It was left for about an hour, filtered, washed with the solvent till the washings did not give any precipitate with vanadium trichloride solution.

In case of Biuret and Michler's ketone the compound was taken in ether to which the vanadium trichloride solution was added slowly till the colour of vanadium trichloride persisted in solution, it was left for 24 hours with frequent shaking, filtered and washed free from VCl_3.

The precipitate was dried over fused calcium chloride in a vaccum desiccator.

Vanadium was estimated in dilute sulphuric acid by reduction with sulphurdioxide, removal of SO_2 by CO_2 and titration with standard solution of potassium permanganate at 70 C. Chlorine was estimated as AgCl by Piria and Schiff's method and the organic matter found by difference.

COMPOUNDS OF VANADIUM TRICHLORIDE WITH ORGANIC SUBSTANCES

S. No.	Organic Substances	Color of the Complex Compounds	M. P. C°	Vanadium %		Chlorine %		Organic Matter %		Probable formulae
				Found.	Calc.	Found.	Calc.	Found.	Calc.	
1.	Diethyl Amine	Black	60	10·76	11·09	22·80	23·71	66·44	65·20	$[V(NH.(C_2H_5)_2)_4]Cl_3$
2.	Triethyl Amine	Black	190	8·97	9·08	19·23	18·97	71·80	71·95	$[V\{N(C_2H_5)_3\}_4]Cl_3$
3.	Diiso Butyl Amine	Greenish Grey	210	7·12	7·57	16·21	15·81	76·67	76·52	$[V(NH\{(CH_3)_2CH.CH_2\}_2)_4]Cl_3$
4.	*m*-Anisidine	Black	150	9·58	10·17	20·91	21·24	69·51	68·59	$[V(NH._2CH_3O.C_6H_4)_4]Cl_3$
5.	8-Hydroxyquinoline	Dark Green	202	6·20	6·91	14·40	13·91	79·89	78·69	$[V(NOC_9H_7)_4]Cl_3$
6.	*O*-Nitraniline	Brownish Yellow	66	7·48	7·19	14·09	15·02	77·43	77·79	$[V(NH_2.C_6H_4.NO_2)_4]Cl_3$
7.	*P*-Nitraniline	Dirty Yellow	154	7·70	7·19	15·50	15·02	76·80	77·79	$[V(NH_2.C_6H_4.NO_2)_4]Cl_3$
8.	*m*-Nitraniline	Greenish Yellow	172	6·80	7·19	14·90	15·02	78·30	77·79	$[V(NH_2.C_6H_4.NO_2)_4]Cl_3$
9.	*O*-Aminobenzoic acid	Bluish Voilet	210	6·96	7·23	15·10	14·95	77·94	77·82	$[V(NH_2.C_6H_4COOH)_4]Cl_3$
10.	*P*-Aminobenzoic acid	Greenish Grey	180	7·35	7·23	14·50	14·95	78·15	77·82	$[V(NH_2.C_6H_4COOH)_4]Cl_3$
11.	*P*-Aminoacetanilide	Pale Green	227	6·40	6·54	14·70	13·98	78·90	79·48	$[V(NH_2.C_6H_4.NH.CO.CH_3)_4]Cl_3$
12.	Amidophenol	Dark Voilet	>250	7·02	7·23	15·45	15·10	77·52	77·62	$[V(NH_2.CO.C_6H_4OH)_4]Cl_3$
13.	Biuret	Cement Green	>250	10·70	10·86	29·06	22·69	66·24	66·45	$[V(NH_2.CO.NH.CO.NH_2)_2]Cl_3$
14.	Michler's Ketone	Yellowish Green	155	3·83	4·13	8·20	8·63	87·97	87·24	$[V\{(CH_3)_2N.C_6H_4.CO.C_6H_4.N(CH_3)_2\}_4]-Cl_3$

General Properties :—Most of the compounds are coloured, slightly hygroscopic, amorphous powder and give sharp melting point. They are insoluble in benzene, carbon tetrachloride or ether but soluble in alcohol. They are easily hydrolysed by hot water, acid or alkali solutions.

DISCUSSION

According to Sidgwick ("Electronic theory of valency" 1927) the maximum co-ordination number that vanadium can exhibit is 6.

In all the cases except Biuret four molecules of organic compound attach themselves to one molecule of VCl_3. It appears that organic compounds are linked to the central atom through the different co-ordinating groups and can be represented as V(4A) Cl_3 where A=organic compound.

In the case of Biuret two molecules of it attach themselves to one molecule of VCl_3, the linking appears to be of chelate type in which only CO groups are reactive. The compounds can be represented as

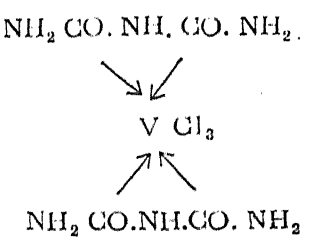

The E. A. N. does not assume the inert gas configuration and therefore the compounds are not very stable.

The authors sincere thanks are due to the authorities of Banaras Hindu University for providing necessary facilities.

REFERENCES

1. Sarju Prasad and K. N. Upadhyaya, *Jour. & Proc. Inst. Chem.*, 32, 257-264 (1960).
2. Wein Land, R. F., and Feige, C., *Ber.*, 36, 252 (1903).

STUDIES IN POLY-SALTS OF VANADIUM

PART I: ELECTROMETRIC STUDY OF THE SYSTEM: $(NH_4)_3VO_4 - HCl - H_2O$

By

P. K. BHATTACHARYA, M. C. SAXENA *and* S. N. BANERJI

Department of Chemistry, University of Saugar, Saugor

[Received on 8th February, 1961]

ABSTRACT

Conductometric and pH studies of the system, ammonium vanadate - hydrochloric acid, have been carried out by adopting the monovariation method. With M/10 solutions each of $(NH_4)_3VO_4$ and HCl, three breaks are obtained in the conductivity and pH curves at points corresponding to 1 : 1, 1 : 2, and 1 : 3·4, ammonium vanadate/HCl ratio. These breaks indicate the completion of aggregation for the formation of the di-, tetra-. and penta-vanadates, respectively, the last being probably formed through an intermediate stage of octavanadate. Further addition of acid results in the formation of the cation VO_2^+ or VO^{++}.

Similar breaks in the experimental curves have been obtained in the case of M/20 solutions of the two reactants. At an increased dilution, using M/40 solutions each of $(NH_4)_3 VO_4$ and HCl, the curves show only one break at 1 : 1 ratio, indicating thereby the absence of further stages of aggregation in dilute solutions.

Vanadium, like molybdenum and tungsten, has a tendency to form poly-acids and poly-salts, though to a lesser extent. Earlier literature describes the existence of vanadates of the ratio, $R_2O : V_2O_5 = 3 : 1, 2 : 1$ and $1 : 1$, similar to orthopyro- and meta-phosphates. Vanadates of the type $R_2O : V_2O_5 = 4 : 5, 3 : 5$ and $2 : 5$, respectively, are also reported by Jander and Jahr[1]. Diffusion coefficient studies[2] of the decomposition of sodium vanadate by acids reveal the existence of mono-, di-, tetra- and penta-vanadates at different H^+ ion concentration. The formation of poly salts by the acidification of ammonium meta-vanadate has been studied by Trujillo[3]. The stages in the formation of the pentavanadate are, however, still not well defined. In the present piece of work, therefore, an electrometric study of the effect of addition of mineral acids on ammonium vanadate has been carried out, the results obtained with hydrochloric acid being reported here.

EXPERIMENTAL

Analysed sample of ammonium vanadate (B. D. H.) and standardized hydrochloric acid have been used. Conductivity and pH measurements have been carried out by Doran Conductivity bridge and glass electrode Beckman pH -meter, respectively.

Monovariation method[4] has been used for the study of the poly vanadates. A series of solutions was prepared, keeping the volume of M/10 ammonium vanadate solution constant (5 ml.), and varying that of M/10 HCl; the total volume was kept constant (30 ml.) by the addition of conductivity water. Similar sets were prepared with M/20 and M/40 solutions, respectively. The conductivity and pH measurements were carried out as usual and the data plotted.

DISCUSSION

A study of the conductivity curves (Fig. 1) shows, that in the case of M/10 solutions (curve A), there is a slow increase in the conductivity with a break at vanadate to HCl ratio nearly 1 : 1 till the addition of about two equivalents of acid,

Fig. (1)

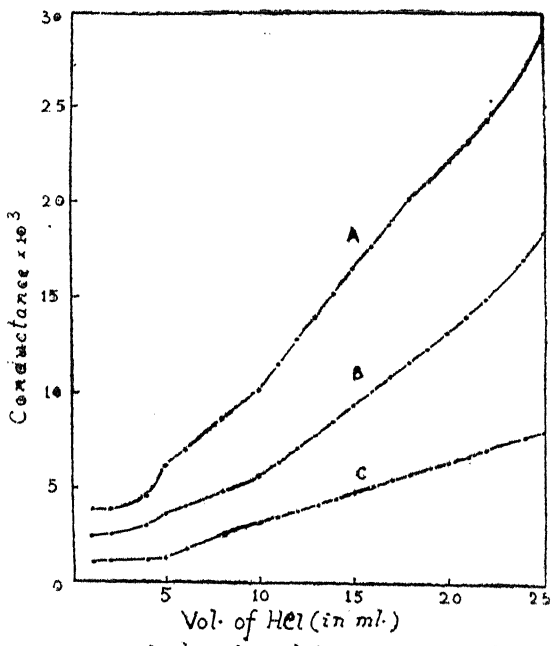

Conductometric study: Effect of addition of HCl on ammonium vanadate

and then the conductance changes more rapidly upto the ratio of about 1 : 3·4, after which the acid added remains unreacted.

Analogous breaks are obtained in the pH curve (Fig. 2, curve A). The above observations can be best explained if the process of aggregation is represented by the following equations, which show that the aggregation takes place gradually and in a continuous manner :

1. $2(NH_4)_3 VO_4 + 2HCl \rightarrow (NH_4)_4 V_2O_7 + H_2O + 2NH_4Cl$

   or,

   $2(NH_4)_3VO_4 + 6HCl \rightarrow 2H_3VO_4 + 6NH_4Cl$

   $2 H_3VO_4 + 4(NH_4)_3VO_4 \rightarrow 3 (NH_4)_4 V_2O_7 + 3H_2O$

2. $2 (NH_4)_4V_2O_7 + 4HCl \rightarrow (NH_4)_4 V_4O_{12} + 2H_2O + 4NH_4Cl$

3. $5 (NH_4)_4 V_4O_{12} + 8HCl \rightarrow 4 (NH_4)_3 V_5O_{14} + 4H_2O + 8NH_4Cl$

4. $(NH_4)_3 V_5O_{14} + 8HCl \rightarrow 5VO_2Cl + 4H_2O + 3NH_4Cl$

The gradual and slight increase in the conductivity of the system upto the ratio 1 : 2 is due to the formation of successive di- and meta- (tetra) vanadates according to the equation (1) and (2). In mixtures of vanadate/acid ratio less than 1 : 1, $(NH_4)_3 VO_4$ also exists in addition to the products $(NH_4)_4 V_2O_7$ and NH_4Cl. The conductivity of the mixture is due to the presence of $(NH_4)_3 VO_4$, $(NH_4)_4 V_2O_7$ and NH_4Cl, which have a greater contribution to the conductivity than the original

Fig. (2)

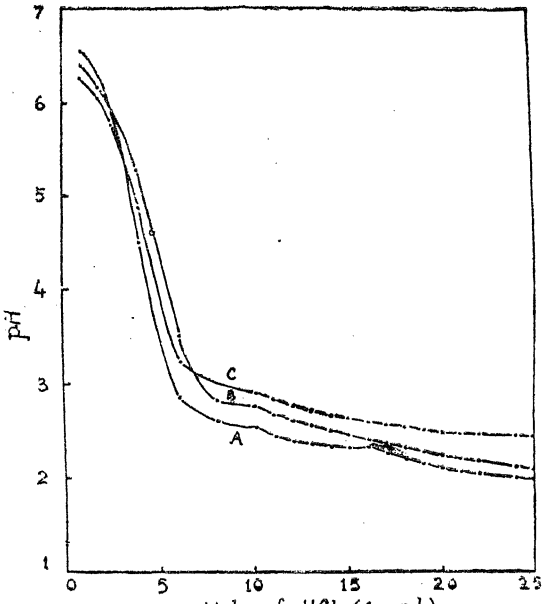

pH study: Effect of addition of HCl on ammonium vanadate

ions. When the composition exceeds 1 : 1, the tetravanadate begins to form and this process continnes till the composition reaches the ratio 1 : 2. There is an increase in conductance due to the resultant ions. The pH (fig. 2. curve A) falls throughout because of the production of the acid salt NH_4Cl and the stable polyvanadates. The further rise in conductivity after the ratio, 1 : 2, is due to the formation of the pentavanadate and this continues upto the ratio 1 : 3·4. The break in the curve at this point may be due to the formation of monomolecular vanadium containing the cation VO_2^+ or VO^{+++}. The sharp fall in pH ceases after the production of the tetravanadate at the ratio 1 : 2.

The ill-defined break at 1 : 2 ratio in fresh solutions is indicative of the fact that the formation of pentavanadate is a slow process. The conclusion is in consonance with Huckel's view[2], that the pentavanadic acid does not come into existence by the simple addition of a vanadate ion to tetravanadic acid, but rather that, continuing the polymerization series, a paring up of the latter acid to octavanadic acid takes place. The yellow pentavanadate is only produced with certainly after the formation of the octavanadate ion. This can be better studied in the aged systems.

The results which have been so far discussed are for the M/10 solutions. The plot of conductance (Fig. 1, curve B) and pH fig. 2, curve B) data in the case of M/20 solutions exhibit similar breaks as are obtained with M/10 solutions, though less pronounced. But with M/40 solutions (fig. 1, curve C) only one break at 1 : 1 ratio is obtained, after which there is a gradual increase in the conductivity and the curve remains smooth. The pH curve (fig. 2, curve C) also exhibits only one break. These results show that the process of aggregation of the vanadate is weakened with the decrease of concentration of ammonium vanadate, though the same vanadate/acid ratios are maintained.

The authors express their thanks to Prof. A. K. Bhattacharya, Head, Department of Chemistry, for his keen interest in the work.

REFERENCES

1. Jander and Jahr, *Z. anorg. Chem*, **211**, 49 (1933).
2. W. Huckel, "Structural Chemistry of Inorganic compounds," Elsevier Publishing Co. Vol. I, P. 202-204.
3. R. Trujillo, *Anales real Soc. Espan fis yu quim*, **50B**, 553-65 (1954).
4 Nayar and Pandey, *Proc. Ind. Acad. Sci.*, **27A**, (1948).

STUDIES IN POLY-SALTS OF VANADIUM

PART II : ELECTROMETRIC STUDY OF THE REACTION BETWEEN AMMONIUM VANADATE AND ORGANIC ACIDS

By

P. K. BHATTACHARYA, M. C. SAXENA *and* S. N. BANERJI

Department of Chemistry, University of Saugar, Saugor

[Received on 8th February, 1961]

ABSTRACT

Conductometric and pH studies of the systems $(NH)_3VO_4$ – acetic acid and $(NH)_3VO_4$ – oxalic acid have been carried out by using the monovariation method. The conductivity and pH curves in the system $(NH_4)_3VO_4$ – acetic acid with M/10 solutions show breaks corresponding to 1 : 1 and 1 : 2 ratios. This indicates the formation of the di- and tetra-vanadates ; the pH for that of the pentavanadate is not reached in this system. In the case of dilute solutions (M/20 and M/40) there is no further aggregation after the production of divanate. Acetic acid, unlike other organic acids, thus, behaves as a mineral acid in bringing about aggregation. The difference in the nature of the pH and conductivity curves is due to anion effect of the acid used.

Conductometric and pH study in the system $(NH_4)_3VO_4$ – oxalic acid reveals the formation of a 1 : 2 vanadium-oxalato-complex. The stoichiometry of the complex has been further confirmed by the Job's method of continuous variations. The probable molecular formula for the complex would be $(NH_4)_3[VO_2(C_2O_4)]$ aq. as suggested by Rosenheim.

The effect of organic acids (excepting acetic) on molybdates[1] and tungstates[2] has been found to be different from that of mineral acids, in that they produce complexes instead of bringing about aggregation, as is done by mineral acids. Oxalato-[3], malonate-[4], citrate-[5] and salicylato-[6] complexes with ammonium vanadate have been referred to in literature. In the present communication, we have studied the systems of ammonium vanadate with acetic acid and oxalic acid, respectively. The work has been further extended to the physico-chemical study of the complex formation between ammonium vanadate and oxalic acid.

EXPERIMENTAL

Analysed ammonium vanadate (B. D. H.), chemically pure acetic acid and AnalaR oxalic acid have been used for experimental studies. The systems $(NH_4)_3VO_4$ – acetic acid and $(NH_4)_3VO_4$ – oxalic acid have been investigated by

using the monovariation method[7]. Different sets of solutions were prepared by taking a constant volume (5 ml.) of M/10, M/20 or M/40 solutions of ammonium vanadate, varying that of equimolecular organic acid and keeping the total volume constant (30 ml.) by the addition of conductivity water.

Recourse has been taken to Job's method of continuous variations[8] for ascertaining the stoichiometry of the complex formed in the system $(NH_4)_3VO_4$ —oxalic acid. The conductivity and pH measurements have been carried out as usual by the Doran Conductivity bridge and glass-electrode Beckman pH-Meter, respectively. The experimental data have been plotted.

DISCUSSION

(*1*) *System* :— *Ammonium Vanadate — acetic acid* :—

Curve A (Fig. 1) of the system with M/10 solutions shows that the conductivity

Fig (1)

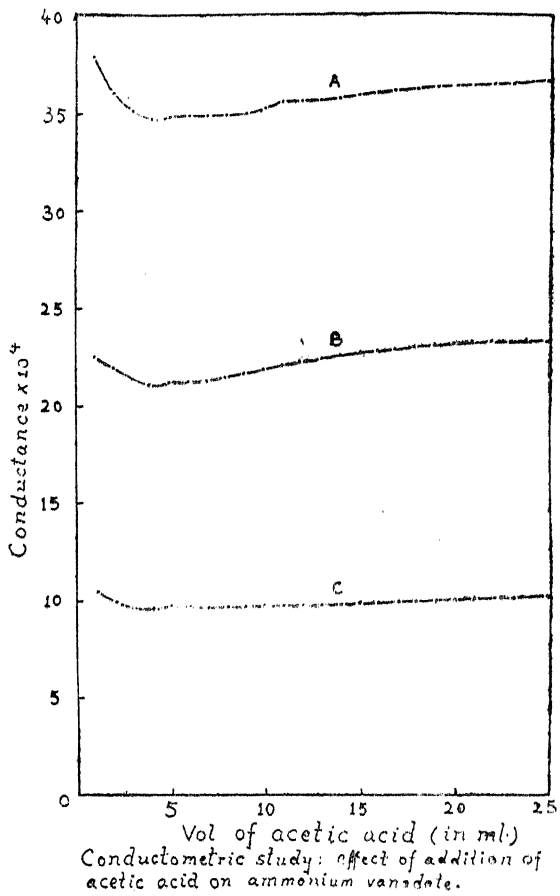

Conductometric study: effect of addition of acetic acid on ammonium vanadate.

falls with the increase of the ratio of vanadate to acetic acid upto 1 : 1, after which it remains almost constant upto the ratio 1 : 2. Further addition of acetic acid shows a smooth rise in conductivity indicating, thereby, that the acid has no further effect. The slight fall in conductivity upto the ratio 1 : 1 is due to the formation of the di-vanadate ($V_2O_7^{4-}$). The conductivity remains constant, thereafter, upto the ratio 1 : 2 due to the aggregation to tetravanadate. Further aggregation for the formation of pentavanadate is not met with in the case of this acid. The conductivity curves (B and C, Fig. 1) with M/20 and M/40 solutions, respectively, show only one break at the ratio 1 : 1 indicating the absence of further stages of aggregation.

The pH results (Fig. 2) are in accord with those of conductance. The curves A, B and C (Fig. 2.) stand for M/10, M/20 and M/40 equimolar solutions,

Fig. (2)

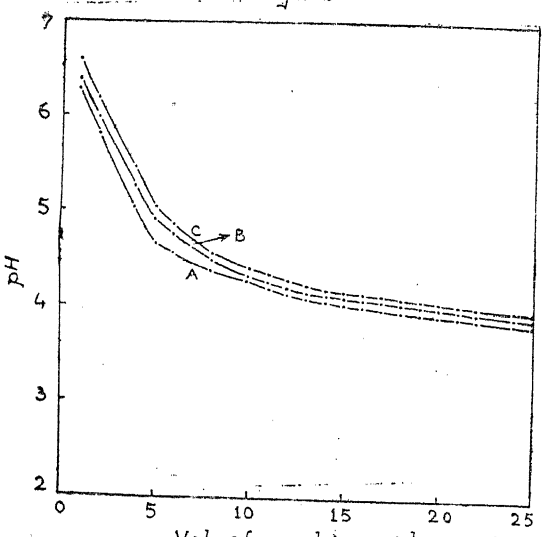

pH study : effect of addition of acetic acid on ammonium vanadate.

respectively, of ammonium vanadate and acetic acid. The data indicate that in the system, ammonium vanadate – acetic acid, the pH required (2·5 – 3) for the formation of pentavanadate is not reached.

Acetic acid, thus, behaves as a mineral acid in bringing about the aggregation of vanadate ions. But the nature of the curve is different from that in the case of HCl. This may be due to the anion of the acid, the role of which can be explained by the consideration of an intermediate stage of the formation of vanadic acid during the polymerization of vandates (see eqn. (1) part I, page 75).

The anion of the acid has a definite influence on the weak and amphoteric vanadic acid before it can bring about the aggregation.

(2) *System :—Ammonium vanadate – Oxalic acid :—*

The experimental curves of conductivity (Fig. 3, curve A, B and C) and pH

Fig.(3)

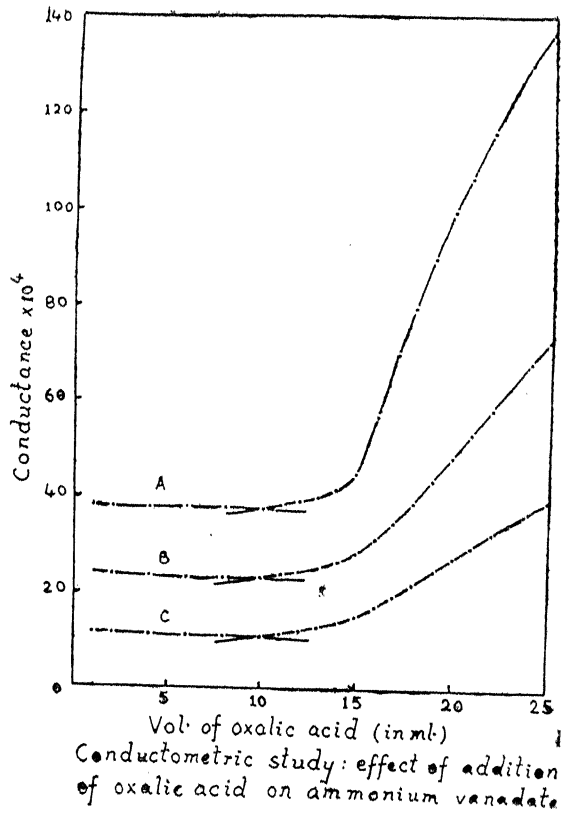

Conductometric study : effect of addition of oxalic acid on ammonium vanadate

(Fig. 4, curves A, B and C) measurements of the system, $(NH_4)_3 VO_4 - C_2H_2O_4$, show breaks only at 1 : 2 ratio of ammonium vanadate to oxalic acid indicating thereby,

Fig. (4)

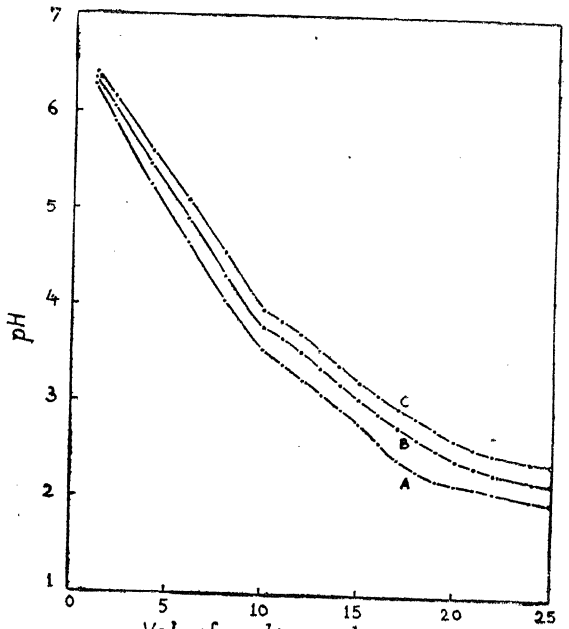

pH study: effect of addition of oxalic acid on ammonium vanadate

Fig. (5)

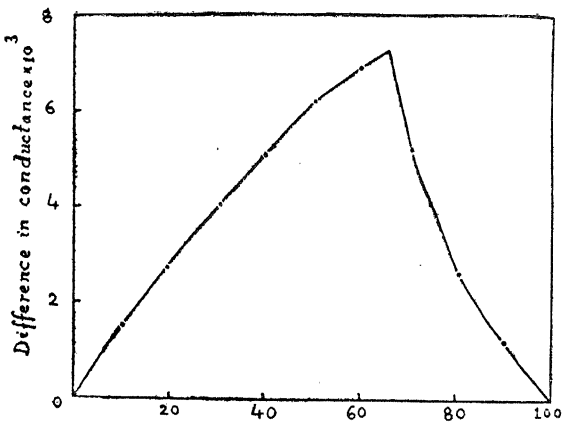

Composition of the vanadium-oxalato-complex by Job's method of continuous variations using equimolar solutions (M/40) of $(NH_4)_3VO_4$ and oxalic acid

the formation of a 1 : 2 vanadium-oxalato complex. This break is obtained irrespective of the dilution of the solutions, and this confirms the formation of a complex and the absence of aggregation. This is further confirmed by Job's continuous variation method (*loc. cit.*) which shows a maximum in the curve (Fig. 5) at a point corresponding to 66% of oxalic acid. The complex should be $(NH_4)_3$ $[VO_2 (C_2O_4)_2]$ aq. as suggested by Rosenheim[9]. The liberation of H^+ ions from oxalic acid for complex formation is clearly indicated by the pH curves (Fig. 4) which show a continuous fall in pH values.

The work with other organic acids is in progress.

The authors express their thanks to Prof. A. K. Bhattacharya for his keen interest in the work.

REFERENCES

1. Rao and Banerji, Proc. Symposium on the Chemistry of Co-ordination Compounds, Agra Part III, 95-101 (1959)
2. Rao and Banerji, *Proc. Nat. Acad. Sci., India*, **23A**, 76 (1954)
3. Kopel and Goldman, *Z. anorg. Chem.*, **36**, 281 (1903)
4. W. Schramm., *Ibid.*, **161**, 231 (1927)
5. G. A. Barbieri, *Atti. R.*, (5), **24**, 1, (1915)
6. A. Rosenheim and Hsin Yu Mong., *Z. anorg. Chem.*, **148**, 25 (1925)
7. Nayar and Pandey, *Proc. Ind. Acad. Sci.*, **27A**, 284 (1948)
8. P. Job, *Ann. Chim.*, **9**, 113 (1928)
9. A. Rosenheim, *Z. anorg. Chem.*, **4**, 368 (1893)

STUDY OF THE EXTENT OF AGGREGATION DURING SOL-GEL TRANSFORMATION OF SOME GEL FORMING SYSTEMS

By

Y. D. UPADHYA *and* S. P. MUSHRAN

Chemical Laboratories, The University, Allahabad

[Received on 1st March, 1961]

ABSTRACT

The sol-gel transformation of the gel yielding zirconium succinate sols employing a Stormer viscosimeter has been investigated. The extent of aggregation during sol-gel transformation has been assessed employing the Staudinger's viscosity relation $\eta_{sp}=KcM$. The results obtained have been discussed and explained.

Various methods have been adopted from time to time to study sol-gel transformation of several gel forming colloidal systems. Von Schroeder[1], Lewites[2], Sheppard[3], Banerji and Ghosh[4], have studied the changes in viscosity during gelation of gelatin gels under various conditions and have concluded that for some time the rate of increase of viscosity is nearly proportional to the time, but afterwards it becomes irregular. Mardles[5] made viscometric studies of gel forming systems in non-aqueous media and Prasad and coworkers[6] in soap gel-forming systems in organic media.

The changes in optical properties during sol-gel transformation have also been investigated. Prakash[7] observed changes in extinction co-efficients and Prasad and coworkers[8] investigated the changes taking place in the intensity and depolarisation factors of the light scattered, using polarised incident light. Recently, the depolarisation factors and the angular variation of the intensity of light scattered from gel forming systems of sodium soaps in organic solvents have been investigated.[9]

Sen and Ghosh[10] investigated the rate of change of turbidity with time of silicic acid sols. According to them the turbidity increases, becomes maximum approximately at or near the time of gelation and then gradually decreases. The time of gelation could be determined graphically from turbidity measurements.

The sol-gel transformation of the gel yielding zirconium succinate sols investigated here have been studied by us employing viscometric methods and in this paper we are presenting our results on such measurements.

The zirconium succinate sols were obtained by the method described by Upadhya and Mushran[11].

Three samples of zirconium succinate sols were prepared by adding to a fixed quantity of the metal nitrate, different amounts of sodium succinate, below the precipitation value, keeping total volume the same. The sols were purified by dialysis at the room temperature. The zirconium content of these samples were estimated, and for the purpose of investigation, the metal content in the sols was

maintained constant by diluting the sols with distilled water, wherever necessary.

Sols (A), (B) and (C) had the following compositions :

Volume of 0·3570 M zirconium nitrate = 150·00 mls.

0·25M sodium succinate :

in sol (A) = 90·00 mls.

in sol (B) = 95·00 mls.

in sol (C) = 100·00 mls.

The sols were purified by dialysis for a period of 96 hours.

These succinate sols yield transparent gels with electrolytes of suitable concentrations. The process of gelation can be easily followed by following the changes in the viscosity of the gel forming sols. As the sols approach the gel state the viscosity increases considerably, the time of flow through a capillary becomes very large, leading to unsuspected errors in the measurements, which therefore become less reliable. The cylindrical rotational viscometers are, however, of great use, in the measurements of the viscosity in such cases, as the rate of shear can be conveniently varied.

A Stormer viscosimeter, cup and rotor type, supplied by Arthur, Thomas Co. U. S. A., was employed for following the viscosity changes during gelation of zirconium succinate sols. The viscosimeter was fitted with a liquid circulating stage to control the temperature of the substance under investigation. Several drops of glycerine were deposited on the surface of the stage for purposes of assuring good contact with the water bath. The inlet and outlet of the circulating stage were connected by means of a rubber hose to a constant temperature bath worked by a thermomix regulator. With this arrangement temperature control was maintained within $0 \pm 0{\cdot}1^{\circ}C$ at $30^{\circ}C$. A fine nylon thread was used to support the weight, which was suitably chosen, in a manner to avoid turbulence until a convenient speed of the rotor is attained. To a fixed amount of sol was added a known amount of electrolyte KCl, and the mixture was taken in the cup and the cylindrical rotor was immersed in the sol electrolyte mixture. By releasing the brake, the rotor was allowed to revolve. The time required for 100 revolutions of the rotor, as indicated by the revolution counter, was recorded at a constant temperature $30^{\circ} \pm 0{\cdot}1^{\circ}C$. from which the number of revolutions per second were calculated. The values of rev. per sec. were found out at suitable intervals. The initial reading of the revolution of the rotor were taken after two minutes of mixing and the results with the three different sols A, B and C are tabulated in Tables 1 to 9.

The relative viscosity is obtained by dividing the reciprocal of revolutions per second for sol with the reciprocal of revolutions per second for water, using the same driving weight. The value of η_{sp}, the specific viscosity is then culculated and is given in column 4.

TABLE 1

Showing the values of 1/rev. per sec., η_{sp} and aggregation with time.

Volume of sol (A) = 60·00 mls.
N/30 KCl = 8·00 mls.
Total volume = 95·00 mls.

Time in mins.	Time for 100 rev. in secs.	1/rev. per sec.	η_{sp}	Aggregation
0	22·90	0·229	0·027	1·000 M_o
10	23·00	0·230	0·031	1·148
20	23·10	0·231	0·036	1·333
30	23·40	0·234	0·049	1·814
40	24·10	0·241	0·080	2·998
50	24·40	0·244	0·094	3·481
60	24·70	0·247	0·108	3·999
70	25·40	0·254	0·139	5·147
80	26·30	0·263	0·179	6·630
90	28·00	0·280	0·255	9·443
100	32·60	0·326	0·461	17·080
105	43·00	0·430	0·928	34·370
110	70·00	0·700	0·139	79·210
115	98·10	0·981	3·399	125·900
120	98·50	0·985	3·417	126·600
125	143·90	1·439	5·453	201·900

TABLE 2

Showing the values of 1/rev. per sec., η_{sp} and aggregation with time.

Volume of sol (A) = 60·00 mls.
N/30 KCl = 10·00 mls.
Total Volume = 95·00 mls.

Time in mins.	Time for 100 rev. in sec.	1/rev. per sec.	η_{sp}	Aggregation
0·00	23·00	0·230	0·031	1·000 M_o
15·00	23·20	0·232	0·040	1·290
25·00	24·50	0·245	0·098	3·161
35·00	24·80	0·248	0·112	3·612
50·00	26·40	0·264	0·184	5·934
65·00	29·90	0·299	0·340	10·960
80·00	64·30	0·643	1·883	60·740
85·00	76·60	0·766	2·435	78·540
90·00	100·50	1·005	3·507	113·200
95·00	139·70	1·397	5·264	169·700

TABLE 3

Showing the values of 1/rev. per sec., η_{sp} and aggregation with time.

Volume of sol (A) = 60·00 mls.
N/30 KCl = 12·00 mls.
Total volume = 95·00 mls.

Time in mins.	Time for 100 rev. in secs.	1/rev. per sec.	η_{sp}	Aggregation
0·00	23·50	0·235	0·053	1·000 M_o
10·00	24·20	0·242	0·085	1·604
20·00	25·00	0·250	0·121	2·283
30·00	26·80	0·268	0·202	3·811
40·00	35·10	0·351	0·574	10·830
45·00	47·60	0·476	1·134	21·396
50·00	77·00	0 770	2·453	46·283
55·00	108·90	1·089	3·883	73·264
60·00	156·70	1·567	6·026	113·698
65·00	211·50	2·115	8·036	151·623

TABLE 4

Showing the values of 1/rev. per sec., η_{sp} and aggregation with times.

Volume of sol (B) = 54·00 mls.
N/30 KCl = 11·00 mls.
Total volume = 90 00 mls.

Time in mins.	Time for 100 rev. in secs.	1/rev. per sec.	η_{sp}	Aggregation
0·00	23·50	0·235	0·0538	1·000 M_o
10·00	23·80	0·238	0·06726	1·251
20·00	24·30	0·243	0·08969	1·666
30·00	24·80	0·248	0·1121	2·083
40·00	26·70	0·267	0·1973	3·667
50·00	28·00	0·280	0·2557	4·755
60·00	33·10	0·331	0·4843	9·018
70·00	48·50	0·485	1·1750	21·840
80·00	116·50	1·165	4·2250	78·500
85·00	139·50	1·395	5·2570	97·700

TABLE 5

Showing the values of 1/rev. per sec., η_{sp} and aggregation with time.

Volume of sol (B) = 54·00 mls.

N/30 KCl = 13·00 mls.

Total Volume = 90·00 mls.

Time in mins.	Time for 100 rev. in secs.	1/rev. per sec.	$\eta_{sp.}$	Aggregation
0·00	23·60	0·236	0·05965	1·000 M_o
10·00	24·00	0·240	0·08072	1·353
20·00	24·80	0·248	0·1119	1·875
30·00	26·40	0·264	0·1839	3·083
40·00	30·30	0·303	0·3588	6·016
50·00	38·50	0·385	0·7263	12·160
60·00	89·00	0·890	2·9900	50·240
70·00	120·00	1·200	4·3810	73·450

TABLE 6

Showing the values of 1/rev. per sec., η_{sp} and aggregation with time.

Volume of sol. (B) = 54·00 mls.

N/30 KCl = 15·00 mls.

Total Volume = 90·00 mls.

Time in mins.	Time for 100 rev. in secs.	1/rev. per sec.	η_{sp}	Aggregation
0·00	24·00	0·240	0·07174	1·000 M_o
10·00	26·30	0·263	0·1794	2·501
20·00	27·20	0·272	0·2198	3·062
30·00	30·40	0·304	0·3633	5·065
40·00	41·70	0·417	0·6910	9·634
45·00	59·60	0·596	1·6730	23·320
50·00	78·20	0·782	2·5070	34·830
55·00	115·50	1·155	4·1780	58·320

TABLE 7

Showing the values of 1/rev. per sec., η_{sp} and aggregation with time.
Valume of sol (C) = 54·00 mls.
N/30 KCl = 7·50 mls.
Total volume = 95·00 mls.

Time in mins.	Time for 100 rev. in secs.	1/rev. per sec.	η_{sp}	Aggregation
0·00	23·80	0·238	0 0680	1·000 M_o
10·00	24·00	0·240	0·0740	1·088
20·00	24·20	0·242	0·0850	1·250
30·00	24·30	0·243	0·0900	1·323
40·00	24·50	0·245	0·0980	1·441
50·00	25·00	0·250	0·1210	1·779
60·00	25·40	0·254	0·1390	2·440
70·00	27·00	0·270	0·2210	3·250
80·00	30·00	0·300	0·3450	5·074
90·00	38·40	0·384	0·7220	10·620
95·00	43·10	0·431	0·9330	13·720
100·00	51·50	0·515	1·3100	19·270
105·00	72·20	0·722	2·2380	32·910
110·00	90·80	0·908	3·0710	45·150
115·00	162·30	1·623	6·2780	92·340

TABLE 8

Showing the values of 1/rev. per sec., η_{sp} and aggregation with time.
Volume of sol (C) = 54·00 mls.
N/30 KCl = 9·00 mls.
Total volume = 95·00 mls.

Time in mins.	Time for 100 rev. in secs.	1/rev. per sec.	η_{sp}	Aggregation
0·00	24·00	0·240	0·0750	1·000 M_o
10·00	24·20	0·242	0·0850	1·133
20·00	24·40	0·244	0·0940	1·253
30·00	24·60	0·246	0·1020	1·360
40·00	24·80	0·248	0·1130	1·507
50·00	25·90	0·259	0·1610	2·146
60·00	28·60	0·286	0·2820	3·795
70·00	36·60	0·366	0·6420	8·559
80·00	55·10	0·551	1·4710	19·610
90·00	61·40	0·614	1·7160	22·880
95·00	77·30	0·773	2·4660	32·880
100·00	96·20	0·962	3·3140	44·180
105·00	130·00	1·300	4·8290	64·370

TABLE 9

Showing the values of 1/rev. per sec., η_{sp} and aggregation with time.

Volume of sol (C) = 54·00 mls.
N/30 KCl = 10·55 mls.
Total volume = 95·00 mls.

Time in mins.	Time for 100 rev. in secs.	1/rev. per sec.	η_{sp}	Aggregation.
0·00	24·20	0·242	0·0840	1·000 M_o
10·00	24·40	0·244	0·0940	1·119
20·00	24·60	0·246	0·1040	1·238
30·00	25·40	0·254	0·1390	1·665
40·00	27·80	0·278	0·2470	2·941
50·00	34·30	0·343	0·5380	6·404
60·00	66·80	0·668	1·9950	23·750
70·00	76·80	0·768	2·4440	29·090
80·00	115·00	1·150	4·1570	49·480

DISCUSSION

A perusal, of the Tables 1 to 9 and of Figs. 1, 2 and 3, shows that the initial viscosities of sols depend upon the concentration. When an electrolyte is

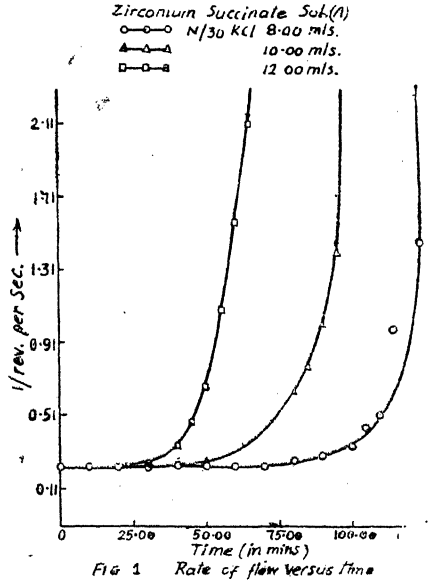

FIG 1 Rate of flow versus time

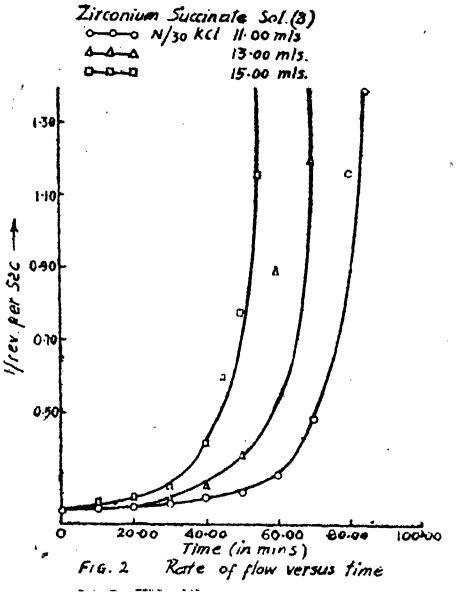

FIG. 2 Rate of flow versus time

added, with the progress of time, the viscosity increases at first very slowly, then with appreciable speed and finally, just before the gelling time it shoots up to a high value,

From the rate of change of viscosity, with time, it has been possible to visualise the degree of aggregation in the succinate sols with the help of Staudinger's viscosity relation :

$$\frac{\eta_{sp}}{c} = K_m.M$$

$$\eta_{sp} = \eta/\eta_o - 1$$

$$= \eta_r - 1$$

where η_{sp} = specific viscosity

η_o = viscosity of the medium

c = Concentration

K_m = Constant

M = Molecular weight.

The extent of aggregation in succinate sole at different intervals of time have been calculated from the above equation in terms of M_o the extent of aggregation in a sol at the time of initial observation. The results are presented in column 5 of the tables.

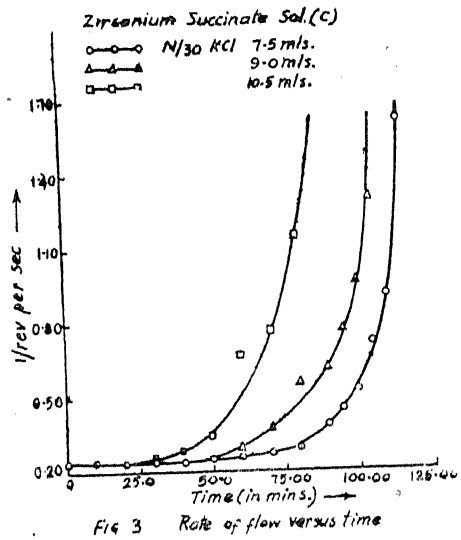

Fig 3 Rate of flow versus time

It will be seen from the tables 1 to 9 that a gradual increase in the extent of aggregation in the succinate sols is noticeable in the beginning but near about the point where gel is obtained, the extent of aggregation increases considerably.

The very steep rise in the viscosity, suggesting a large increase in aggregation during the last stage of gelation region, is due to the considerable increase in structuration, essential for gel formation.

ACKNOWLEDGEMENTS

Thanks of the authors are due to Professor S. Ghosh, D.Sc., F.N.I., for his interest in these investigations and to the U. P. Scientific Research Committee for the grant of a research scholarship to one of the authors (Y.D.U.) to support this work.

REFERENCES

1. Von Schroeder, K. : *Z. physikal. Chem.*, **45**, 75 (1903)
2. Lewites, S. J. : *Kolloid-Z.*, **2**, 208 (1907)
3. Sheppard, S. E. : *J. Phys. Chem.*, **14**, 273 (1910)
4. Banerji, S. and Ghosh, S. : *J. Ind. Chem. Soc.*, **31**, 923 (1930)
5. Mardless, F. W. : *Trans. Faraday Soc.*, **18**, 327 (1923)
6. Prasad, M. : *Proc. Ind. Acad. Sci.*, **24A**, 295 (1946)
7. Prakash, S. : *J. Phys. Chem.*, **36**, 1324 (1932)
8. Prasad, M. : *J. Coll. Sci.*, **7**, 178 (1952)
9. Sundaram, S. : *Proc. Ind. Acad. Sci.*, **60A**, 176 (1954)
10. Sen, K. C. and Ghosh, B. N. : *J. Ind. Chem. Soc.*, **33**, 403 (1956)
11. Upadhya, Y. D. and Mushran, S. P. : *Kolloid-Z.*, **171**, 31 (1960)

ON MUTUAL RELATIONSHIPS BETWEEN VARIOUS INTEGRAL TRANSFORMS*

By

C. B. L. VERMA

T. R. S. College, Rewa, M. P.

[Received on 24th February, 1961]

1. In the present paper we investigate the inter-relationships between the various integral transforms including the generalizations of the well-known Laplace Transform. The transforms considered are :

(*a*) The Laplace Transform,

$$\phi(p) = \int_0^\infty e^{-pt} f(t)\, dt\,, \quad R(p) > 0 \tag{1.1}$$

which we symbolically denote as

$$\phi(p) \doteq f(t)$$

(*b*) Varma's generalization of Laplace Transform (10)

$$\phi_1(p) = \int_0^\infty e^{-\frac{1}{2}pt}\ (pt)^{m-\frac{1}{2}}\ W_{k,m}(pt)\, f(t)\, dt\,, \quad R(p) > 0 \tag{1.2}$$

$$\text{or } \phi_1(p) \overset{V}{\underset{k,m}{\doteq}} f(t)$$

(*c*) Meijer's generalized transforms :

$$(i)\ \psi_1(p) = \int_0^\infty e^{-\frac{1}{2}pt}\ (pt)^{-k-\frac{1}{2}}\ W_{k+\frac{1}{2},m}(pt) f(t)\, dt\,, \quad R(p) > 0 \tag{1.3}$$

$$\text{or } \psi_1(p) \overset{M}{\underset{k,m}{\doteq}} f(t)$$

$$(ii)\ \psi_2(p) = \int_0^\infty (pt)^{\frac{1}{2}} K_\nu(pt) f(t)\, dt \qquad R(p) > 0$$

$$\text{or } \psi_2(p) \overset{K}{\underset{\nu}{\doteq}} f(t) \tag{1.4}$$

*Read at the 30th Annual Session of the Academy on February 3, 1961.

(*d*) The Hankel Transform [(2) (p. 5)]

$$g(p) = \int_0^\infty (pt)^{\frac{1}{2}} \; J_\nu \; (pt) f \; (t) \, dt, \; R \; (p) > 0 \tag{1.5}$$

$$\text{or } g(p) \underset{\nu}{\overset{J}{=}} f(t)$$

(*e*) The H-Transform [(2) p. 157]

$$g_1(p) = \int_0^\infty (pt)^{\frac{1}{2}} \; H_\nu \; (pt) f(t) \, dt, \; R \; (p) > 0 \tag{1.6}$$

$$\text{or } g_1(p) \underset{\nu}{\overset{H}{=}} f(t)$$

2. *Theorem* 1. If $\phi(p) \doteqdot f(t)$

$$\text{and } \psi(p) \underset{k,m}{\overset{V}{=}} f(t)$$

then

$$\psi(p) = \frac{\Gamma(2m+1)}{\Gamma(m-k+{}^3/_2)} \; \frac{1}{2\pi i p} \int_{c-i\infty}^{c+i\infty} {}_2F_1 \left[{2m+1, 1 \atop m-k+{}^3/_2} : \frac{z}{p} \right] \phi(z) \, dz, \tag{2.1}$$

where R $(2m+1) > 0$, R $({}^3/_p) < 1$ and if p is real then $p > c$ and provided that [(4) p. 177]

(*i*) $f(t)$ belongs to L (o, ∞)

(*ii*) All the singularities of $\phi(z)$ are on the left side of $c \pm i\infty$

(*iii*) $|\phi(z)| \sim 0 \; (z^\alpha)$ uniformly with respect to phase z as $|z| \to \infty$ in the range

$$-\tfrac{1}{2}\pi \leqslant \text{phase } z \leqslant \tfrac{1}{2}\pi, \quad R \; (\alpha) < -1$$

Proof: We have

$$\psi(p) = \int_0^\infty e^{-\frac{1}{2}pt} \; (pt)^{m-\frac{1}{2}} \; W_{k,m} \; (pt) f \; (t) \, dt \tag{2.2}$$

and

$$\phi(p) = \int_0^\infty e^{-pt} f \; t) \, dt \tag{2.3}$$

then the Mellin - inversion formula for (2,3) gives under conditions (*i*) & (*ii*) stated above

$$f(t) = \frac{1}{2\pi i} \int_{c-i\infty}^{c+i\infty} e^{zt}\, \phi(z)\, dz \tag{2.4}$$

Substituting this value of $f(t)$ in (2·2) and inverting the order of integration which is permissible because of uniform and absolute convergence (Fubini's theorem), We obtain

$$\psi(p) = \frac{1}{2\pi i} \int_{c-i\infty}^{c+i\infty} \phi(z)\, dz \int_0^\infty e^{-(\frac{1}{2}p - z)\,t}\ (pt)^{m-\frac{1}{2}}\, W_{k,m}(pt)\, dt \tag{2·5}$$

The latter integral may be evaluated by using Goldstein's result (3) *viz* :

$$\int_0^\infty x^{l-1} e^{-(a^2+\frac{1}{2})\,x}\, W_{k,m}(x)\, dx$$

$$= \frac{\Gamma(\frac{1}{2} + l \pm m)}{\Gamma(1 - k + l)}\ {}_2F_1\left[\begin{matrix}\frac{1}{2} \pm m + l \\ 1 - k + l\end{matrix} : -a^2\right] \tag{2·6}$$

$$R(a^2 + 1) > 0,\ R(\tfrac{1}{2} + l \pm m) > 0$$

Hence the theorem.

3. *Theorem* 2 :

If $\phi(p) \cdot\!\!-\!\!\circ\ f(t)$

and $\psi(p) \underset{k,m}{\overset{M}{-\!\!\circ}} f(t)$

then

$$\psi(p) = \frac{\Gamma(1 - k \pm m)}{\Gamma(1 - 2k)}\ \frac{1}{2\pi i p} \int_{c-i\infty}^{c+i\infty} {}_2F_1\left[\begin{matrix}1 - k \pm m \\ 1 - 2k\end{matrix} : \frac{z}{p}\right] \phi(z)\, dz$$

$$R(1 - k \pm m) > 0,\ R(z/p) < 1 \tag{3·1}$$

and under the same conditions as in theorem 1.

The proof is also exactly similar to that followed in § 2.

4. *Theorem* 3 :

If $\phi(p) \underset{\lambda,\mu}{\overset{M}{-\!\!\circ}} f(t)$

and $\psi(p) \underset{k,m}{\overset{V}{-\!\!\circ}} f(t)$

then

$$\psi(p) = \frac{\Gamma(1 \pm \lambda + \mu)\,\Gamma(1 + \mu + \lambda + 2m)}{\Gamma(1 + 2\mu)\,\Gamma(\lambda + \mu + 3/2 + m - k)} \quad \frac{1}{2\pi i}\, p^{-\lambda-\mu-1} \tag{4·1}$$

$$\times \int_{c-i\infty}^{c+i\infty} {}_3F_2\left[\begin{matrix} 1 + \lambda + \mu + 2m,\ 1 \pm \lambda + \mu \\ 1 + 2\mu,\ \lambda + \mu + \frac{3}{2} + m - k \end{matrix} : \frac{z}{p}\right] z^{\lambda+\mu}\,\phi(z)\,dz$$

$$R(1 \pm \lambda + \mu) > 0, \qquad R(1 + \mu + \lambda + 2m) > 0$$

and under the same conditions as in theorem 1.

Proof: Since

$$\phi(p) = \int_0^\infty e^{-\frac{1}{2}pt}\,(pt)^{-\lambda-\frac{1}{2}} W_{\lambda+\frac{1}{2},\mu}(pt)\,f(t)\,dt \tag{4.2}$$

we have by Inversion theorem (5)

$$f(t) = \frac{\Gamma(1 - \lambda + \mu)}{\Gamma(1 + 2\mu)} \quad \frac{1}{2\pi i} \int_{c-i\infty}^{c+i\infty} e^{\frac{1}{2}tz}(tz)^{\lambda-\frac{1}{2}} M_{\lambda-\frac{1}{2},\mu}(tz)\,\phi(z)dz \tag{4.3}$$

$$R(1 - \lambda + \mu) > 0.$$

Substituting this value of $f(t)$ in

$$\psi(p) = \int_0^\infty e^{-\frac{1}{2}pt}\,(pt)^{m-\frac{1}{2}} W_{k\,m}(pt)\,f(t)\,dt$$

and inverting the order of integration which is permissible as before, we obtain

$$\psi(p) = \frac{\Gamma(1 - \lambda + \mu)}{\Gamma(1 + 2\mu)} \cdot \frac{1}{2\pi i} \int_{c-i\infty}^{c+i\infty} z^{\lambda+\mu}\,\phi(z)dz \int_0^\infty e^{-\frac{1}{2}pt}\,(pt)^{m-\frac{1}{2}} W_{k,m}(pt)$$

$$t^{\lambda+\mu}\left\{ e^{\frac{1}{2}tz}\,(zt)^{-\mu-\frac{1}{2}} M_{\lambda-\frac{1}{2},\mu}(zt) \right\} dt$$

The latter integral may evaluated by expanding $M_{\lambda-\frac{1}{2},\mu}$ in series, (11) p. 336 and then integrating term by term and using ((8) p. 30)

$$\frac{\Gamma(\nu + 1 + m \pm m)}{\Gamma(\nu + \frac{3}{2} + m - k)}\; p^{-\nu-1}\, \overline{\overline{V}}_{k,m}\, t^{\nu}$$

We therefore obtain

$$\psi(p) = \frac{\Gamma(1 \pm \lambda + \mu)\,\Gamma(1 + \lambda + \mu + 2m)}{\Gamma(1 + 2\mu)\,\Gamma(\lambda + \mu + {}^3/_2 + m - k)} \frac{1}{2\pi i} p^{-\lambda-\mu-1}$$

$$\times \int_{c-i\infty}^{c+i\infty} z^{\lambda+\mu}\, {}_3F_2\left[\begin{matrix} 1 \pm \lambda + \mu,\ 1 + \lambda + \mu + 2m \\ 1 + 2\mu,\ \lambda + \mu + \frac{3}{2} + m - k \end{matrix} : \frac{z}{p}\right] \phi(z)\, dz$$

$$R(1 \pm \lambda + \mu) > 0,\ R(1 + \mu + \lambda + 2m) > 0$$

and under the conditions stated in the theorem.

If we put $\lambda = -\mu$, ${}_3F_2$ degenerates into ${}_2F_1$ and we get theorem 1.

5. *Theorem* 4: If $f(t)$ and $t^{\rho-1} f\left(\frac{1}{t}\right)$ belong to $L(0, \infty)$

and if $g(p) \underset{\nu}{\overset{J}{=}} f(t)$

and $\phi(p) \underset{\mu}{\overset{K}{=}} t^{\rho-1} f\left(\frac{1}{t}\right)$

then

$$\phi(p) = 2^{\rho-2}\, p^{-\rho+\frac{1}{2}} \int_0^\infty z^{\frac{1}{2}}\, G^{3,0}_{0,4}\left(\frac{p^2z^2}{16} \,\middle|\, \begin{matrix} \frac{\nu}{2}, & \frac{\rho+\mu}{2}, & \frac{\rho-\mu}{2}, & \frac{-\nu}{2} \end{matrix}\right) g(z)\, dz \tag{5.1}$$

$$R(p) > |R(\mu)| - {}^3/_2;\ R(z) > 0,\ R(p) > 0,\ R(\nu) > -\tfrac{1}{2}.$$

Proof: Since $g(p)$ is the Hankel Transform of order ν of we have

$$f(t) = \int_0^\infty (tz)^{\frac{1}{2}}\, J_\nu(tz)\, g(z)\, dz \tag{5.2}$$

and

$$\phi(p) = \int_0^\infty (pt)^{\frac{1}{2}}\, K_\mu(pt)\, t^{\rho-1} f\left(\frac{1}{t}\right) dt \tag{5.3}$$

Sustituting the value of $t^{\rho-1} f\left(\frac{1}{t}\right)$ from (5.2) in (5.3) and inverting the order of integration we get

$$\phi(p) = p^{\frac{1}{2}} \int_0^\infty z^{\frac{1}{2}}\, g(z)\, dz \int_0^\infty t^{\rho-1}\, K_\mu(pt)\, J_\nu(zt^{-1})\, dt$$

Evaluating the latter integral by (2) p. 375 (21), we get the reasult.

6. *Theorem* 5 : If $f(t)$ and $t^{\rho-1} f\left(\frac{1}{t}\right)$ belong to L $(0, \infty)$

and if $g(p) \underset{\nu}{\overset{H}{=}} f(t)$

and $\phi(p) \underset{\mu}{\overset{K}{=}} t^{\rho-1} f\left(\frac{1}{t}\right)$

then

$$\phi(p) = 2^{\rho-2}\, p^{-\rho+\frac{1}{2}} (-1)^{m+1}$$

$$\times \int_0^\infty z^{\frac{1}{2}} G_{1,5}^{4,0}\left(\frac{p^2 z^2}{16} \middle| \begin{matrix} \frac{1-\nu}{2} - m \\ \frac{\nu}{2}, -\frac{\nu}{2}, \frac{\rho+\nu}{2}, \frac{\rho-\mu}{2}, \frac{1-\nu}{2} - m \end{matrix}\right) g(z)\, dz$$

m integer, $p > 0$, $\rho > |\mathrm{R}(\mu)| - 3/2$, $-\frac{1}{2} < \nu < \frac{1}{2}$ (6.1)

Proof: Since $g(p)$ is the H=Transform of $f(t)$ we have (2) p. 157,

$$f(t) = \int_0^\infty (tz)^{\frac{1}{2}}\, Y_\nu(tz)\, g(z)\, dz;\ -\tfrac{1}{2} < \mathrm{R}(\nu) < \tfrac{1}{2} \qquad (6.2)$$

Substituting the value of $t^{\rho-1} f\left(\frac{1}{t}\right)$ from (6.2) in

$$\phi(p) = \int_0^\infty (pt)^{\frac{1}{2}}\, K_\mu(pt)\, t^{\rho-1} f\left(\frac{1}{t}\right) dt$$

and following the method of § 5, we get the theorem in view of the result [(2) p. 375 (20)]

$$\int_0^\infty x^{\rho-1} K_\mu(ax)\, Y_\nu(bx^{-1})\, dx$$

$$= (-1)^{m+1}\, 2^{\rho-2}\, a^{-\rho}\, G_{1,5}^{4,0}\left(\frac{a^2 b^2}{16} \middle| \begin{matrix} \frac{1-\nu}{2} - m \\ \frac{\nu}{2}, -\frac{\nu}{2}, \frac{\rho+\nu}{2}, \frac{\rho-\mu}{2}, \frac{1-\nu}{2} - m \end{matrix}\right)$$

m, integer, $b > 0$ $\mathrm{R}(a) > 0$, $\mathrm{R}(\rho) > |\mathrm{R}(\mu)| - 3/2$

7. We may utilize the above theorems to evaluate some line-integrals. By way of illustration we take a few examples.

Example 1. In theorem 1. taking

$$f(t) = t^{\nu-1}\, \mathrm{E}\left[\begin{matrix}\alpha_1 & \cdots & \alpha_h \\ \beta_1 & \cdots & \beta_r\end{matrix} : \frac{1}{t}\right]$$

we have (1) p. 222 (33)

$$\phi(p) = p^{-\nu}\, \mathrm{E}\left[\begin{matrix}\alpha_1 & \cdots & \alpha_h, \nu \\ \beta_1 & \cdots & \beta_r\end{matrix} : p\right]$$

$$\mathrm{R}(\nu) > 0$$

and Roopnarain [(8) p. 30] gives

$$\psi(p) = p^{-\nu}\, \mathrm{E}\left[\begin{matrix}\alpha_1 & \cdots & \alpha_h, \nu, \nu+2m \\ \beta_1 & \cdots & \beta_r, \nu+\frac{1}{2}+m-k\end{matrix} : p\right]$$

$$\mathrm{R}(\nu+m\pm m) > 0,\ \mathrm{R}(p) > 0$$

Substituting in theorem 1, and putting $m = \frac{a-1}{2}$, $k = 1-b+\frac{a}{2}$ we get after a little adjustment

$$\frac{1}{2\pi i}\int_{c-i\infty}^{c+i\infty} z^{-\nu}\, \mathrm{E}\left[\begin{matrix}\alpha_1 \cdots \alpha_h, \nu \\ \beta_1 \cdots \beta_r\end{matrix} : z\right]\, {}_2\mathrm{F}_1\left[\begin{matrix}a, 1 \\ b\end{matrix} : \frac{z}{p}\right] dz$$

$$= \frac{\Gamma(b)}{\Gamma(a)}\, p^{-\nu+1}\, \mathrm{E}\left[\begin{matrix}\alpha_1 \cdots \alpha_h, \nu, \nu+a-1 \\ \beta_1 \cdots \beta_r, \nu+b-1\end{matrix} : p\right] \qquad (7.1)$$

$$\mathrm{R}(b) > 0,\ \mathrm{R}(a) > 0,\ \mathrm{R}(\nu) > 0,\ \mathrm{R}(\nu+a-1) > 0,\ \mathrm{R}\left(\frac{z}{p}\right) < 1$$

Example 2 : Again in theorem 1, if we take

$$f(t) = t^{-\lambda}\, e^{-a/2t}\, \mathrm{W}_{\lambda,\mu}\left(\frac{a}{t}\right)$$

then [(1) p. 217 (22)]

$$\phi(p) = 2a^{\frac{1}{2}}\, p^{\lambda-\frac{1}{2}} \mathrm{K}_{2\mu}(2\sqrt{ap}),$$

$$\mathrm{R}(a) > 0,\ \mathrm{R}(p) > 0$$

and [(9) p. 273]

$$\psi(p) = a^{1-\lambda}\, \mathrm{G}^{4,0}_{2,4}\left(ap \,\middle|\, \begin{matrix}\frac{1}{2}-k+m, 0 \\ 2m, 0, \lambda+\mu-\frac{1}{2}, \lambda-\mu-\frac{1}{2}\end{matrix}\right)$$

Hence the theorem gives after putting $m = \frac{c-1}{2}$, $k = 1-d+\frac{c}{2}$

$$\frac{1}{2\pi i}\int_{c-i\infty}^{c+i\infty} z^{\lambda-\frac{1}{2}} \mathrm{K}_{2\mu}\left(2\sqrt{az}\right)\, {}_2\mathrm{F}_1\left[\begin{matrix}c, 1 \\ d\end{matrix} ; \frac{z}{p}\right] dz \qquad (7.2)$$

$$\frac{a^{\frac{1}{2}-\lambda}\,\Gamma(d)}{\Gamma(c)} \cdot \frac{p}{2}\, \mathrm{G}^{4,0}_{2,4}\left(ap \,\middle|\, \begin{matrix}d-1, 0 \\ c-1, 0, \lambda+\mu-\frac{1}{2}, \lambda-\mu-\frac{1}{2}\end{matrix}\right)$$

$$\mathrm{R}(d) > 0,\ \mathrm{R}(c) > 0.\quad \mathrm{R}(z/p) < 1$$

Example 3 : In theorem 2 let us take

$$f(t) = t^{\mu-1}(1+t)^{-\mu-\frac{1}{2}}$$

then we have (1) p. 139

$$\phi(p) = 2^{\mu}\,\Gamma(\mu)\,e^{\frac{1}{2}p}\,D_{-2\mu}(\sqrt{2p}),\quad R(\mu), R(p)>0$$

and by Rathie (6)

$$\psi(p) = \frac{p^{-\mu}}{\Gamma(\mu)+\frac{1}{2}}\,E\left[\begin{matrix}\mu-k+m,\ \mu-k-m,\ \mu+\frac{1}{2}\\ \mu-2k\end{matrix};p\right]$$

$$R(\mu)>1,\ R(p)>0$$

Putting $m = \frac{a-b}{2}$ and $k = 1-\frac{a+b}{2}$

we obtain

$$\frac{1}{2\pi i}\int_{c-i\infty}^{c+i\infty} e^{\frac{1}{2}z}\,D_{-2\mu}(\sqrt{2z})\;{}_2F_1\left[\begin{matrix}a, b\\ a+b-1\end{matrix}:\frac{z}{p}\right]dz$$

$$\frac{\Gamma(a+b-1)2^{-\mu}p^{-\mu+1}}{\Gamma(a)\,\Gamma(b)\,\Gamma(\mu)\,\Gamma(\mu+\frac{1}{2})}E\left[\begin{matrix}\mu+a-1,\ \mu+b-1,\ \mu+\frac{1}{2}\\ \mu+a+b-2\end{matrix}:p\right] \qquad (7.3)$$

$$R(a)>0,\ R(b)>0,\ R(\mu)>0,\ R(\mu+a-1)>0,\ R\left(\frac{z}{p}\right)<1$$

I am indebted to Dr. P. L. Srivastava for his valuable guidance.

REFERENCES

1. Erdelyi A., (1954) Tables of Integral Transforms Vol. 1.
2. Erdelyi A., (1954) Tables of Integral Transforms Vol. 2.
3. Goldstein S., (1932) *Proc. Lond. Math. Soc.* **34**, 103-125.
4. Mclachlan N. W. (1948, Modern Operational Calculus.
5. Meijer C. S. (1941) *Proc. Nederl. Akad. wet. Amsterdam*, 44.
6. Meijer C. S. (1940) *Proc. Amsterdam Akad. wet* 43.
7. Rathie C. B. (1953-54) *Univer. Rajputana Studies, phy. sec.* III.
8. Roopnarain (1957) *Ganit.* Vol. 8. No. 1.
9. Roopharain (1957) *Math. Zeit. Bd.* 68, 272-281.
10. Varma R. S. (1951) *Proc. Nat. Acad. Sci. India*, A-20, 219-16.
11. Whittaker E. T. & Watson G. N. (1927) Modern Analysis.

RELATIONS BETWEEN HANKEL AND GENERALIZED LAPLACE TRANSFORMS*

By

C. B. L. VERMA

T. R. S. College, Rewa, M. P.

[Received on 24th February, 1961]

1. The Laplace Transform of a function $f(t) \in L\ (0, \infty)$ is defined by the equation

$$L\left\{ f; p\right\} = \int_0^\infty e^{-pt} f(t)\, dt, \quad R(p) > 0 \tag{1.1}$$

while its Hankel Transform of order ν by the equation [6]

$$H_\nu \left\{ f; \xi \right\} = \int_0^\infty t f(t)\, J_\nu (\xi t)\, dt, \quad \xi > 0 \tag{1.2}$$

Tricomi (7) discovered a relation between the Hankel and Laplace Transforms. Recently Bhonsle (1) has obtained a relation between the Laplace Transform of $t^\mu f(t)$ and Hankel Transform of $f(t)$. The object of this paper is to generalize the result of Bhonsle by investigating the relations existing between the Hankel Transform and the generalizations of the Laplace Transform as given by Meijer (3) and Varma (8).

Meijer's generalization is

$$K_\lambda \left\{ f; p \right\} = \sqrt{\frac{2}{\pi}} \int_0^\infty (pt)^{\frac{1}{2}} K_\lambda (pt) f(t)\, dt \quad R(p) > 0 \tag{1.3}$$

while Varma generalized (1.1) in the form

$$V_{k,m} \left\{ f; p \right\} = \int_0^\infty e^{-\frac{1}{2} pt} (pt)^{m-\frac{1}{2}} W_{k,m}(pt)\, f(t)\, dt, \quad R(p) > 0 \tag{1.4}$$

*Read at the 30th Annual Session of the Academy on February 3, 1961.

(1.3) and (1.4) reduce to (1.1) when $\lambda = \pm \frac{1}{2}$ and

$k + m = \frac{1}{2}$ respectively.

2. *Theorem* 1. If $f(t)$ and $H_\nu \{f, \xi\}$ belong to L $(0, \infty)$

and if $R(p) > 0$, $|p| > |\xi|$

and $R(\mu \pm \lambda + \frac{1}{2}) > 0$, $R(\mu + \nu \pm \lambda + \frac{3}{2}) > 0$

then

$$K_\lambda \left\{ t^\mu f; p \right\} = \int_0^\infty \chi(p,\xi)\, H_\nu \left\{ f; \xi \right\} d\xi \tag{2.1}$$

where

$$\chi(p,\xi) = \frac{2^\mu\, \Gamma\frac{1}{2}(\mu + \nu \pm \lambda + \frac{3}{2})}{\sqrt{\pi}\, \Gamma(\nu+1)\, p^{\mu+\nu+1}}\, \xi^{\nu+1}\, {}_2F_1 \left[\begin{matrix} \frac{1}{2}(\mu+\nu\pm\lambda+\frac{3}{2}) \\ \nu+1 \end{matrix} ; -\frac{\xi^2}{p^2} \right]$$

Proof: Since f belong to L $(0, \infty)$, we have by Hankel's Inversion theorem [(6) p. 52].

$$f(t) = \int_0^\infty \xi\, H_\nu \{f, \xi\}\, J_\nu (t\xi)\, d\xi \tag{2.2}$$

Multiplying both sides by $\sqrt{\frac{2}{\pi}}\, t^\mu\, (pt)^{\frac{1}{2}} . K_\lambda . (pt)$ and

integrating between $(0, \infty)$, we have, after inverting the order of integration which is justified by Fubini's theorem under conditions stated,

$$K_\lambda \{t^\mu f(t); p\} = \int_0^\infty \xi\, H_\nu \{f, \xi\}\, K_\lambda \left\{ t^\mu\, J_\nu (t\xi) \right\} d\xi$$

Now, since (2) p. 137,

$$K_\lambda \left\{ t^\mu\, J_\nu (t\xi); p \right\} = \frac{2^\mu\, \Gamma\frac{1}{2}(\mu + \nu \pm \lambda + \frac{3}{2})}{\sqrt{\pi}\, \Gamma(\nu+1)}\, \xi^\nu\, p^{-\mu-\nu-1}$$

$$\times\, {}_2F_1 \left[\begin{matrix} \frac{1}{2}(\mu+\nu\pm\lambda+\frac{3}{2}) \\ \nu+1 \end{matrix} ; -\frac{\xi^2}{p^2} \right]$$

$$R(\mu + \nu - \tfrac{1}{2}) > |R(\lambda)| - 2; |p| > |\xi|$$

the result follows.

Putting $\lambda = \pm \frac{1}{2}$ we get after a little simplification

Bhonsle's result (1), *viz.* :

$$L \{ t^{\mu} f; p \} = \int_0 K(p, \xi) H_{\nu} \{ f; \xi \} d\xi \tag{2.3}$$

Where

$$K(p\ \xi) = \Gamma(\mu+\nu+1)\ \xi\ (p^2+\xi^2)^{-\frac{1}{2}(\mu+1)}\ P_{\mu}^{-\nu} \left\{ \frac{p}{\sqrt{p^2+\xi^2}} \right\}$$

$$R(\mu) > -1, R(\mu+\nu) > -1, R(p) > 0$$

Example : Taking

$$f(t) = t^{\lambda-\mu+\frac{1}{2}}\ {}_2F_1\left[\begin{matrix}\alpha, \beta \\ \lambda+1\end{matrix}; -b^2t^2\right]$$

we have (2) p. 81, $H_{\nu}\ \{f; \xi\}$

$$= \frac{2^{\lambda-\mu+3/2}\ \Gamma(\lambda+1)}{\Gamma(\alpha)\ \Gamma(\beta)\ \xi^{\lambda-\mu+5/2}}\ G^{3,1}_{2,4}\left(\frac{\xi^2}{4b^2}\middle| \begin{matrix}1,\ 1+\lambda \\ \frac{5}{2}+\lambda-\mu+\nu \\ \hline 2\end{matrix},\ \alpha,\ \beta,\ \begin{matrix}\frac{5}{2}+\lambda-\mu-\nu \\ \hline 2\end{matrix}\right)$$

$-R(\nu)-1 < R(\lambda-\mu+3/2) < 2\ max\ [R(\alpha), R(\beta)] - \frac{1}{2}$, $R(b) > 0$
and (2) p. 152 gives

$$K_{\lambda} \{ t^{\mu} f; p \} = \sqrt{\frac{2}{\pi}}\ \frac{2^{\lambda+1}\ \Gamma(\lambda+1)}{b^{\alpha+\beta}}\ p^{\alpha+\beta-\lambda-\frac{3}{2}}\ S^{(p/b)}_{1-\alpha-\beta,\ \alpha-\beta}$$

$$R(\lambda) > -1, R(p) > 0$$

$S_{\mu,\nu}(z)$ being the Lommel-Function.

Substituting in the theorem and putting $\mu = a+c-d-\frac{1}{2}$, $\nu = d-1$, $\lambda = a-c$, we get after a slight simplification

$$\int_0^{\infty} \xi^{2c-3}\ {}_2F_1\left[\begin{matrix}a, c \\ d\end{matrix}; -\frac{\xi^2}{p^2}\right] G^{3,1}_{2,4}\left(\frac{\xi^2}{4b^2}\middle| \begin{matrix}1,\ 1-c+a \\ 1-c+d,\ \alpha,\ \beta,\ 2-c\end{matrix}\right) d\xi$$

$$= \frac{\Gamma(\alpha)\ \Gamma(\beta)\ \Gamma(d)}{\Gamma(a)\ \Gamma(c)\ b^{\alpha+\beta}}\ p^{\alpha+\beta+2c-2}\ S^{(p/b)}_{1-\alpha-\beta,\ \alpha-\beta} \tag{2.4}$$

$-R(d) < 2(d-2c+2) < 2\ max\ [R(\alpha), R\delta(\beta)] - \frac{1}{2}$; $R(p), R(b) > 0$

$R(2a-d) > 0$, $R(2c-d) > 0$, $R(1-c+a) > 0$

3. *Theorem* 2. : If f and $H_\nu \{ f; \xi \}$ belong to L $(0, \infty)$

and if R $(\mu+\nu+1+m\pm m) > 0$ and R (p), R $(\xi) > 0$

then

$$V_{k,m} \left\{ t^\mu f; p \right\} = \int_0^\infty \psi(p, \xi)\, H_\nu \{ f; \xi \}\, d\xi \tag{3.1}$$

where

$$\psi(p, \xi) = \frac{\Gamma^*(\mu+\nu+1+m\pm m)\, \xi^{\nu+1}}{2^\nu\, \Gamma(\nu+1)\, \Gamma(\mu+\nu+{}^3/_2+m-k)}\, p^{-\mu-\nu-1}$$

$$\times {}_4F_3\left[\begin{matrix} \frac{1}{2}(\mu+\nu+{}^3/_2+m\pm m\pm\frac{1}{2}) \\ \nu+1;\ \frac{1}{2}(\mu+\nu+2+m-k\pm\frac{1}{2}) \end{matrix};\ -\frac{\xi^2}{p^2} \right]$$

The proof is exactly similar to that given in theorem 1.

The result follows since Roopnarain ((4) p. 31) gives

$$V_{k,m} \left\{ t^\mu\ J_\nu(\xi t; p \right\} = \frac{(\frac{1}{2}\xi)^\nu\ \Gamma^*(\mu+\nu+1+m\pm m)}{\Gamma(\nu+1)\ \Gamma(\mu+\nu+{}^3/_2+m-k)} p^{-\mu-\nu-1}$$

$$\times {}_4F_3\left[\begin{matrix} \frac{1}{2}(\mu+\nu+{}^3/_2+m\pm m\pm\frac{1}{2}) \\ \nu+1,\ \frac{1}{2}(\mu+\nu+2+m-k\pm\frac{1}{2}) \end{matrix};\ -\frac{\xi^2}{p^2} \right] \tag{3.2}$$

$$R(\mu+\nu+1+m\pm m)>0.\quad R(p)>0,\ |p| > |\xi|$$

Again putting $k+m=\frac{1}{2}$, ${}_4F_3$ degenerates into ${}_2F_1$ giving Bhonsle's result (2.3) as before.

Example : If

$$f(t)=t^{1-2\mu}\, G^{l,n}_{r,s}\left(\lambda t^2 \,\middle|\, \begin{matrix} \alpha_1 \ldots \alpha_r \\ \beta_1 \ldots \beta_s \end{matrix}\right)$$

we get (2) p. 91 (20)

$$H_\nu \left\{ f;\ \xi \right\} = \frac{2^{2-2\mu}}{\xi^{3-2\mu}}\ G^{l,n+1}_{r+2,s}\left(\frac{4\lambda}{\xi^2} \middle| \begin{matrix} h, \alpha_1 \ldots \alpha_r\ k \\ \beta, \ldots \ldots \beta_s \end{matrix} \right)$$

$$h = -\tfrac{1}{2}+\mu-\tfrac{1}{2}\nu,\ k = -\tfrac{1}{2}+\mu+\tfrac{1}{2}\nu$$

$$r+s<2(l+n), \qquad R(\alpha_j-\mu) < -\tfrac{1}{2},\ j=1, \ldots n$$

$$|\arg\lambda| < (l+n-\tfrac{1}{2}r-\tfrac{1}{2}s)\pi \quad R(\beta_j-\mu+\tfrac{1}{2}\nu) > -{}^3/_2,\ j=1, \ldots l,$$

and by Roopnarain (5) p. 91,

$$V_{k,m}\left\{ t^{\mu} f; p \right\}$$

$$= \frac{p^{\mu-2}}{\sqrt{\pi}\; 2^{\mu-\frac{1}{2}-k-m}} G^{\,l,n+4}_{r+4,\,s+2}\left(\frac{4\lambda}{p^2} \middle| \begin{matrix} \frac{\mu-1}{2}, & \frac{\mu}{2}, & \frac{\mu-1}{2}-m, \frac{\mu}{2}-m, \alpha_1 \ldots \alpha_r \\ \beta_1 \ldots \beta_s, & \frac{\mu-1}{2}+\frac{k-m}{2}, & \frac{\mu}{2}-\frac{1}{4}+\frac{k-m}{2} \end{matrix} \right)$$

$$\left| \arg \frac{p}{\lambda} \right| < (l+n-\tfrac{1}{2}r-\tfrac{1}{2}s-\tfrac{1}{2})\pi$$

$$(r+s+1) < 2\,(l+n)$$

$$R\left(\frac{\mu}{2}-1-m \pm m\right) < R(\beta j);\; j = 1, 2 \ldots . l.$$

Hence we get by putting

$$\mu = 2a-c,\; \nu = c-1,\; m = b-a,\; k = a+b-2d+\tfrac{1}{2}$$

and simplifying

$$\int_0^{\infty} \xi^{4a-c-3}\, {}_4F_3\left[\begin{matrix} a,\; a+\frac{1}{2},\; b,\; b+\frac{1}{2} \\ c,\; d,\; d+\frac{1}{2} \end{matrix};\; -\frac{\xi^2}{p^2} \right] G^{\,l,n+1}_{r+2,\,s}\left(\frac{4\lambda}{\xi^2} \middle| \begin{matrix} 2a-\frac{3c}{2}, & \alpha_1 \ldots \alpha_r, & 2a-\frac{c}{2}-1 \\ & \beta_1 \ldots \beta_s & \end{matrix} \right) d\xi$$

$$= \frac{\Gamma(c)\,\Gamma(2d)}{\Gamma(2a)\,\Gamma(2b)\,\sqrt{\pi}\; 2^{2(a-b-c+d)}}\, p^{4a-c-2}$$

$$\times G^{\,l,n+4}_{r+4,\,s+2}\left(\frac{4\lambda}{p^2} \middle| \begin{matrix} a-\frac{c}{2}-\frac{1}{2},\; a-\frac{c}{2},\; 2a-b-\frac{c}{2}-\frac{1}{2},\; 2a-b-\frac{c}{2},\; \alpha_1 \ldots \alpha_r \\ \beta_1 \ldots \beta_s,\; 2a-d-\frac{c}{2}-\frac{1}{4},\; 2a-d-\frac{c}{2} \end{matrix} \right) \qquad (3.3)$$

$$R(a) > R(b) > 0,\; R(p) > 0,\; |p| > |\xi|$$

$$R(\alpha_j + c - 2a) < -\tfrac{1}{4},\; j = 1 \ldots n;\; \left| \arg \frac{p}{\lambda} \right| < (l+n-\tfrac{1}{2}r-\tfrac{1}{2}s-\tfrac{1}{2})\pi$$

$$\left.\begin{aligned} R(\beta_j + \tfrac{3c}{2} - 2a) > -1 \\ R(\beta_j - 3a + \tfrac{c}{2} + 2b) > -1 \end{aligned}\right\} j = 1 \ldots l;$$

$$(r+s+1) < 2\,(l+n)$$

$$R(\beta_j + \tfrac{c}{2} - a) > -1,\; j = 1 \ldots l$$

I am thankful to Dr. B. R. Bhonsle for suggesting me the problem and to Dr. P. L. Srivastava for his guidance during the preparation of this paper.

REFERENCES

1. Bhonsle B. R.———"A Relation between Laplace and Hankel Transform"—to be published in *Glas. Math. Ass.*
2. Erdelyi A., (1954), Tables of Integral Transforms, Vol. 2.
3. Meijer C. S., (1940), *Proc. Amsterdam Akad. wet.* 43.
4. Roopnarain (1957), *Gcnit.*, Vol. 8, No. 1.
5. Roopnarain (1957-58), *Rend. det. semi. Mat.* Vol. 1.
6. Sneddon I. N. (1951), Fourier Transforms, Mcgraw Hill.
7. Tricomi F, (1935), *Rend. del. Lincei.* (6) 22-564-571.
8. Varma R. S, (1951), *Proc. Nat. Acad. Sei. India*, A20, 209-16.

THE POTENTIOMETRIC DETERMINATION OF AROMATIC AMINES BY DIAZOTIZING*

By

ERNST DACHSELT†

[Received on 15th June 1961]

With great interest I read a report about the above mentioned publication in the "Chemisches Zentralblatt 132 (1961), p. 4118." As far as I conclude from these short indications (I am sorry not to be in possession of the original work) they are identical with the results of my own investigations which I carried out in collaboration with Prof. Dr. Erich Müller from 1924 to 1925 at the Institute of Electrochemistry and Physical Chemistry of the Saxon Polytechnical University in Dresden. We published the results of this research entitled "Die potentiometrische Indikation der Diazotierung und quantitative Bestimmung von Aminen" in the "Zeitschrift für Elektrochemie" vol. 31 (1925), p. 662-66. I beg to draw your attention to this publication.

*Note to the publication of G. Sitaramaiah and R. S. Sharma in the "Proceedings of the National Academy of Sciences, India, Sect. A 26, 129-33, March 1957".

†Present Address : Rudolf-Breitscheidstrasse 5^{I}, Graz (Germany).

FORM IV

(*See* Rule 8)

Statement about ownership and other particulars about newspaper (Proceedings of The National Academy of Sciences, India, Section A-Physical Sciences) to be published in the first issue every year after the last day of February.

1.	Place of Publication	... The National Academy of Sciences, India, Lajpatrai Road, Allahabad-2 (U.P.)
2.	Periodicity of its publication	... Quarterly.
3.	Printer's Name	... M. Sarwat Husain.
	Nationality	... Indian.
	Address	... 170, Noorulla Road, Allahabad.
4.	Publisher's Name	... Dr. R. K. Saksena.
	Nationality	... Indian.
	Address	... 1, B-Beli Road, Allahabad-2.
5.	Editor's Name	... Dr. R. K. Saksena.
	Nationality	... Indian.
	Address	... 1, B-Beli Road, Allahabad-2.
6.	Names and addresses of individuals who own the newspaper and partners or shareholders holding more than one per cent of the total capital.	The National Academy of Sciences, India, Lajpatrai Road, Allahabad-2 (U. P.)

I, R. K. Saksena, hereby declare that the particulars given above are true to the best of my knowledge and belief.

Dated March 1, 1961.

R. K. SAKSENA.
Signature of Publisher

CONTENTS

The Mass-frequency Function in Galactic Clusters . . . . . O. P. Gupta *and* R. S. Kushwaha 1

Physico-chemical Studies on the Compositions of Complex Arsenite, Thiosulphate and Arsenate of Metals—Part I . . . . . M. S. Bhadraver *and* J. N. Gaur 10

Effect of Phosphorus on Availability of Nitrogen . . J. S. P. Yadav 14

Chemistry of Vanadium—Part VII . . . . . Sarju Prasad *and* Kailash Nath Upadhyaya 20

Potentiometric Studies on the Oxalato-complexes of Titanium (IV) . . . . . Sarju Prasad *and* Jaibeni Prasad Tripathi 24

Chemistry of Vanadium—Part VIII . . . . . Sarju Prasad *and* Kailash Nath Upadhyaya 29

Study of the V^{IV} Precipitates by Physico-chemical Methods—Parts I and II . . . . . P. K. Bhattacharya *and* S. N. Banerji 33, 39

Physico-chemical Study of the Insoluble Compounds of Trivalent Cerium—Parts I and II . . M. C. Saxena *and* A. K. Bhattacharya 44, 51

Studies in Chromium Arsenite Sol—Parts II and III . . . . . P. C. Jain *and* S. N. Banerji 58, 66

Chemistry of Vanadium—Part IX . . . . . Sarju Prasad *and* P. V. S. Jagannadha Sarma 72

Studies in Poly-salts of Vanadium—Parts I and II . . . . . P. K. Bhattacharya, M. C. Saxena *and* S. N. Banerji 75, 79

Study of the Extent of Aggregation during Sol-Gel Transformation of some Gel forming Systems . . . . . Y. D. Upadhya *and* S. P. Mushran 85

On Mutual Relationships between Various Integral Transforms . . . . . C. B. L. Verma 94

Relations between Hankel and Generalized Laplace Transforms . . . . . C. B. L. Verma 102

The Potentiometric Determination of Aromatic Amines by Diazotizing . . . . . Ernst Dachselt 108

Published by Dr. R. K. Saksena, for the National Academy of Sciences, India, Allahabad and Printed by M. Sarwat Husain at The Mission Press, Allahabad

Secretary, Editorial Board—**Dr. R. K. Saksena**